## INFORMATION TO USERS

8703780

Wenig, Robert Wayne

VANADIUM-PHOSPHORUS-OXYGEN INDUSTRIAL CATALYSTS FOR C-4
HYDROCARBON SELECTIVE OXIDATION TO MALEIC ANHYDRIDE

*Iowa State University*                                    PH.D.          1986

Vanadium-phosphorus-oxygen industrial catalysts for

$C_4$ hydrocarbon selective oxidation to maleic anhydride

by

Robert Wayne Wenig

A Dissertation Submitted to the

Graduate Faculty in Partial Fulfillment of the

Requirements for the Degree of

DOCTOR OF PHILOSOPHY

Major: Chemical Engineering

Approved:

Signature was redacted for privacy.

In Charge of Major Work

Signature was redacted for privacy.

For the Major Department

Signature was redacted for privacy.

For the Graduate College

Iowa State University
Ames, Iowa

1986

## TABLE OF CONTENTS

GENERAL INTRODUCTION

## Selective Oxidation Processes

Selective oxidation reactions with transition metal oxide catalysts have found commercial application for the conversion of hydrocarbons into chemical intermediates. The partial oxidation of napththalene to phthalic anhydride and benzene to maleic anhydride by supported $V_2O_5$ catalysts are examples of selective oxidation processes. A current application of hydrocarbon selective oxidation involves the partial oxidation of $C_4$ hydrocarbons to maleic anhydride by vanadium-phosphorus mixed oxide catalysts. A survey of industrial selective oxidation reactions is presented in Table 1 (1).

Selective oxidation catalysts provide a controlled donation of oxygen to the hydrocarbon molecule in order to restrict the formation of complete oxidation products. Active centers are provided by the metal oxide catalysts to assist in the transformation of the reactant into reaction intermediates and oxidation products. The nature of this interaction and the reaction mechanism for commercial selective oxidation reactions are poorly understood.

## Catalysts for Maleic Anhydride Synthesis

Maleic anhydride is an important intermediate in the formation of unsaturated polyester resins and specialty chemicals (2). Worldwide capacity for maleic anhydride production now exceeds 700,000 tonnes per year (3). An important recent advance in this process is the development of vanadium-phosphorus-oxygen (V-P-O) catalysts which are capable of selectively oxidizing n-butane and 1-butene to maleic anhydride. The

Table 1. Industrial selective oxidation processes

| Reaction | Catalyst | Reactor |
|---|---|---|
| naphthalene $+ \frac{9}{2} O_2 \rightarrow$ phthalic anhydride $+ 2CO_2 + 2H_2O$ | Supported $V_2O_5$ | Fluidized bed |
| benzene $+ \frac{9}{2} O_2 \rightarrow$ maleic anhydride $+ 2CO_2 + 2H_2O$ | Supported $V_2O_5 + MoO_3$ | Fluidized bed |
| $H_2C=CHCH_2CH_3 + 3 O_2 \rightarrow$ maleic anhydride $+ 3H_2O$ | Promoted V-P-O | Fixed bed |
| $CH_3CH_2CH_2CH_3 + \frac{7}{2} O_2 \rightarrow$ maleic anhydride $+ 4H_2O$ | Promoted V-P-O | Fixed bed |
| $CH_3OH + \frac{1}{2} O_2 \rightarrow HCHO + H_2O$ | $Fe(MoO_4)_3 + MoO_3$ | Fixed bed |
| $H_2C=CH_2 + \frac{1}{2} O_2 \rightarrow H_2C\overset{O}{-}CH_2$ | Supported Ag | Fixed bed |
| $H_2C=CHCH_3 + \frac{3}{2} O_2 \rightarrow H_2C=CHCO_2H$ | Mixed molybdates | Fixed bed |

2

$C_4$ hydrocarbon based oxidation processes are favored by higher theoretical yields and lower feedstock costs than is possible with the earlier benzene based oxidation processes (2). Industrial V-P-O catalysts often contain Zn, Ti, Co, or Mo promoters and are reported to give high conversions of n-butane and high selectivities for maleic anhydride (3, 4).

A survey of patented catalysts for the selective oxidation of n-butane to maleic anhydride is presented in Table 2 (3). Typically these catalysts are prepared by dissolving $V_2O_5$ in water or alcohol solvents, then reducing the vanadium with acids or alcohols under reflux. After formation of a uniform $V^{4+}$ solution, phosphoric acid is added to achieve the desired P-to-V ratio. Following several hours of reaction, the solvent is evaporated to give a catalyst precursor which is activated under a controlled environment at 350-500°C. Catalyst promoters are often co-precipitated or impregnated onto the catalyst precursor prior to calcination. Variations in reducing agent, solvent, P-to-V ratio, and activation conditions has been found to result in the formation of ten or more distinct V-P-O phases of unique catalytic properties (Table 3) (3, 5).

Recent studies have attempted to relate V-P-O phase composition to catalyst activity, catalyst selectivity, and reaction mechanism. Bordes and Courtine (6) have postulated the existence of active catalyst sites at phase boundaries between the $\alpha$-VOPO$_4$ and the $(VO)_2P_2O_7$ phases in olefin oxidation studies. The selective oxidation of 1-butene was reported to involve a redox mechanism between these vanadium(V) and vanadium(IV) catalyst phases. Hodnett et al. (7, 8) describes a dependence of catalyst phase composition and selectivity in n-butane oxidation on the nominal catalyst P-to-V ratio. Catalysts prepared in aqueous solution with higher

Table 2. Patented catalysts for n-butane selective oxidation to maleic anhydride

| Year | Composition | P:V:X | Solvent | Feed | Temperature | Yield %[a] |
|------|-------------|-------|---------|------|-------------|------------|
| 1975 | V-P-O | 1.06:1 | Water | 1.5% butane in air | 440 | 43 |
| 1975 | V-P-O | 1.20:1 | Isobutanol | 1.5% butane in air | 374 | 62 |
| 1975 | V-P-O | 1.20:1 | Methanol | 1.5% butane in air | 468 | 53 |
| 1977 | V-P-O | 1.08:1 | Water | butane-air | 370 | 54 |
| 1981 | V-P-O | 1.10:1 | Isobutanol | 1.4% butane in air | 446 | 62 |
| 1975 | V-P-Zn-O | 1.15:1:0.19 | Water | 1% butane in air | 450 | 51 |
| 1979 | V-P-Ti-O | 1.15:1:0.06 | Water | 1.5% butane in air | 460 | 47 |
| 1980 | V-P-Co-O | 1.20:1:0.065 | Water | 1.5% butane in air | 420 | 59 |
| 1982 | V-P-Mo-O | 1.20:1:0.025 | Water | 14% butane 18% oxygen | 360 | 56 |
| 1982 | V-P-Zn-O | 1.28:1:0.3 | Methanol | butane-air | 411 | 48 |

[a]The yield is defined as $\dfrac{\text{moles of maleic anhydride produced}}{\text{moles of n-butane introduced}} \times 100$.

Table 3. Phases of V-P-O catalysts

| $V^{5+}$ phase | Description | $V^{4+}$ phase | Description |
|---|---|---|---|
| $VPO_5 \cdot 2 H_2O$ | Dihydrate phase | $VO(H_2PO_4)_2$ (phase E) | Detrimental effect on selectivity |
| $VPO_5 \cdot 1 H_2O$ | Hydrate phase | $(VO)_2P_2O_7 \cdot 1 H_2O$ | Catalyst precursor decomposed at 380°C |
| $\beta$-$VOPO_4$ | Isostructural with $\beta$-$VOSO_4$. Features corner-sharing $VO_6$ octahedra | $(VO)_2P_2O_7$ | Features edge-sharing $VO_6$ octahedra |
| $\alpha$-$VOPO_4$ | Isostructural with $\alpha$-$VOSO_4$. Features corner-sharing $VO_6$ octahedra | B-phase | Patented catalyst for industrial processes |
| Phase X | Patent | $\beta$-phase | The $V^{4+}$ part of the B-phase. Tripolyphosphate structure |
| $(\alpha'$-$VOPO_4)$ | Similar structure to $\alpha$-$VOPO_4$; contains trapped water | $\beta^*$-phase | Transforms into B'-phase at 450°C and $\beta$-$VOPO_4$ at 500°C |
| B'-phase | Reported to be oxidized equivalent to the $\beta$- or B-phase | $VO(PO_3)_2$ | P/V $\sim$ 2:1 |

phosphorus loadings were·found to have a reduced vanadium surface and higher selectivities for maleic anhydride.

Although the selective oxidation of $C_4$ hydrocarbons is a process of great industrial importance, both the reaction pathway and mechanism for maleic anhydride formation remain poorly understood. In the following sections possible reaction pathways and reaction mechanisms are presented for n-butane and 1-butene selective oxidation.

## Reaction Pathways

The reaction pathways which have been presented for the oxidation of n-butane to maleic anhydride have been very simple. The models by Escardino et al. (9), Wohlfahrt and Hofmann (10), and Wüstneck et al. (11) do not propose any involvement of olefins in the oxidation mechanism. The reaction pathway described by Escardino (9) proposes the direct formation of maleic anhydride and carbon oxides from n-butane with the subsequent combustion of maleic anhydride to carbon oxides:

n-butane ⟶ maleic anhydride

$CO_x$ $(H_2O)$
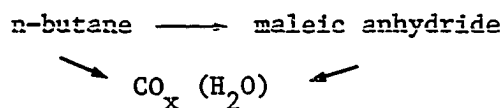
The rate controlling step in this paraffin oxidation scheme for maleic anhydride synthesis appears to involve the rupture of a methylene carbon-hydrogen bond of n-butane on the V-P-O catalyst surface (12). Abstraction of a hydrogen radical seems to allow the formation of an activated ·$C_4H_9$ species which could be readily oxidized to maleic anhydride.

The reaction pathway for 1-butene selective oxidation is generally
believed to proceed with 1,3-butadiene (13) and furan (14) as intermediates.
Crotonaldehyde and 2-butenes are usually considered to be side products.
The reaction pathway proposed by Varma and Saraf (15) involves the
selective oxidation of 1-butene to maleic anhydride via a 1,3-butadiene
surface intermediate (furan is described as a secondary intermediate). The
combustion of 1-butene, butadiene, and maleic anhydride to carbon oxides
and water was proposed in parallel reactions. The reaction pathway
proposed by Varma and Saraf (15) follows:

$$1\text{-butene} \longrightarrow \text{butadiene} \longrightarrow \text{maleic anhydride}$$
$$\searrow \quad CO_x, \ (H_2O) \quad \swarrow$$
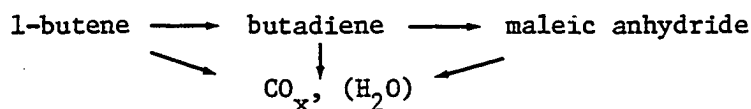
### Peroxide Mechanisms

The dehydrogenation of 1-butene to 1,3-butadiene suggests the
possibility of peroxide intermediates in olefin selective oxidation.
Trimm (16) proposes the addition of two oxygen molecules to butadiene to
form a diperoxide species. Subsequently hydroperoxides are formed and
react to give maleic acid or di-aldehydes—which readily dehydrate to
form maleic anhydride.

$$CH_2=CH-CH=CH_2 + 2O_2 \longrightarrow \cdot OOH_2C-CH=CH-CH_2OO\cdot$$

$$\cdot OOH_2C-CH=CH-CH_2OO\cdot + 2RH \longrightarrow HOOH_2C-CH=CH-CH_2OOH + 2R\cdot$$

$$HOOH_2C-CH=CH-CH_2OOH \xrightarrow[O_2]{-2H_2O} \underset{HO}{\overset{O}{\diagdown}}C-CH=CH-C\overset{O}{\underset{OH}{\diagup}}$$

$$HOOC-CH=CH-COOH \xrightarrow{-H_2O} \text{(maleic anhydride)}$$
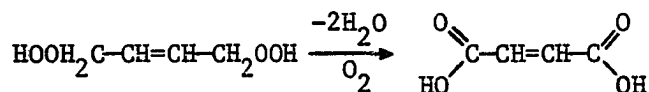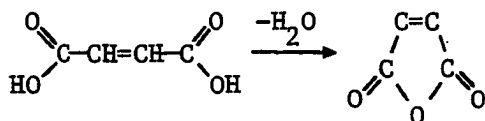
The addition of a single oxygen to 1,3-butadiene could lead to the formation of a peroxide species on the catalyst surface (16). Subsequently hydroperoxides and 2-butenoic acid species could be formed before the second addition of oxygen to give maleic acid. The dehydration of maleic acid to maleic anhydride would follow:

$$CH_2=CH-CH=CH_2 + O_2 \longrightarrow \cdot H_2C-CH=CH-CH_2OO\cdot$$

$$\cdot H_2C-CH=CH-CH_2OO\cdot + RH \longrightarrow \cdot H_2C-CH=CH-CH_2OOH + R\cdot$$

$$\cdot H_2C-CH=CH-CH_2OOH \xrightarrow[O_2]{-H_2O} \cdot H_2C-CH=CH-C\overset{O}{\underset{OH}{}}$$

$$\cdot H_2C-CH=CH-C\overset{O}{\underset{OH}{}} + RH \xrightarrow{O_2} \overset{O}{\underset{HO}{}}C-CH=CH-C\overset{O}{\underset{OH}{}} + R\cdot$$

$$\overset{O}{\underset{HO}{}}C-CH=CH-C\overset{O}{\underset{OH}{}} \xrightarrow{-H_2O} \text{(maleic anhydride)}$$
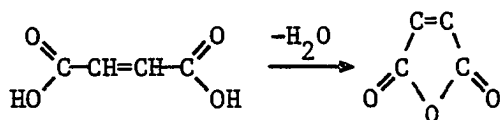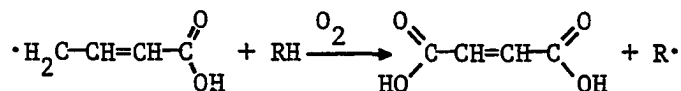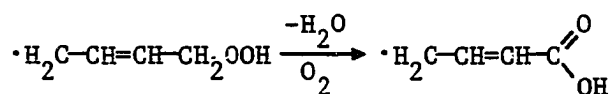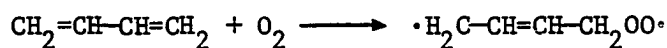
A cyclic peroxide route to maleic anhydride could involve the addition of oxygen to butadiene since intramolecular peroxide formation across a double bond is also possible (16), leading to epoxides and carbonyls.

$$\text{(butadiene)} \xrightarrow{O_2} \text{(cyclic peroxide)} \xrightarrow[-H_2O]{O_2} \text{(carbonyl product)}$$
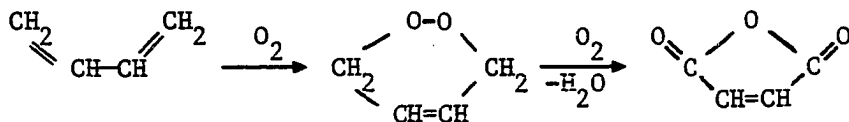
## Redox Mechanism

The redox mechanism is attributed to changes in metal oxidation state which occur when the catalyst is reduced during hydrocarbon oxidation and subsequently reoxidized by oxygen in the feed. Mars and van Krevelen first introduced this mechanism in 1954 (17). For 1-butene oxidation to 1,3-butadiene, Batist (18) describes a $Mo^{6+}/Mo^{4+}$ redox process in which catalyst anion vacancies ($\square$) and surface oxygen species assist in the formation of a $\pi$-allyl surface intermediate ($[Mo=C_4H_7]^{5+}$).

$$C_4H_8 + \square + O^{2-} \rightleftarrows C_4H_7^- + OH^-$$

$$Mo^{6+} + C_4H_7^- \rightarrow [Mo=C_4H_7]^{5+}$$

$$[Mo=C_4H_7]^{5+} + O^{2-} \rightarrow Mo^{4+} + \square + OH^- + C_4H_6$$

$$2OH^- \rightleftarrows O^{2-} + \square + H_2O$$

$$O_2 + 2\square + 2Mo^{4+} \rightarrow 2O^{2-} + 2Mo^{6+}$$
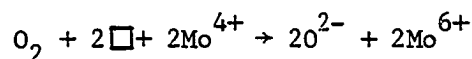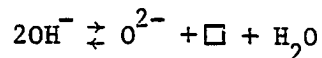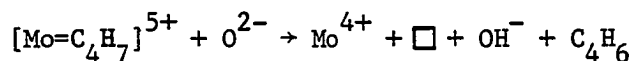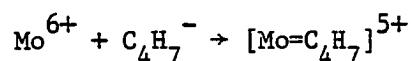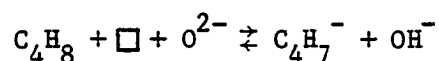
A convincing reaction scheme for n-butane selective oxidation should be able to incorporate catalyst redox properties and peroxide type mechanisms for molecular transformations into the reaction pathways for maleic anhydride synthesis described earlier. In addition, the influence of catalyst composition on phase structure, catalyst activity and selectivity, and the reaction mechanism need to be explored for industrial-type V-P-O catalysts.

## Research Objectives

Although evidence exists that the nominal (preparative) P-to-V ratio is a key parameter in determining the catalytic behavior of vanadium-phosphorus-oxygen catalysts, a fundamental understanding of the operation of these catalysts is still lacking. The purpose of this study is to investigate the synthesis and characterization of V-P-O catalysts having variable P-to-V ratio, and to examine the dependence of catalyst activity, selectivity, and reaction mechanism on phase composition. Catalyst characterization techniques including X-ray diffraction, laser Raman spectroscopy, infrared spectroscopy, X-ray photoelectron spectroscopy, scanning electron microscopy, X-ray energy dispersive spectroscopy, and BET surface area measurements will be used. Kinetic measurements are to be undertaken in order to relate the compositional and structural characteristics of these catalysts to activity and selectivity in n-butane partial oxidation, and to activity for maleic anhydride combustion. In addition, the reaction mechanism for n-butane selective oxidation to maleic anhydride is to be probed by _in situ_ Fourier transform infrared spectroscopy.

## Explanation of Dissertation Format

This dissertation contains six sections, each of which is written in a form suitable for publication in a technical journal. References cited in the General Introduction are found at the end of the dissertation. The research presented in each section has been conducted by the author.

SECTION I.  V-P-O INDUSTRIAL CATALYSTS FOR n-BUTANE OXIDATION:
CHARACTERIZATION AND KINETIC MEASUREMENTS

ABSTRACT

Vanadium-phosphorus-oxygen (V-P-O) catalysts prepared in alcohol
solution with P-to-V ratios from 0.9 to 1.2 were characterized by X-ray
diffraction, infrared spectroscopy, laser Raman spectroscopy, scanning
electron microscopy, and X-ray photoelectron spectroscopy. A strong effect
of P-to-V synthesis ratio on catalyst structure, catalyst morphology,
vanadium oxidation state, and reactivity in n-butane selective oxidation to
maleic anhydride was observed. A slight "excess" of catalyst phosphorus
(P/V = 1.1 catalyst) was found to stabilize a $(VO)_2P_2O_7$ phase which was
active and selective in n-butane oxidation. A larger "excess" of phosphorus
was found to enhance selectivity of the $(VO)_2P_2O_7$ phase at the expense of
catalyst activity. Used V-P-O catalysts without "excess" phosphorus
contained the active but nonselective $\alpha$-$VOPO_4$ phase.

# INTRODUCTION

Vanadium-phosphorus mixed oxide catalysts are used industrially for the selective oxidation of $C_4$ hydrocarbons to maleic anhydride. The development of V-P-O catalysts which are capable of activating paraffin feedstocks is an important new development in this process.

Catalysts which are prepared in organic media often possess high surface areas and reduced vanadium(IV) phases which are active and selective in n-butane oxidation (1-3). The effects of reducing agent, solvent, activation conditions, and P-to-V ratio on phase structure and reactivity are poorly understood (4-5). This paper presents a systematic study of the effects of nominal (preparative) P-to-V ratio on phase composition, vanadium oxidation state, catalyst morphology, and catalyst reactivity for n-butane selective oxidation by V-P-O catalysts prepared in organic solution.

## EXPERIMENTAL METHODS

### Catalyst Preparation

Four vanadium-phosphorus oxide catalysts were prepared according to the preparation method reported by Katsumoto and Marquis (1). Phosphorus to vanadium (P-to-V) ratios of 0.9, 1.0, 1.1, and 1.2 were selected for the catalyst preparations. The precipitation equipment included a heated (1000 ml) three neck round bottom flask, a cooled reflux condenser, and a water trap. Thirty grams of $V_2O_5$ were suspended by rapid stirring in 60 ml of isobutyl alcohol and 40 ml of benzyl alcohol. The vanadium-oxide-alcohol mixture was refluxed for three hours at 120°C. During this period the solution changed in color from brown to black and approximately 2 ml of water was collected and removed. The apparently reduced vanadium suspension was cooled to 40°C prior to the addition of ortho-$H_3PO_4$. The suspension was again heated to 120°C and refluxed for an additional three hours. During this time a reduced vanadium phosphate (probably $V^{4+}$) was formed as indicated by a change in color from black to blue. The resulting catalyst was separated by filtration, dried for twelve hours at 125°C, and activated in air for three hours at 380°C.

### Characterization Techniques

#### Surface area measurements

Surface areas were measured using a Micromeretics 2100E Accusorb instrument with nitrogen as the adsorbate.

## X-ray diffraction

X-ray powder diffraction patterns were obtained with a Siemans D500 diffractometer using Cu $K_\alpha$ radiation. The samples were rotated in the X-ray beam.

## Fourier transform infrared spectroscopy

Transmission infrared spectra were recorded using a Nicolet 60-SX Fourier transform infrared spectrometer with single beam optics. Each spectrum represents the accumulation of 100 scans at 1 $cm^{-1}$ resolution.

## Laser Raman spectroscopy

Raman spectra was obtained in the backscattering mode using a Spex 1403 laser Raman spectrometer. The 514.3 nm line of a Spectra Physics argon ion laser operating at 200 mw output was the primary excitation source. A spectral resolution of 5 $cm^{-1}$ and a central slit setting of 60 μm were used. Spectral accumulation was provided by a Nicolet 1180E computer system. All spectra reported were obtained with 50 scans at scan drives of 3.125 $cm^{-1}$/s.

## Scanning electron microscopy

Scanning electron microscopy studies were conducted using a Joel Model JSM-U3 scanning electron microscope. Samples were prepared by depositing catalyst powder onto a thin film of carbon black on a graphite sample mount. A gold thickness of 300 $\overset{o}{A}$ was then sputtered onto the sample mount. Micrographs were obtained at a potential difference of 25 kV. A Tracor/Northern 2000 microanalyzer was used for the energy dispersive X-ray analysis.

## X-ray photoelectron spectroscopy

X-ray photoelectron spectra were obtained with an AEI 200B

spectrometer using Al $K_\alpha$ radiation. Signal averaging was performed using

a Nicolet 1180 computer system, all samples were referenced to the carbon

ls binding energy of 284.6 eV. Catalyst samples were sealed in evacuated

Pyrex tubes which were opened in a helium dry box attached directly to the

photoelectron spectrometer.

### Catalyst Activity Measurements

The selective oxidation of n-butane to maleic anhydride was performed

using a continuous flow, fixed bed reactor, and gas chromatograph

analytical system described previously (6). The reactor was packed with

2 g of catalyst homogeneously mixed with 40 g of SiC. Both the catalyst

and SiC particles were in the 2 mm size range. Reaction temperatures from

350°C to 450°C were investigated at a space velocity of 750 $hr^{-1}$. The

following reactor conditions were established for each experimental run:

oxygen partial pressure—0.22 atm; n-butane partial pressure—0.015 atm;

nitrogen partial pressure—0.765 atm; volumetric flow rate of n-butane—

540 $cm^3$ (STP)/h; total molar flow rate—1.61 g-mol/h.

For these studies the percent conversion is defined as

$$\frac{\text{moles of n-butane consumed}}{\text{moles of n-butane in feed}} \times 100\%$$

The selectivity to product A is defined as

$$\frac{\text{moles of A produced}}{\text{moles of n-butane consumed}} \times \frac{1}{\gamma} \times 100\%$$

where $\gamma$ is the ratio of the number of C atoms in the reactant to the number of C atoms in the product. Rates of n-butane disappearance, maleic anhydride formation, and $CO_2$ formation are based on the surface area of the used catalyst.

EXPERIMENTAL RESULTS

Characterization of Precipitated Catalysts

Surface area measurements

The BET surface area measurements for the precipitated and air-activated catalysts are presented in Table 1. In general, an increase in nominal P-to-V ratio was found to result in somewhat lower surface areas for the precipitated catalyst, and significantly higher surface areas for the air activated catalysts. Surface areas in excess of 60 $m^2$/g were observed for the activated P/V = 1.2 catalyst.

X-ray diffraction

The X-ray powder diffraction patterns of the precipitated catalysts having composition P/V = 0.9, 1.0, 1.1, and 1.2 are given in Figure 1[a], 1[b], 1[c], and 1[d], respectively. Each of the precipitated catalysts were found to possess the X-ray diffraction lines at 5.72, 4.53, 3.68, 3.29, 3.11, 2.94, 2.79, and 2.66 Å reported by Stefani and Fontana (7) and by Cavani et al. (2) for the B-phase precursor. Additional X-ray diffraction lines were observed at 2.40, 1.91, 1.85, and 1.76 Å. Johnson et al. (8) describes the precatalyst as a $VO(HPO_4) \cdot 0.5H_2O$ phase.

Following three hours of activation in air an extensive transformation of the $VO(HPO_4) \cdot 0.5H_2O$ phase was observed for the P/V = 0.9 catalyst; only small changes were observed in the XRD pattern of the P/V = 1.0, 1.1, and 1.2 catalysts. The air-activated P/V = 0.9 catalyst (Figure 2[a]) was
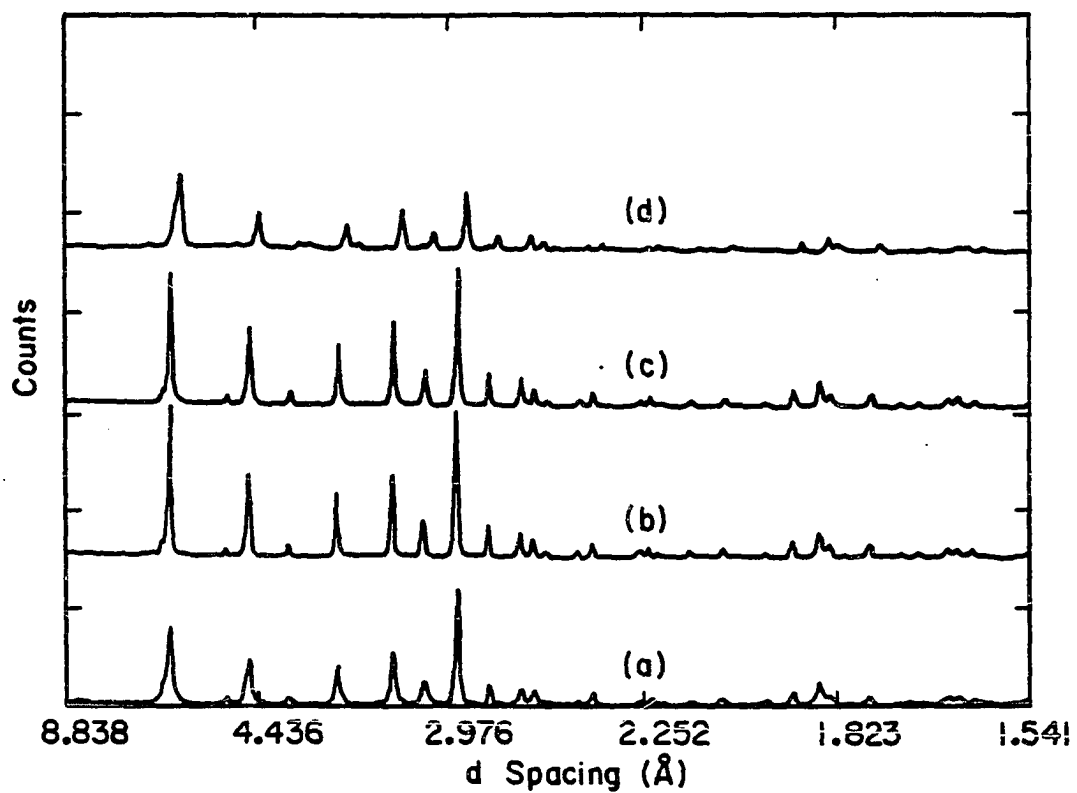
Figure 1.  X-ray diffraction patterns of precipitated catalysts:

        (a) P/V = 0.9
        (b) P/V = 1.0
        (c) P/V = 1.1
        (c) P/V = 1.2
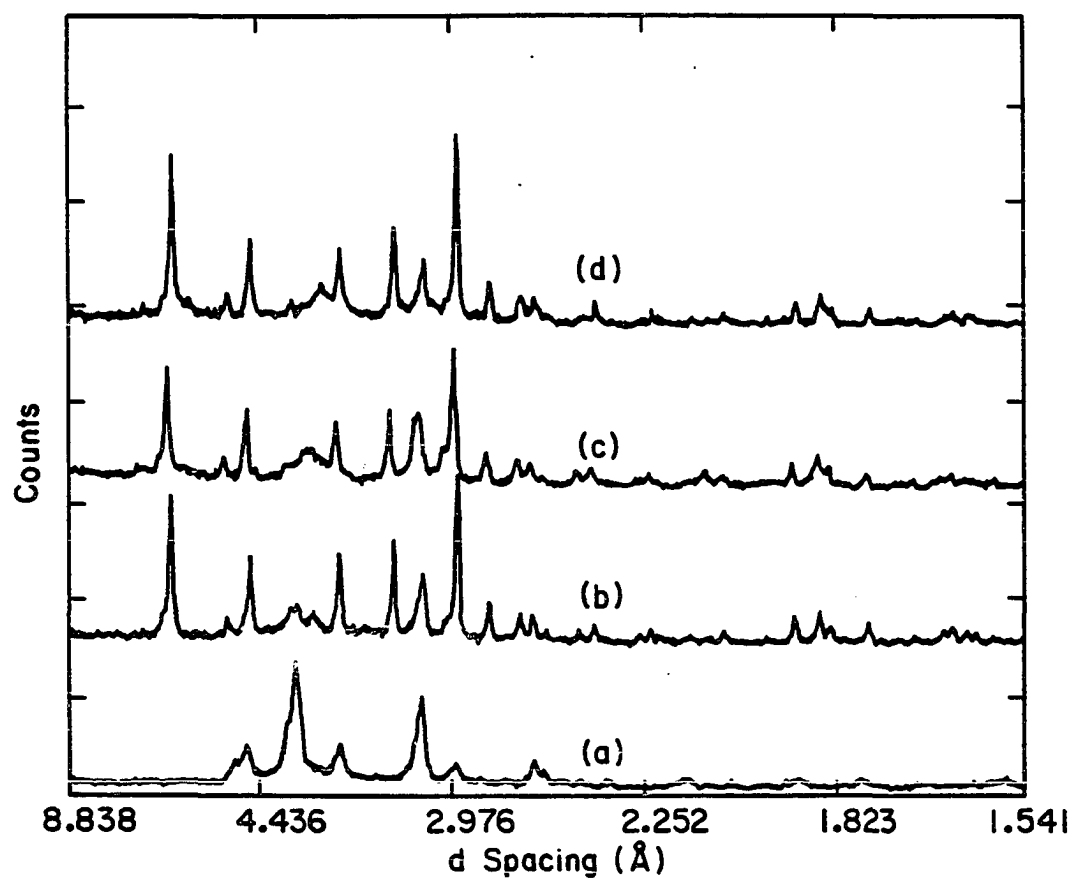
Figure 2. X-ray diffraction patterns of air-activated catalysts:

(a) P/V = 0.9
(b) P/V = 1.0
(c) P/V = 1.1
(d) P/V = 1.2

Table 1. Surface area of precipitated and air-activated catalysts

| P-to-V Ratio | 0.9 | 1.0 | 1.1 | 1.2 |
|---|---|---|---|---|
| Precipitated catalyst $(m^2/g)$ | 14.3 | 4.5 | 1.6 | 3.2 |
| Air-activated catalyst $(m^2/g)$ | 12.5 | 16.8 | 33.0 | 60.9 |

found to have principal XRD lines at 4.72, 4.57, 4.04, 3.67, 3.13, 2.96, and 2.61 Å. These lines are assigned to an oxidized form of the $VO(HPO_4) \cdot 0.5H_2O$ phase referred to as the B' phase (9). The activated P/V = 1.0, 1.1, and 1.2 catalysts (Figures 2[b], 2[c], and 2[d]) were found to have very weak lines at these positions as well as stronger $VO(HPO_4) \cdot 0.5H_2O$ diffraction lines. The P/V = 0.9 catalyst was completely oxidized to the B' phase, whereas the catalysts having greater phosphorus loadings exhibited only trace amounts of this oxidized $V^{5+}$ phase.

Laser Raman spectroscopy

Characterization of the air-calcined catalysts having P-to-V ratios of 0.9 and 1.0 was obtained by laser Raman spectroscopy (Figures 3[a] and 3[b], respectively). Other air-calcined and precipitated catalyst samples did not yield informative Raman spectra due to fluorescence. Raman bands were observed for the air-calcined P/V = 0.9 catalyst at 287, 305, 406, 486, 529, 702, and 994 $cm^{-1}$. These bands were assigned to semicrystalline $V_2O_5$ (10) present in a nearly amorphous B'phase. Very weak $V_2O_5$ bands
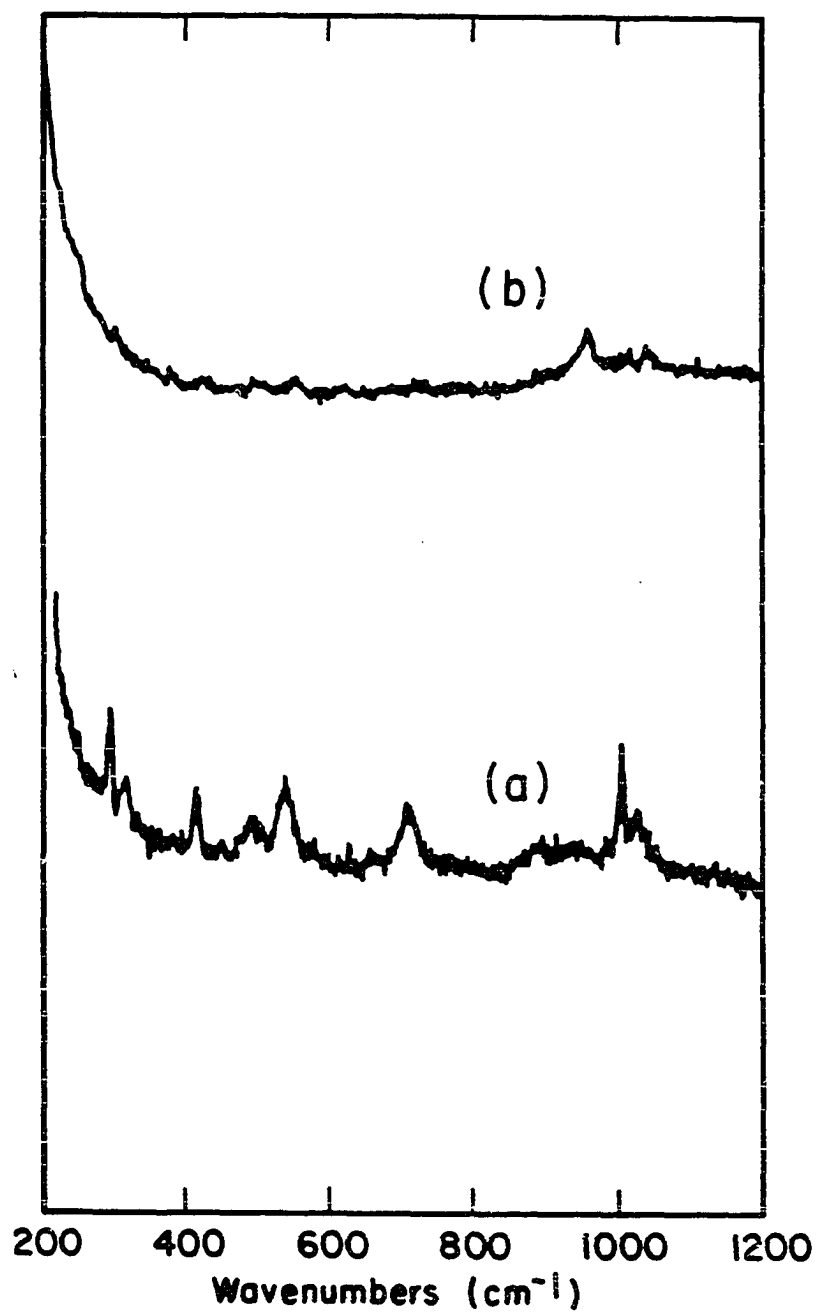
Figure 3. Raman spectra of air-activated catalysts having composition:

(a) P/V = 0.9
(b) P/V = 1.0

were also observed for the air-calcined P/V = 1.0 catalyst. In addition, a band at 922 $cm^{-1}$ was assigned to a P-O stretching vibration of a disordered $VO(HPO_4) \cdot 0.5H_2O$ phase.

## Infrared spectroscopy

Infrared spectroscopy was used to identify vibrational bands for the precipitated catalysts having P-to-V ratios from 0.9 to 1.2 (Figures 4[a]-4[d]). Each precatalyst possessed infrared bands at 416, 485, 529, 547, 645, 686, 929, 975, 1048, 1102, 1133, and 1198 $cm^{-1}$. Catalysts prepared with "excess" phosphorus (P/V = 1.1 and P/V = 1.2) displayed additional infrared bands at 735 and 696 $cm^{-1}$.

Infrared bands at 416, 485, 529, 547, and 645 $cm^{-1}$ were assigned to P-O bending vibrations; the bands at 696 and 735 $cm^{-1}$ were assigned to P-O stretching vibrations for catalysts incorporating excess phosphorus. The 686 $cm^{-1}$ band was assigned to $H_2O$ bending vibrations while the 929 $cm^{-1}$ infrared band was associated with a P-(OH) stretch of the $VO(HPO_4) \cdot 0.5H_2O$ phase (11). An intense band at 975 $cm^{-1}$ was assigned to a V=O stretching vibration by analogy to the 1018 $cm^{-1}$ $\nu_{V=O}$ observed for $V_2O_5$ (10). A symmetric $PO_3$ stretching vibration was assigned to the 1048 $cm^{-1}$ band. Asymmetric $PO_3$ stretching vibrations were observed at 1102, 1133, and 1198 $cm^{-1}$. These assignments are consistent with those reported for the $P_2O_7^{-4}$ ion (12) and are made in analogy to model compound assignments (13, 14).

Infrared spectroscopy was also used to characterize the air-calcined catalysts having P-to-V ratios from 0.9 to 1.2. The P/V = 0.9 (Figure 5[a]) catalyst was found to undergo a phase transformation during air activation. Infrared bands were observed at 423, 601, 642, 932, 993, 1020,
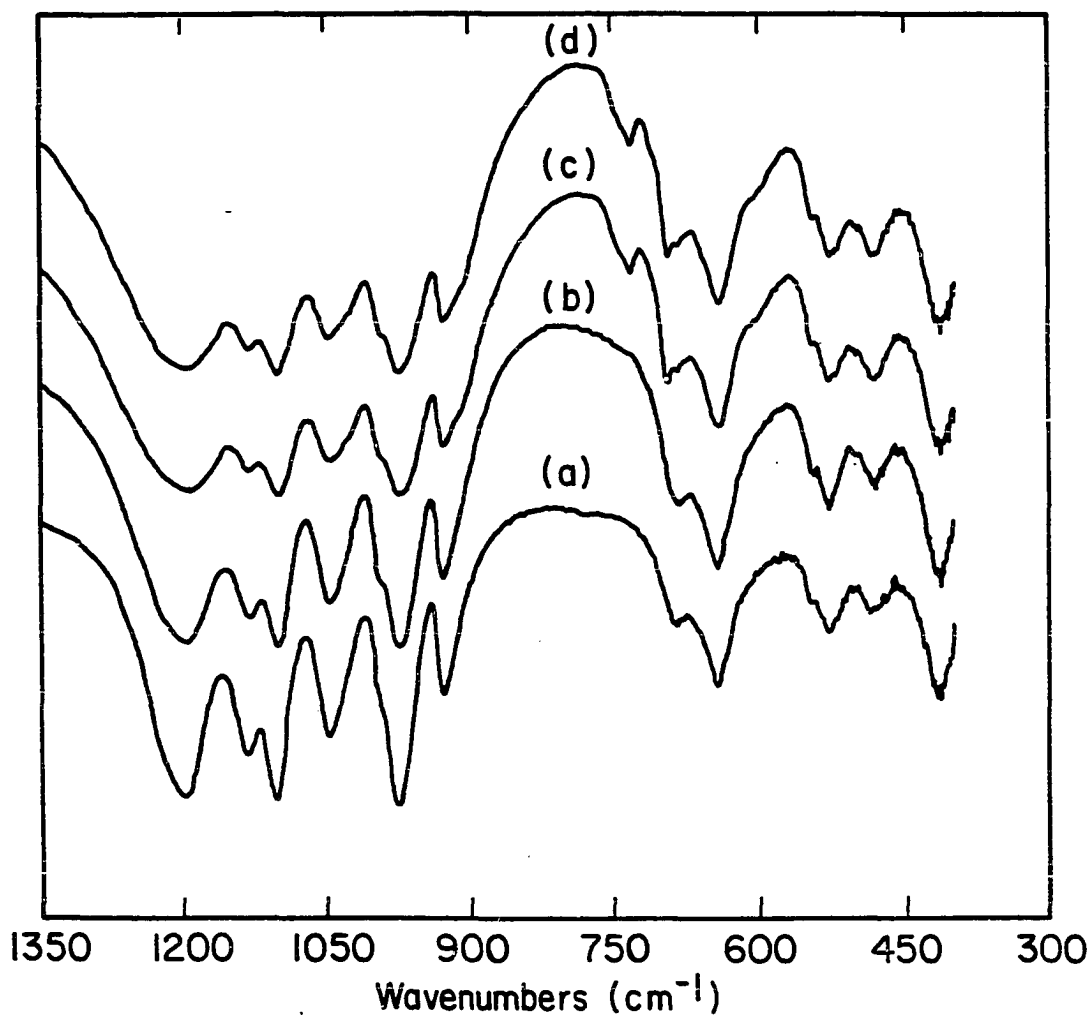
Figure 4. Infrared spectra of precipitated catalysts having composition:

(a) P/V = 0.9
(b) P/V = 1.0
(c) P/V = 1.1
(d) P/V = 1.2
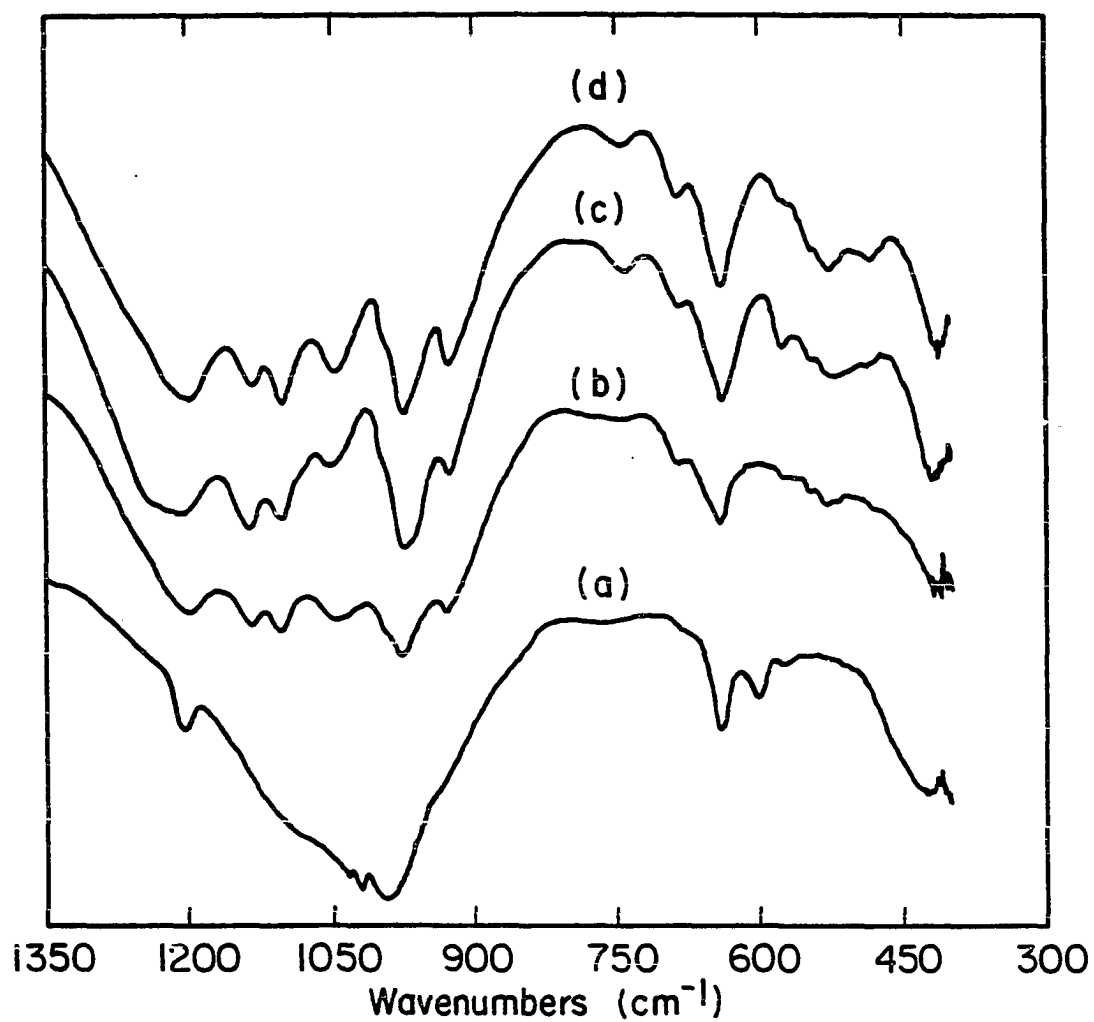
Figure 5.  Infrared spectra of air-activated catalysts having composition:

(a) P/V = 0.9
(b) P/V = 1.0
(c) P/V = 1.1
(d) P/V = 1.2

1033, and 1205 $cm^{-1}$. Coupled V-O and P-O bending vibrations were assigned to the 423 $cm^{-1}$ band. Infrared bands at 601 and 642 $cm^{-1}$ were attributed to P-O bending vibrations of the B' phase identified by X-ray diffraction. The intense band at 975 $cm^{-1}$ was assigned to a V=O stretching vibration (10). A symmetric P-O stretching vibration was assigned to the 932 $cm^{-1}$ band; asymmetric P-O stretching vibrations were assigned to infrared bands at 1020, 1033, and 1205 $cm^{-1}$. These assignments are in agreement with those reported in the literature for oxidized V-P-O phases (12, 13, 14).

Only subtle changes were observed in the infrared spectra of the P/V = 1.0, 1.1, and 1.2 catalysts following air activation (Figure 5[b]), 5[c] and 5[d], respectively). An additional P-O bending vibration was observed at 578 $cm^{-1}$. The P-O stretching band observed for precatalysts with "excess" phosphorus at 696 $cm^{-1}$ was no longer apparent. The P-O bending vibrations at 485, 529, and 547 $cm^{-1}$ were observed to broaden and to decrease in intensity. No changes were observed in the remaining infrared bands. These subtle changes in structure which occur upon activation in air seem to indicate mild restructuring and possible distortion of the $P_2O_7^{-4}$ ion during calcination.

## Scanning electron microscopy

Scanning electron micrographs of the precipitated and air-calcined catalysts were obtained for catalysts having P-to-V ratios of 0.9 to 1.2. The $VO(HPO_4) \cdot 0.5H_2O$ precatalyst was found to consist of 3 x 5 x 0.5 μm hexagonal platelets. Johnson et al. (8) has described these catalysts as lamellar platelets whose crystallographic orientation changes upon activation. Representative micrographs of the precipitated and air-activated

catalysts are given in Figure 6. X-ray energy dispersive spectroscopy
(Figure 7) established that vanadium and phosphorus were well dispersed
in a homogeneous mixed oxide catalyst.

## X-ray photoelectron spectroscopy

X-ray photoelectron spectra of the precipitated and air-calcined
catalysts are shown in Figures 8 and 9; Table 2 provides the observed
binding energies. Each of the precipitated catalysts (Figures 8[a]-8[d])
were characterized by a band at 517.0-517.2 which was assigned to the
$2p_{3/2}$ binding energy of vanadium (IV) (16). Multiple oxygen oxidation
states are indicated by one or more shoulder bands in the oxygen 1s
photoelectron spectrum of the precipitated catalysts. The XPS spectra for
the air-calcined catalysts (Figures 9[a]-9[d]) yielded V $2p_{3/2}$ binding
energies of 517.9, 517.6, 517.4, and 517.3 eV for the P/V = 0.9, 1.0, 1.1,
and 1.2 catalysts. These results indicate that the surfaces of the
catalysts are oxidized during air activation—especially for the catalysts
not having "excess" phosphorus.

## Kinetic Measurements for n-Butane Oxidation

## Conversion and selectivity of V-P-O catalysts

Reactivity measurements were obtained at 350-450°C for vanadium-
phosphorus-oxygen catalysts having P/V ratios of 0.9, 1.0, 1.1, and 1.2.
The percent selectivity for maleic anhydride and percent n-butane conver-
sion are displayed in Figures 10 and 11, respectively. Since only maleic
anhydride and carbon dioxide reaction products were observed, the
selectivity for carbon dioxide has not been shown ($S_{MA} + S_{CO_2}$ = 100%).

Figure 6a.   Scanning electron micrograph of precipitated P/V = 0.9
             catalyst

4μ
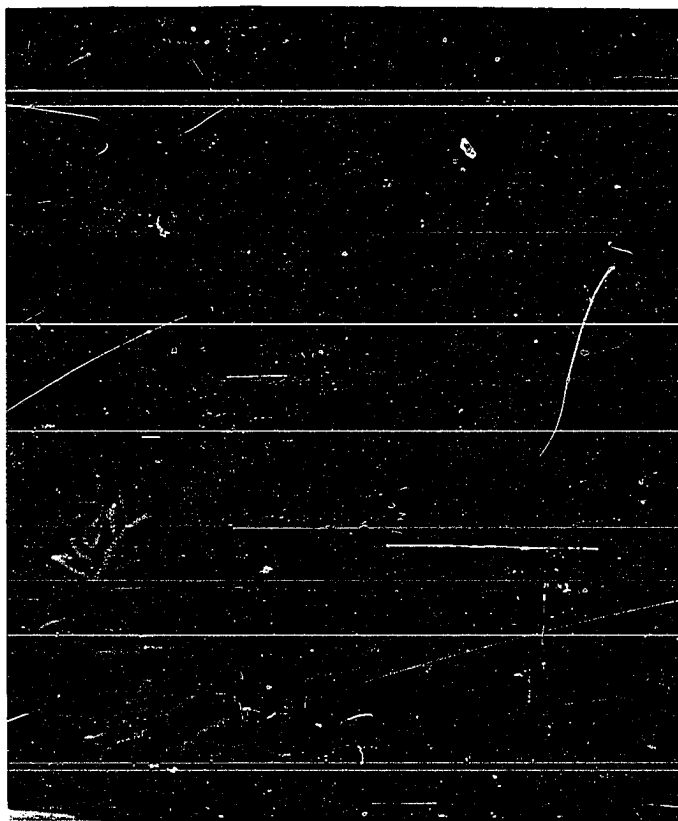
Figure 6b. Scanning electron micrograph of air-activated P/V = 1.0
catalyst
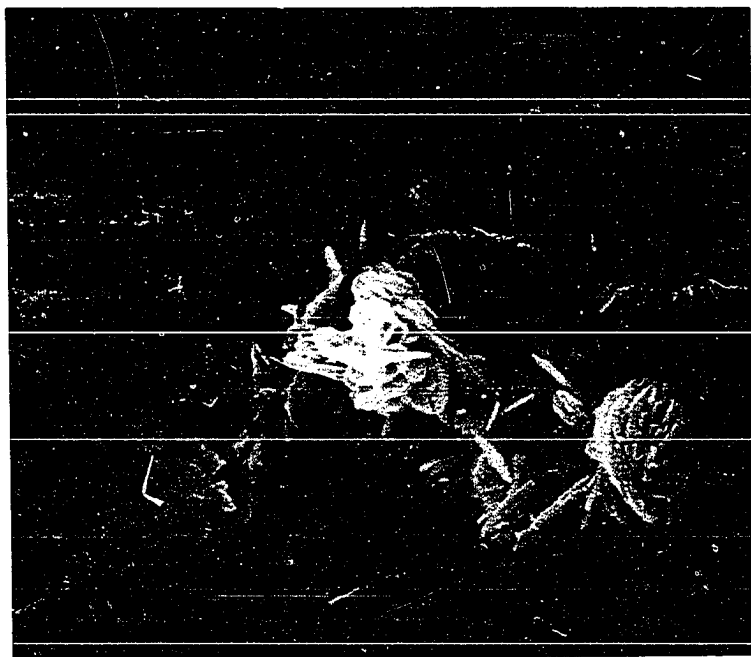
6μ

Figure 6c.  Scanning electron micrograph of air-activated P/V = 1.0
            catalyst

2μ
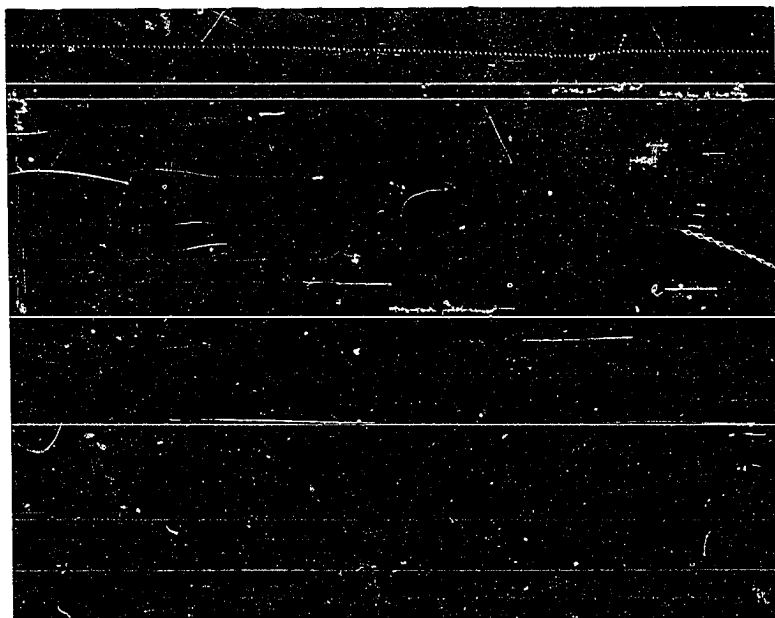
Figure 6d. Scanning electron micrograph of air-activated P/V = 1.2
catalyst
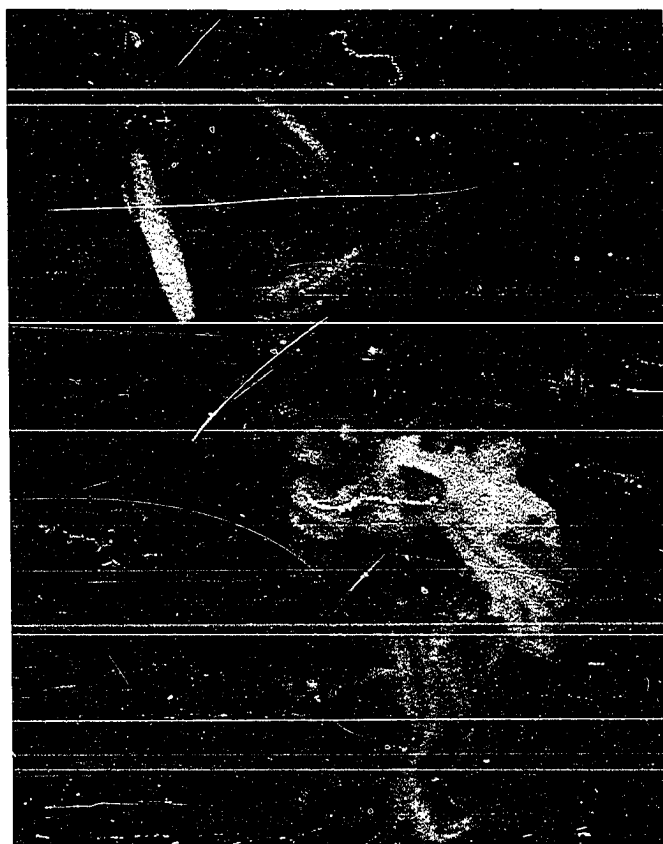
3μ

Figure 7.  X-ray energy dispersive spectrum of air-activated P/V = 0.9 catalyst:

      (a) elemental map for phosphorus
      (b) scanning electron micrograph of catalyst particle
      (c) elemental map for vanadium

5μ

(a)

5μ

(b)

5μ
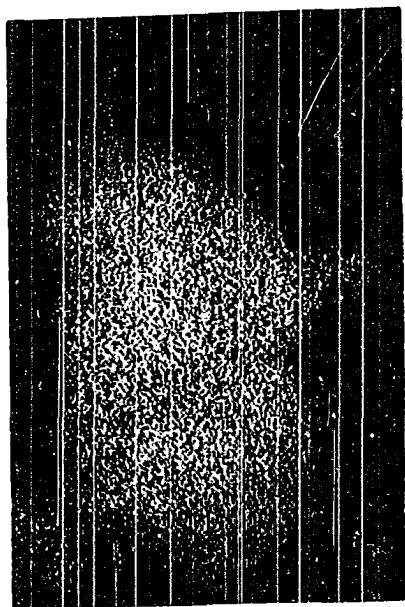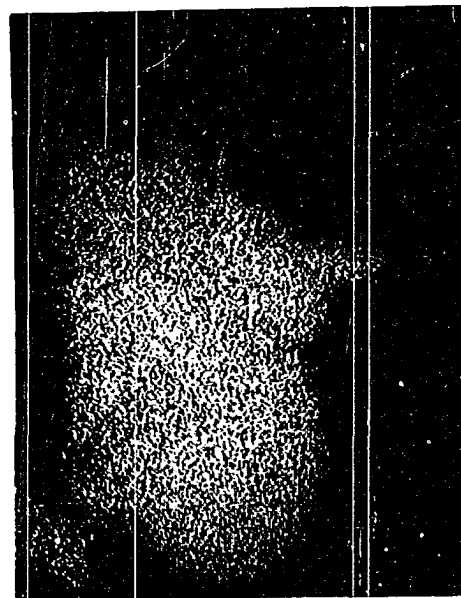
(c)
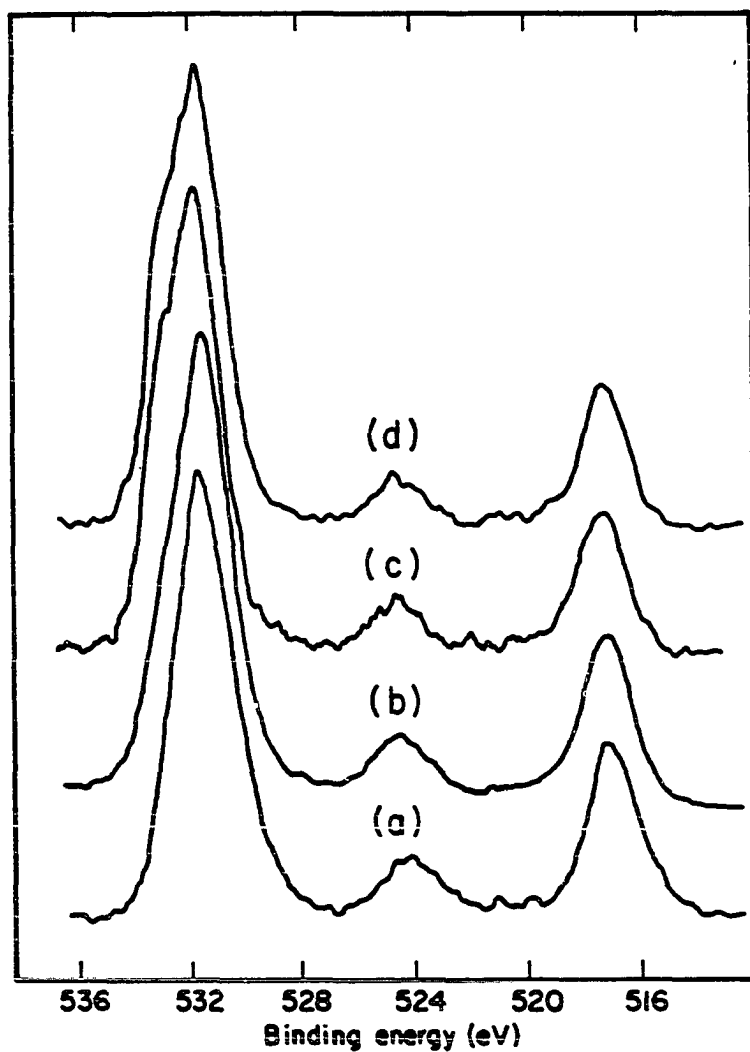
Figure 8. X-ray photoelectron spectra of precipitated V-P-O catalysts:

(a) P/V = 0.9
(b) P/V = 1.0
(c) P/V = 1.1
(d) P/V = 1.2
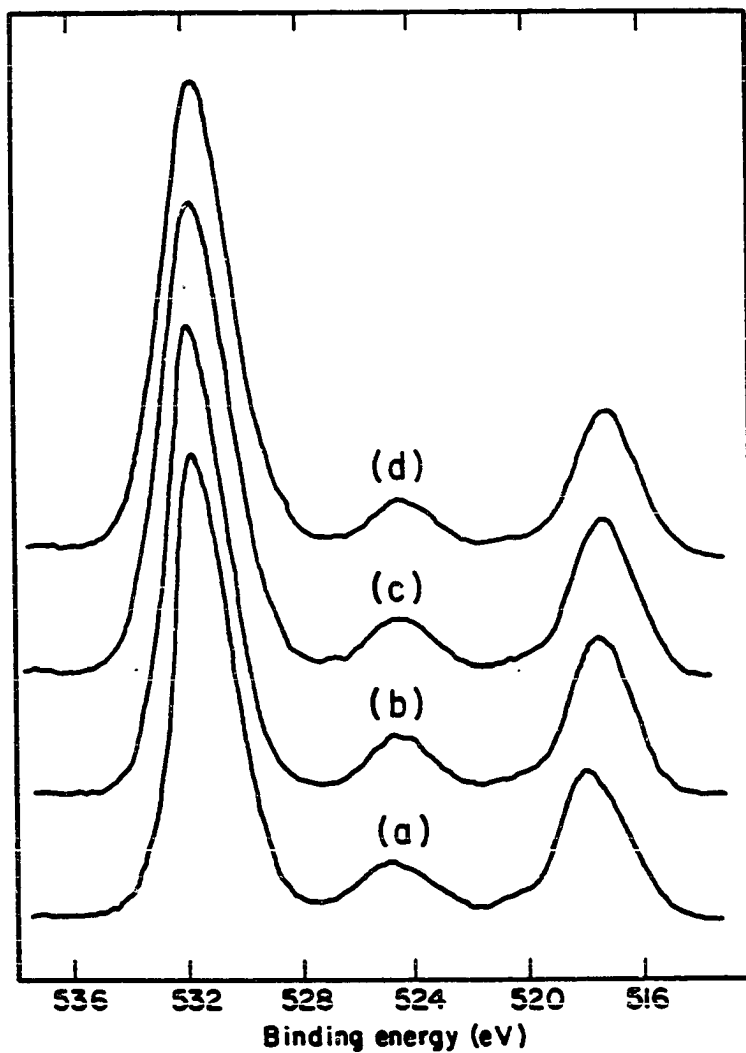
Figure 9. X-ray photoelectron spectra of air-activated V-P-O catalysts:

(a) P/V = 0.9
(b) P/V = 1.0
(c) P/V = 1.1
(d) P/V = 1.2
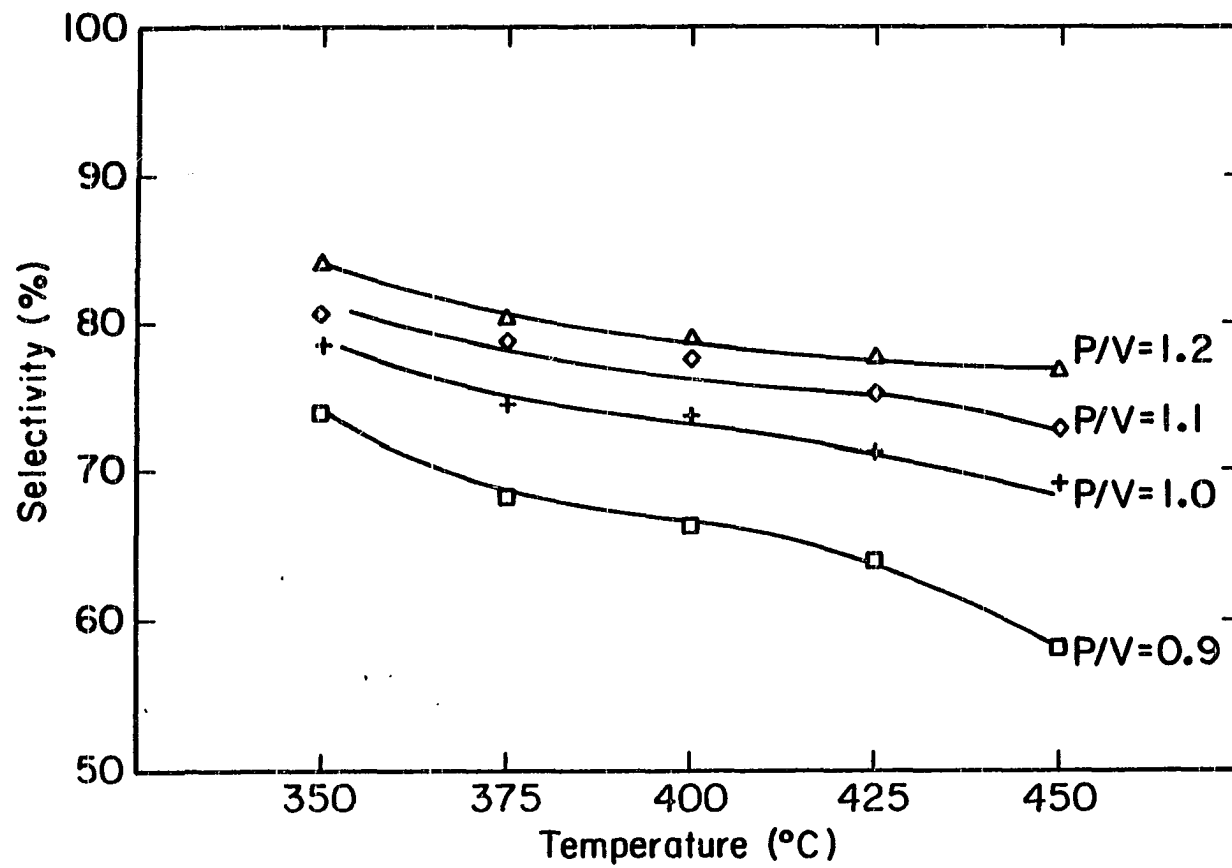
Figure 10. V-P-O catalyst selectivity for maleic anhydride as a function of catalyst P-to-V ratio and reaction temperature
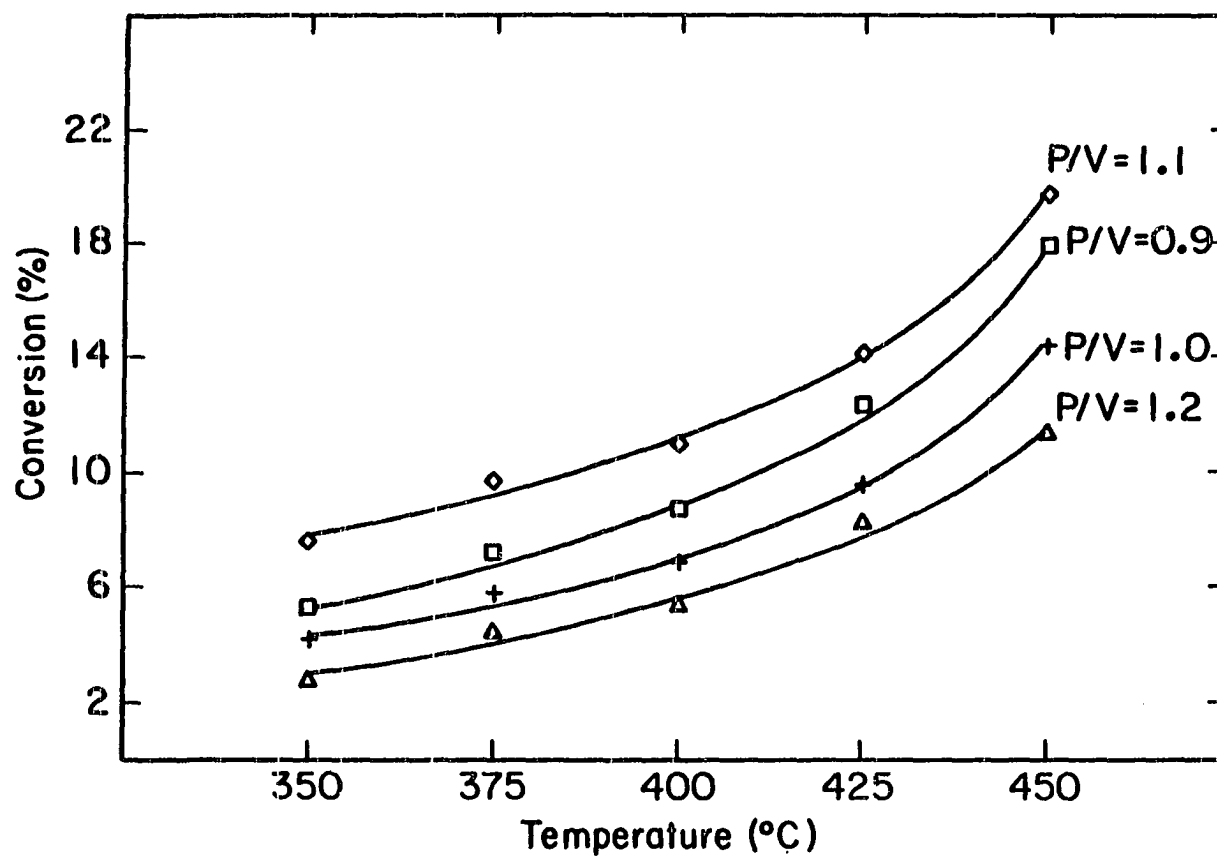
Figure 11. n-Butane conversion as a function of catalyst P-to-V ratio and reaction temperature

Table 2.  V $2p_{3/2}$ photoelectron spectra binding energies for precipitated
and air-activated catalysts

| P-to-V Ratio | 0.9 | 1.0 | 1.1 | 1.2 |
|---|---|---|---|---|
| Precipitated catalyst (eV) | 517.0 | 517.0 | 517.2 | 517.2 |
| Air-activated catalyst (eV) | 517.9 | 517.6 | 517.4 | 517.3 |

The selectivity for maleic anhydride was found to decrease with an
increase in reaction temperature and to increase with catalyst phosphorus
loading.  Consequently, the selectivity for carbon dioxide formation was
found to increase with increasing reaction temperatures and to decrease
with additional catalyst phosphorus content.  In general the n-butane
conversion was found to decrease with catalyst P-to-V ratio; however
the P/V = 1.1 catalyst displayed an unusually high conversion of n-butane.

Product yields

Maleic anhydride and carbon dioxide yields were obtained as a
function of reaction temperature and catalyst phosphorus loading (Table 3).
The highest yields of maleic anhydride were obtained with the catalyst
having a P-to-V ratio of 1.1.  Catalysts having P-to-V ratios of 0.9 and
1.0 displayed intermediate maleic anhydride yields, whereas the catalyst
having a P-to-V ratio of 1.2 demonstrated a relatively low yield of maleic
anhydride.  The highest $CO_2$ yields were observed with the catalyst having
a P-to-V ratio of 0.9.  Catalysts having P-to-V ratios of 1.0 and 1.1

Table 3. Product yields as a function of catalyst P-to-V ratio and reaction temperature

| P-to-V | Maleic anhydride yield (%) | | | | Carbon dioxide yield (%) | | | |
|---|---|---|---|---|---|---|---|---|
| | 0.9 | 1.0 | 1.1 | 1.2 | 0.9 | 1.0 | 1.1 | 1.2 |
| 350°C | 3.4 | 3.0 | 5.4 | 2.1 | 1.2 | 0.8 | 1.3 | 0.4 |
| 375°C | 4.2 | 3.7 | 6.6 | 3.1 | 2.0 | 1.2 | 1.8 | 0.8 |
| 400°C | 5.0 | 4.5 | 7.1 | 3.7 | 2.4 | 1.6 | 2.0 | 1.0 |
| 425°C | 6.6 | 6.0 | 8.7 | 5.4 | 3.7 | 2.3 | 2.9 | 1.6 |
| 450°C | 8.7 | 8.1 | 12.0 | 7.1 | 6.0 | 3.6 | 4.3 | 2.1 |

displayed intermediate $CO_2$ yields; very low $CO_2$ yields were observed for the P/V = 1.2 catalyst.

## Specific rates of oxidation

Catalyst phosphorus loading was observed to affect catalyst activity, selectivity, and surface area. In order to isolate these effects, rates of n-butane disappearance, maleic anhydride formation, and carbon dioxide formation were normalized to catalyst surface area (see Figures 12-14). Each of these specific rates were observed to decrease with an increase in catalyst P-to-V ratio. As a result, an increase in catalyst phosphorus content was found to decrease the specific activity of both selective and nonselective oxidation reactions. Furthermore, since "excess" phosphorus more strongly depressed the specific rate of carbon oxide formation, catalyst selectivity was favored by increased P-to-V ratios.

## Characterization of Used Catalysts

Following n-butane selective oxidation, the used V-P-O catalysts were cooled to room temperature in the presence of feed gas mixtures. Thus the used catalysts were not exposed to air until room temperature was reached. No significant changes in catalyst surface area were observed following reaction.

## X-ray diffraction

The X-ray powder diffraction patterns of the used catalysts having composition P/V = 0.9, 1.0, 1.1, and 1.2 are shown in Figure 15. The used P/V = 0.9 (Figure 15[a]) catalyst was found to have broad XRD lines at
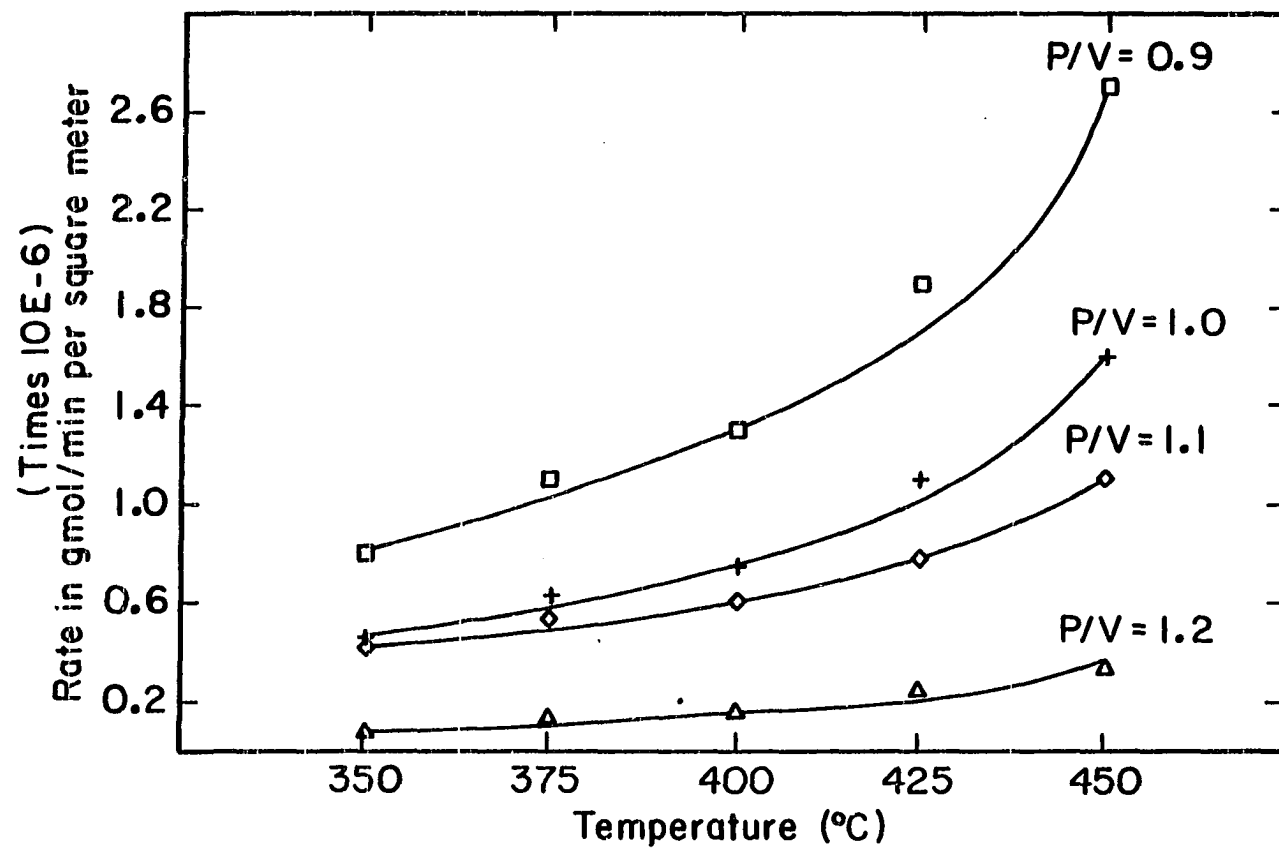
Figure 12. Specific rate of n-butane disappearance as a function of catalyst P-to-V ratio and reaction temperature
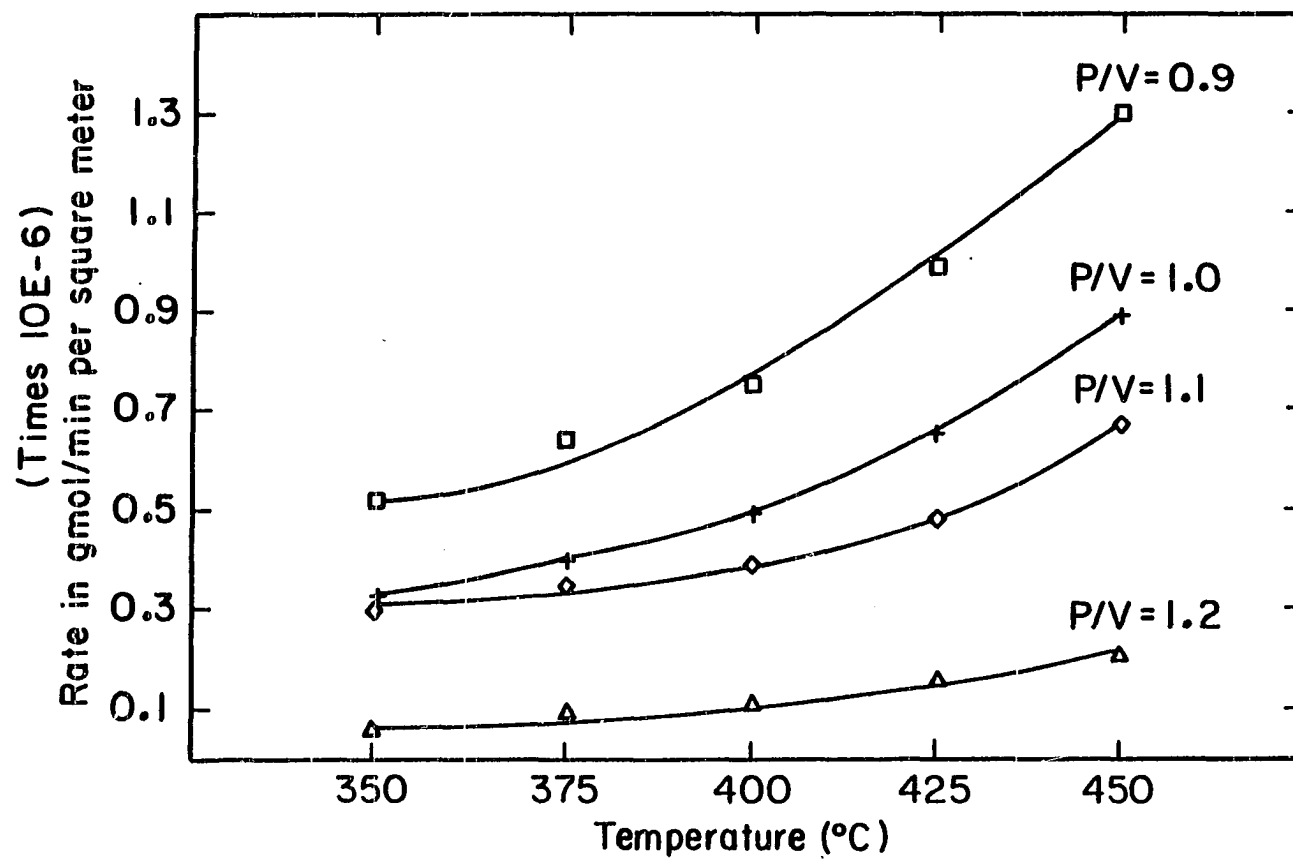
Figure 13. Specific rates of maleic anhydride formation as a function of catalyst P-to-V ratio and reaction temperature
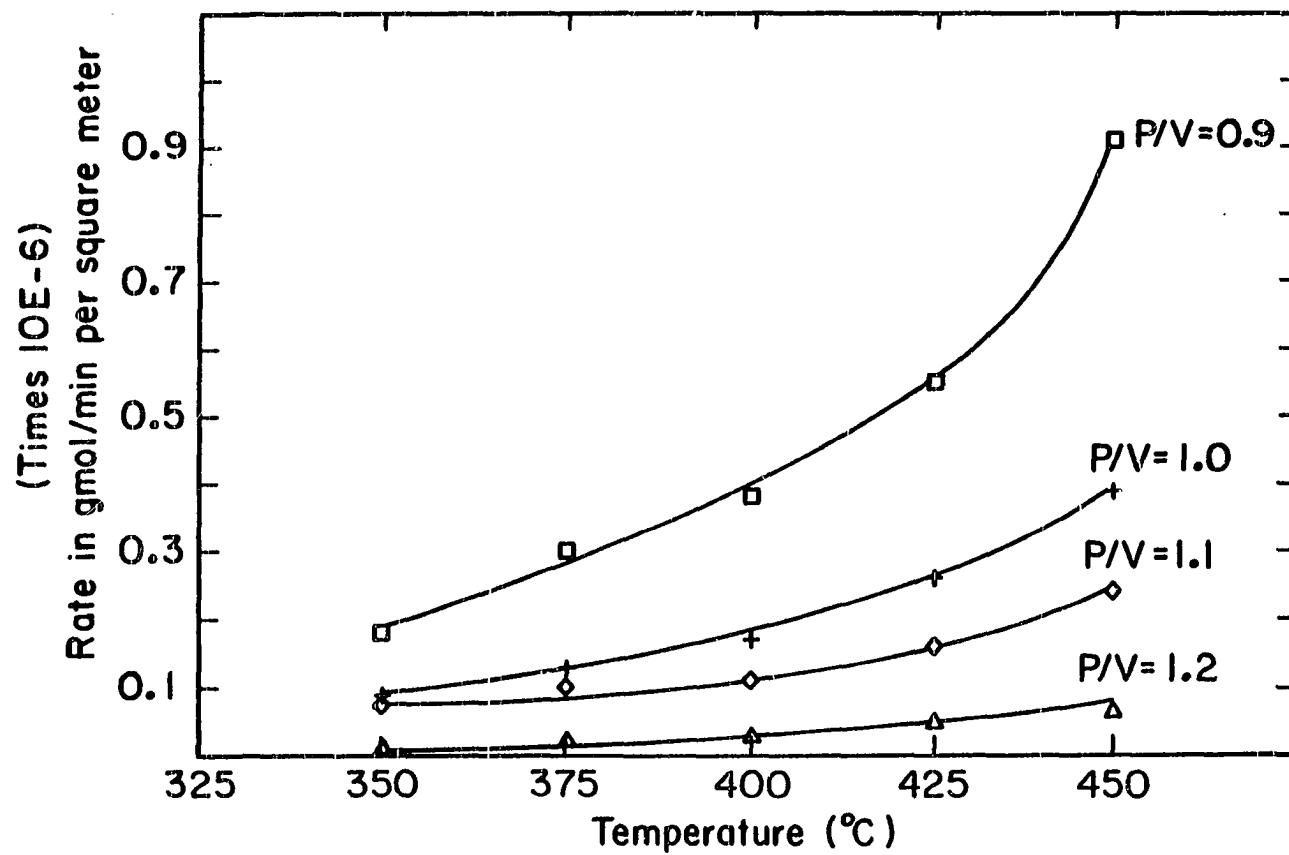
Figure 14. Specific rates of carbon dioxide formation as a function of catalyst P-to-V ratio and reaction temperature
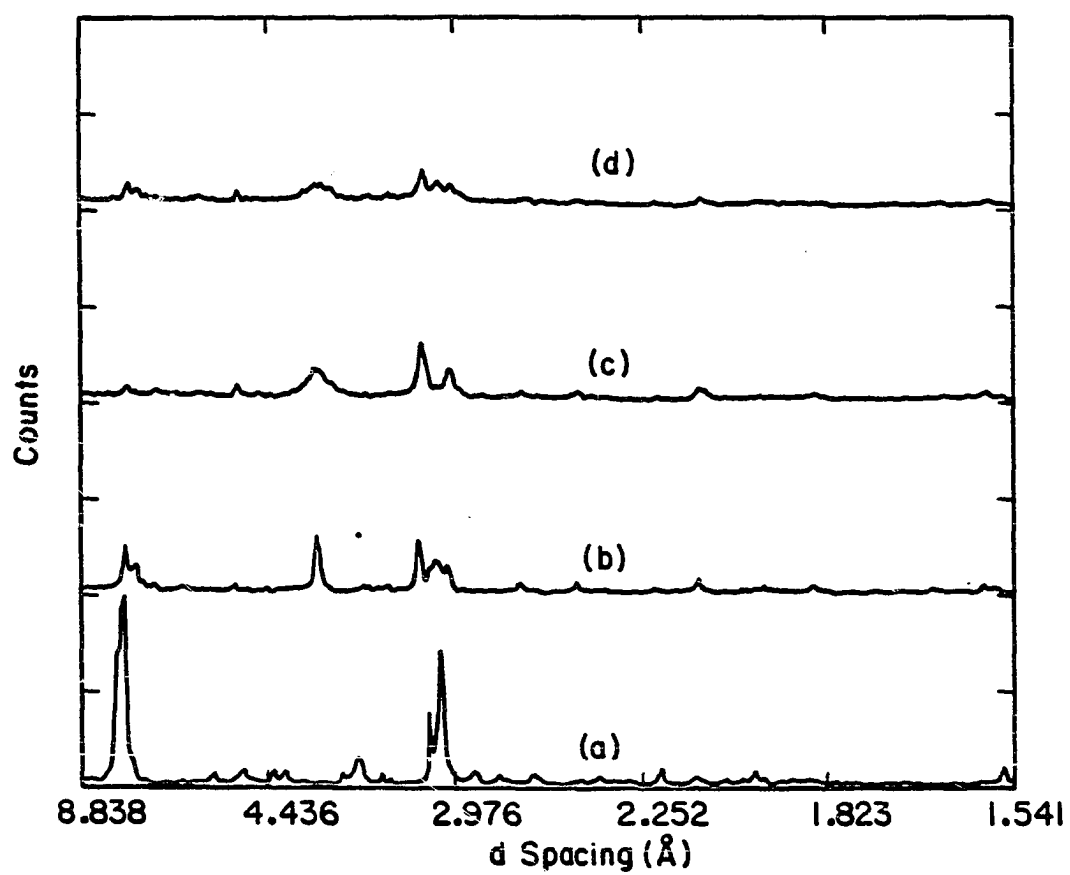
Figure 15.   X-ray diffraction patterns of used catalysts:

        (a) P/V = 0.9
        (b) P/V = 1.0
        (c) P/V = 1.1
        (d) P/V = 1.2

7.2, 6.8, 3.58, 3.10, and 3.04 $\overset{o}{A}$. Diffraction lines at these positions correspond to mixtures of $V^{5+}$ phases. Gopal and Calvo (17) assign lines at 3.57, 3.07, and 3.01 to $\alpha$-VOPO$_4$; diffraction lines at 3.10, 3.00, and 1.96 $\overset{o}{A}$ correspond to $\alpha'$-VOPO$_4$; broad diffraction lines near 7.2 $\overset{o}{A}$ are indicative of a VPO$_5\cdot$2H$_2$O phase (18).

The used P/V = 1.0 catalyst (Figure 15[b]) was found to have XRD lines at 7.2, 6.8, 3.90, 3.15, 3.06, and 3.00 $\overset{o}{A}$. The vanadium(IV) phase(s) described earlier are indicated by diffraction lines at 7.2, 6.8, and 3.06 $\overset{o}{A}$. The broad lines at 3.90, 3.15, and 3.00 $\overset{o}{A}$ indicate the presence of a patented B-phase catalyst (4) which seems to closely resemble the (VO)$_2$P$_2$O$_7$ phase (5). Progressively broader XRD lines at 3.90, 3.15, and 3.00 $\overset{o}{A}$ indicated smaller B-phase crystallites were formed for used catalysts which incorporate "excess" phosphorus (Figures 15 [c] and 15[d]).

## Laser Raman spectroscopy

Characterization of used catalysts having P-to-V ratios of 0.9 to 1.2 was obtained by laser Raman spectroscopy (Figure 16). Unreacted V$_2$O$_5$ was observed in the P/V = 0.9 catalyst (Figure 16[a]) as indicated by vibrational bands at 287, 305, 406, 486, 529, 702, and 994 cm$^{-1}$ (10). The presence of a second possibly amorphous phase was indicated by broad Raman bands at 567, 872, 1014, and 1127 cm$^{-1}$. Raman bands at these frequencies cannot be assigned to V-O and P-O stretching vibrations of any previously observed V-P-O phase (12, 13, 14).

Raman bands were observed for the used P/V = 1.0 catalyst (Figure 16[b]) at 435, 892, 922, 934, 993, and 1018 cm$^{-1}$. The strong 922 and 934 cm$^{-1}$ bands were assigned to P-O stretching vibrations of the (VO)$_2$P$_2$O$_7$
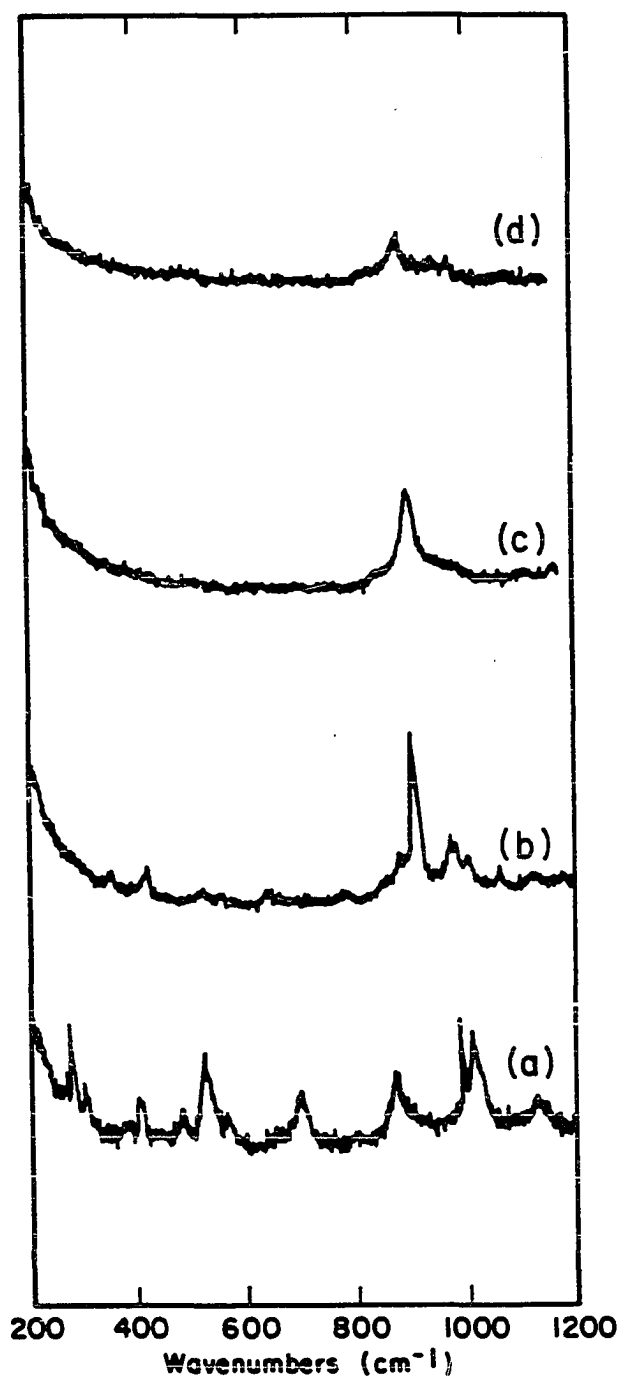
Figure 16. Raman spectra of used catalysts having composition:

(a) P/V = 0.9
(b) P/V = 1.0
(c) P/V = 1.1
(d) P/V = 1.2

phase (15). The very weak Raman bands at 435, 892, 993, and 1018 $cm^{-1}$ indicate P-O vibrations of an unidentified amorphous phase.

The used P/V = 1.1 and 1.2 catalysts (Figure 16[c] and 16[d]) were also found to exhibit very broad Raman bands near 922 $cm^{-1}$ which are characteristic of the $(VO)_2P_2O_7$ phase. The progressive broadening of these P-O stretching bands with increased P-to-V ratio indicates a distortion of the $P_2O_7^{-4}$ crystal environment by "excess" catalyst phosphorus.

## Infrared spectroscopy

Fourier transform infrared spectroscopy was employed to characterize the used V-P-O catalysts (Figure 17). The used P/V = 0.9 catalyst (Figure 17[a]) was found to have infrared bands at 565, 679, 749, 956, 990, 1040, 1088, and 1171 $cm^{-1}$. These vibrational bands are assigned to vibrations of the $PO_4^{-3}$ group and to a 990 $cm^{-1}$ V=O stretching vibration. The infrared spectrum of the used P/V = 0.9 catalyst is assigned to the $\alpha$-$VOPO_4$ phase (3, 19).

The used catalysts having composition P/V = 1.0, 1.1, and 1.2 were found to have broad infrared bands at 510, 576, 635, 743, 967, 1078, 1137, 1249, and 1268 $cm^{-1}$ (Figures 17[b], 17[c], and 17[d]). The infrared spectrum of these catalysts is in agreement for $(VO)_2P_2O_7$ and mixtures of $(VO)_2P_2O_7$ with B-phase (3).

## Scanning electron microscopy

Scanning electron micrographs of the used V-P-O catalysts having P-to-V ratios of 0.9, 1.0, 1.1, and 1.2 are shown in Figure 18. A strong
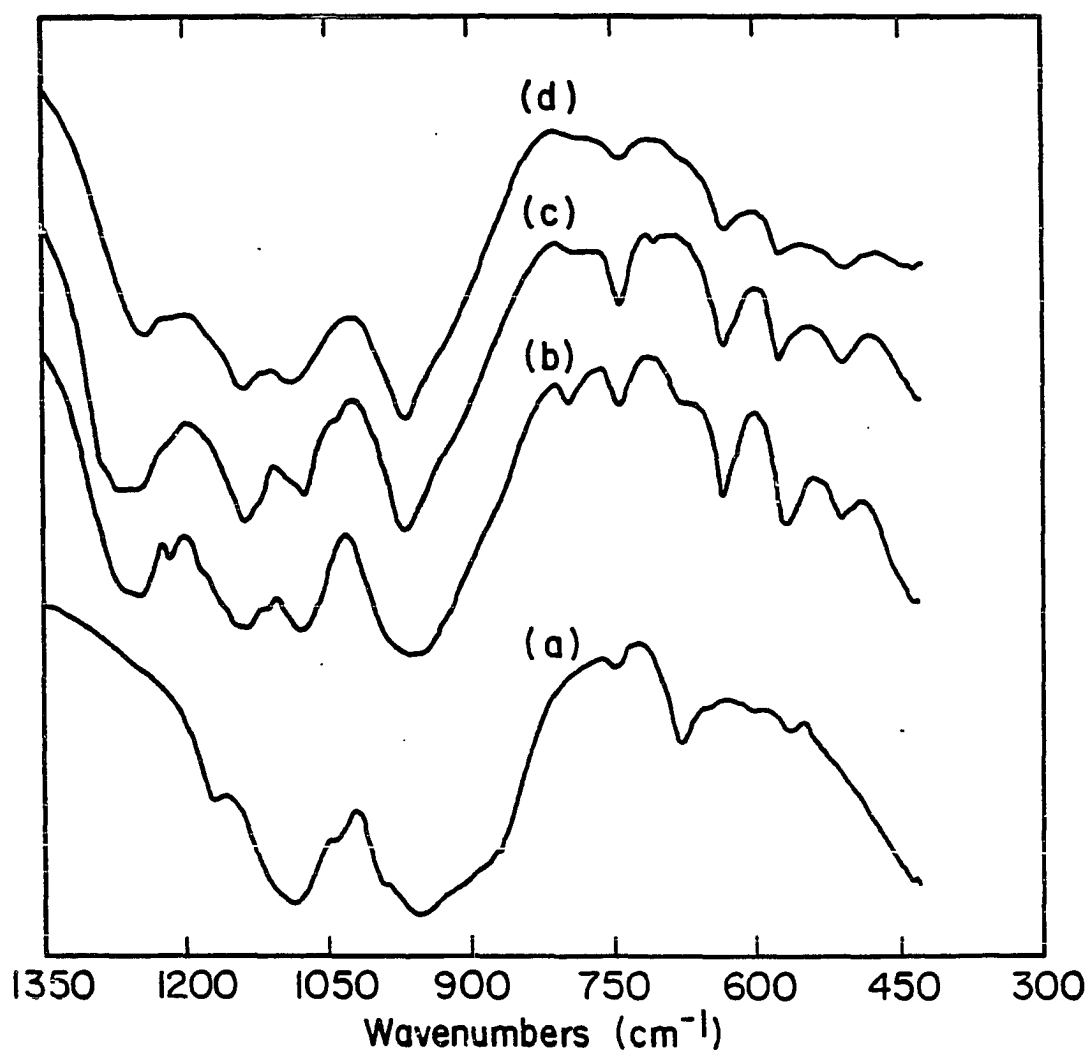
Figure 17. Infrared spectra of used catalysts having composition:

        (a) P/V = 0.9
        (b) P/V = 1.0
        (c) P/V = 1.1
        (d) P/V = 1.2

Figure 18. Scanning electron micrographs of used catalysts having composition:

(a) P/V = 0.9
(b) P/V = 1.0
(c) P/V = 1.1
(d) P/V = 1.2

(d) ⊢ 5μ

(c) ⊢ 5μ

(b) ⊢ 5μ

(a) ⊢ 5μ
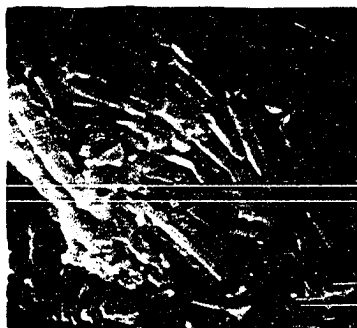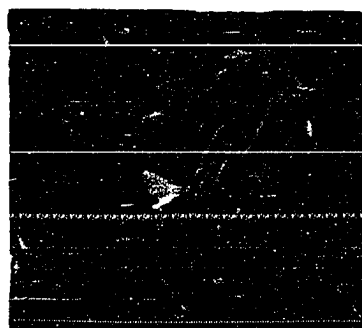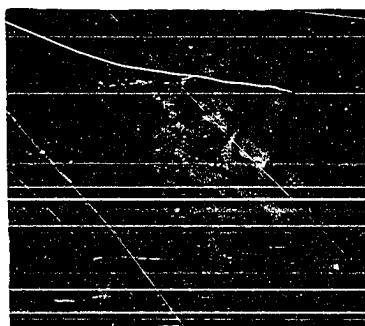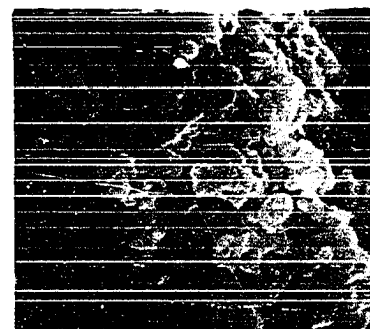
effect of nominal P-to-V ratio on catalyst morphology is observed. The

used P/V = 0.9 catalyst (Figure 18[a]) was found to consist of irregular

platelets while the used P/V = 1.2 (Figure 18[d]) catalyst displayed a

block style morphology. The used P/V = 1.0 and 1.1 catalysts (Figures

18[b] and 18[c]) were found to display a transition from platelet to

block morphology.

X-ray photoelectron spectroscopy

X-ray photoelectron spectra of the used V-P-O catalysts are shown in

Figure 19. The used catalysts were characterized by V $2p_{3/2}$ binding

energies of 517.6, 517.5, 517.4, and 517.3 eV for the P/V = 0.9, 1.0, 1.1,

and 1.2 catalysts, respectively. A decrease in binding energy from 517.9

to 517.6 for the P/V = 0.9 catalyst (Figure 19[a]), and from 517.6 to

517.5 for the P/V = 1.0 catalyst (Figure 19[b]) suggests a partial reduc-

tion of the surface occurred during hydrocarbon-air flow. No change in

V $2p_{3/2}$ binding energy was observed for the used catalysts with "excess"

phosphorus having composition P/V = 1.1 and 1.2 (Figures 19[c] and 19[d]).
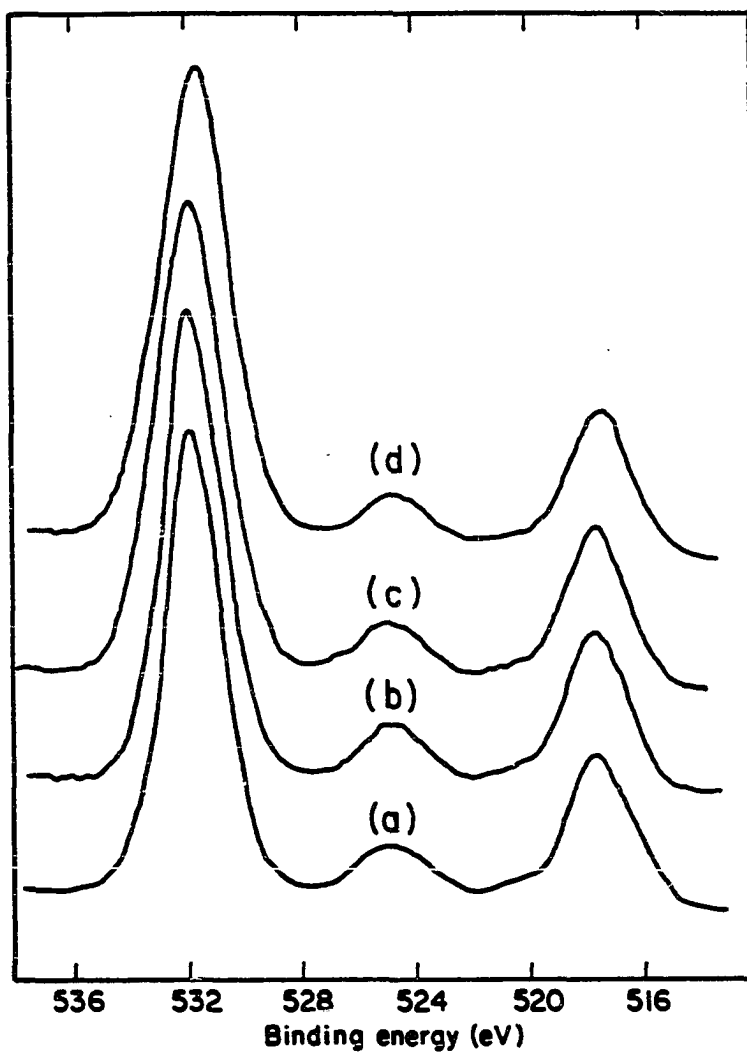
Figure 19. X-ray photoelectron spectra of used V-P-O catalysts:

(a) P/V = 0.9
(b) P/V = 1.0
(c) P/V = 1.1
(d) P/V = 1.2

## DISCUSSION OF RESULTS

Reaction kinetics experiments with vanadium-phosphorus-oxygen catalysts of varying P-to-V ratio have shown that catalyst phosphorus loading is a key parameter in determining catalyst selectivity, catalyst activity, and specific rates of oxidation. Catalyst characterization studies provide structural and compositional explanations for the observed kinetic results.

The precipitated P/V = 0.9 catalyst was found to consist of $VO(HPO_4) \cdot 0.5H_2O$ with vanadium(IV) present on the catalyst surface. Following activation in air, an oxidized B' phase was formed with both surface and bulk vanadium(V). Used catalysts having composition P/V = 0.9 were found to contain unreacted $V_2O_5$ and $\alpha$-$VOPO_4$; the surface of these catalysts possessed both vanadium(IV) and vanadium(V) states. (Assignment of the V $2p_{3/2}$ binding energies to vanadium oxidation states is assisted by model compound studies (16).) The low selectivity for maleic anhydride and moderate conversion of n-butane observed for the P/V = 0.9 catalyst is attributed to the formation of active, but relatively nonselective, $\alpha$-$VOPO_4$. High specific rates of n-butane consumption, maleic anhydride formation, and $CO_2$ formation appear to occur as a result of only mild suppression of activity by catalyst phosphorus.

The precipitated and air-calcined P/V = 1.0 catalysts were found to contain $VO(HPO_4) \cdot 0.5H_2O$; some B' phase was detected in the air-calcined samples. XPS results indicated the surface of the precipitated catalyst was vanadium(IV), while both vanadium(IV) and vanadium(V) were observed for the air-calcined and used P/V = 1.0 catalysts. Intermediate values of

maleic anhydride selectivity and n-butane conversion are attributed to the formation of $(VO)_2P_2O_7$ with some $\alpha$-$VOPO_4$ in the used P/V = 1.0 catalyst. Intermediate specific rates of n-butane consumption, maleic anhydride formation, and $CO_2$ formation result from a moderate suppression of activity by phosphorus.

The precipitated and air-calcined P/V = 1.1 and 1.2 catalysts were found to contain $VO(HPO_4) \cdot 0.5H_2O$. XPS results indicated the surface of the precipitated catalysts was primarily vanadium(IV). A slight oxidation of the surface was indicated during air-activation; no change in vanadium oxidation state was observed for the used V-P-O catalysts containing "excess" phosphorus. High values for maleic anhydride selectivity were observed for both the P/V = 1.1 and 1.2 catalysts. However, n-butane conversion was found to be highest for the P/V = 1.1 catalyst and very low for the P/V = 1.2 catalyst. It appears that the optimal V-P-O catalyst is made by incorporating just enough "excess" phosphorus to stabilize the active and selective $(VO)_2P_2O_7$ phase. Too much "excess" phosphorus can dramatically reduce n-butane conversion by "blocking" the selective, as well as the nonselective, oxidation pathways. The very low specific rates of n-butane consumption, maleic anhydride formation, and $CO_2$ formation observed for the P/V = 1.1 and 1.2 catalysts indicate a dramatic reduction in catalyst activity with the incorporation of "excess" phosphorus.

## CONCLUSIONS

These studies have established that a slight "excess" of catalyst phosphorus (P/V = 1.1) is required to stabilize a $(VO)_2P_2O_7$ phase which is both active and selective in the oxidation of n-butane to maleic anhydride. A larger "excess" of catalyst phosphorus was found to further enhance the selectivity of this phase but this was accomplished only at the expense of catalyst activity. Used V-P-O catalysts without "excess" phosphorus contained the active but nonselective $\alpha-VOPO_4$ phase.

Specific rates of $CO_2$ formation and maleic anhydride formation were found to decrease with increasing catalyst P-to-V ratio. Since $CO_2$ formation rates were more strongly depressed by added phosphorus, maleic anhydride selectivity was favored by an increase in catalyst phosphorus.

REFERENCES

1. Katsumoto, K.; Marquis, M.  U.S. Patent 4 132 670; 1979.

2. Cavani, F.; Centi, G.; Trifiro, F.  The chemistry of catalysts based on vanadium-phosphorus oxides note IV:  catalytic behavior of catalysts prepared in organic medium in the oxidation of $C_4$ fraction.  Appl. Catal. 9:  192-202; 1984.

3. Centi, G.; Manenti, I.; Riva, A.; Trifiro, F.  The chemistry of catalysts based on vanadium-phosphorus oxides note III:  catalytic behavior of different phases in 1-butene oxidation to maleic anhydride.  Appl. Catal. 9:  177-190; 1984.

4. Schneider, R.  U.S. Patent 3 864 280; 1970.

5. Hodnett, B. K.  Vanadium-phosphorus oxide catalysts for the selective oxidation of $C_4$ hydrocarbons to maleic anhydride.  Catal. Rev.-Sci. Eng. 27(3):  374-424; 1985.

6. Ozkan, U.; Schrader, G. L.  $NiMoO_4$ selective oxidation catalysts containing excess $MoO_3$ for the conversion of $C_4$ hydrocarbons to maleic anhydride.  J. Catal. 95:  120-136; 1985.

7. Stefani, G.; Fontana, P.  U.S. Patent 4 100 106; 1978.

8. Johnson, J. W.; Johnson, D. C.; Jacobson, A. J.; Brody, J. F.  Preparation and characterization of $VO(HPO_4) \cdot 0.5H_2O$ and its topotactic transformation to $(VO)_2P_2O_7$.  J. Am. Chem. Soc. 106:  8123-8128; 1984.

9. Hutchings, G.; Higgins, R.  U.S. Patent 4 209 423; 1980.

10. Sanchez, C.; Livage, J.; Lucazeau, G.  Infrared and Raman study of amorphous $V_2O_5$.  Journal of Raman Spectroscopy 12(1):  68-72; 1982.

11. Busca, G.; Cavani, F.; Centi, G.; Trifiro, F.  Nature and mechanism of formation of vanadyl pyrophosphate:  active phase in n-butane selective oxidation.  J. Catal. 99:  400-418; 1986.

12. Greenfield, S.; Clift, M.  Analytical chemistry of the condensed phosphate.  Oxford:  Pergamon Press; 1975.

13. Bhargava, R. N.; Condrate, R. A.  The vibrational spectra of $VPO_5$ crystal phases and related glasses.  Applied Spectroscopy 31(3):  230-236; 1977.

14. Bordes, E.; Courtine, P. Some selectivity criteria in mild oxidation catalysis: V-P-O phases in butene oxidation to maleic anhydride. J. Catal. 57: 236-252; 1979.

15. Moser, T. P.; Schrader, G. L. Selective oxidation of n-butane to maleic anhydride by model V-P-O catalysts. J. Catal. 92: 216-231; 1985.

16. Moser, T. P.; Schrader, G. L. Stability and redox properties of model V-P-O catalysts. J. Catal., submitted.

17. Gopal, R.; Calvo, C. Crystal structure of $\beta$-VOPO$_4$. J. Solid State Chem. 5: 432-435; 1972.

18. Ladwig, V. G. Über die Konstitution des VPO$_5$($\cdot$nH$_2$O). Zeitschrift für anorganische und allgemeine Chemie. Band 338: 266-278; 1965.

19. Shimoda, T.; Okuhara, T.; Misono, M. Preparation of vanadium-phosphorus mixed oxide (P/V = 1) catalysts and their application in butane oxidation to maleic anhydride. Bull. Chem. Soc. Jpn. 58: 2163-2171; 1985.

SECTION II.  MALEIC ANHYDRIDE CONVERSION BY V-P-O CATALYSTS

ABSTRACT

The vapor phase conversion of maleic anhydride was studied using a series of industrial-type vanadium-phosphorus-oxygen (V-P-O) catalysts having P-to-V ratios of 0.9, 1.0, 1.1, and 1.2. A molten maleic anhydride saturator system was used to feed maleic anhydride vapor directly to an integral flow reactor at 350, 400, and 450°C. Direct evidence for the combustion of maleic anhydride and the formation of maleic acid was gathered. The conversion of maleic anhydride was observed to increase with reaction temperature for each catalyst P-to-V ratio studied. The incorporation of "excess" phosphorus in the V-P-O catalyst suppressed maleic anhydride combustion by stabilizing the $(VO)_2P_2O_7$ phase.

## INTRODUCTION

The synthesis of maleic anhydride from n-butane is an important commercial example of paraffin selective oxidation. Vanadium-phosphorus-oxygen (V-P-O) catalysts with P-to-V ratios near unity have found special application for this process (1). Detailed characterization and catalytic activity results for model V-P-O phases (2) and high surface area industrial-type (3) catalysts have been reported. Although this process represents an important commercial advance, the mechanism of n-butane selective oxidation to maleic anhydride remains poorly understood.

The reaction pathways which have been presented for n-butane selective oxidation to maleic anhydride are very simple. The models proposed by Wohlfahrt and Hofmann (4) and Escardino et al. (5) have implied the direct conversion of n-butane to maleic anhydride. The reaction pathway proposed by Escardino (5)

$$\text{n-butane} \longrightarrow \text{maleic anhydride} \qquad (1)$$
$$\searrow CO, CO_2, H_2O \nearrow$$
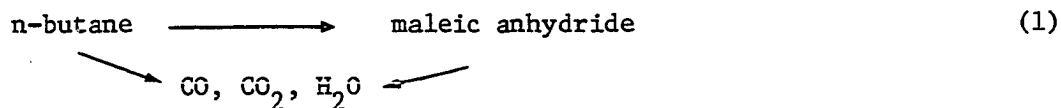
involves the formation of maleic anhydride and carbon dioxdes from n-butane and the combustion of maleic anhydride to CO, $CO_2$, and $H_2O$. Kinetic modeling (Centi et al. (6), Cavani et al. (7)) also indicates the possible combustion of maleic anhydride.

This investigation provides direct evidence for the combustion of maleic anhydride by V-P-O model compounds and industrial catalysts. The effects of reaction temperature, residence time, oxygen partial pressure,

· and catalyst P-to-V ratio on the rates of maleic anhydride disappearance

and $CO_2$ formation are presented.

## EXPERIMENTAL PROCEDURE

### Catalyst Preparation

Industrial-type vanadium-phosphorus mixed oxide catalysts were prepared having P-to-V ratios of 0.9, 1.0, 1.1, and 1.2. The synthesis procedures and characterization results are reported elsewhere (3).

### Maleic Anhydride Conversion Measurements

The vapor phase conversion of maleic anhydride was studied using an integral flow reactor operating at near atmospheric pressure (Figure 1). The reactor was constructed from 316 stainless-steel tubing have a 1-in. outer diameter and ½-in. inner diameter. The overall reactor bed length was 15-in., including the ½-in. thickness of each flange. The temperature along the reactor length and at varying radial depths was monitored by using 13 subminiature thermocouple probe assemblies; the entire reactor was submerged in a heated fluidized sand bath. Zoned heating of the reactor was maintained by seven independently controlled resistance elements. Typically, the temperature of the reactor bed could be controlled to within ±2°C.

Residual activity of the reactor was suppressed by conditioning the reactor wall and the silicon carbide chips with a wash of 85 wt. % $H_3PO_4$ followed by calcination in oxygen at 600°C. The reactor was charged with catalyst and No. 8 mesh (2.38 mm) silicon carbide which served as a diluent. The catalyst bed consisted of a homogeneous mixture of 5.00 g of catalyst and 45 g of conditioned silicon carbide. Catalyst powder was pressed and sieved between Nos. 10 and 20 mesh screens to provide catalyst particles from 1.68 to 0.84 mm.

O.D. 1.00"
I.D. 0.50"

thermocouple

graphite gasket

stainless steel mesh
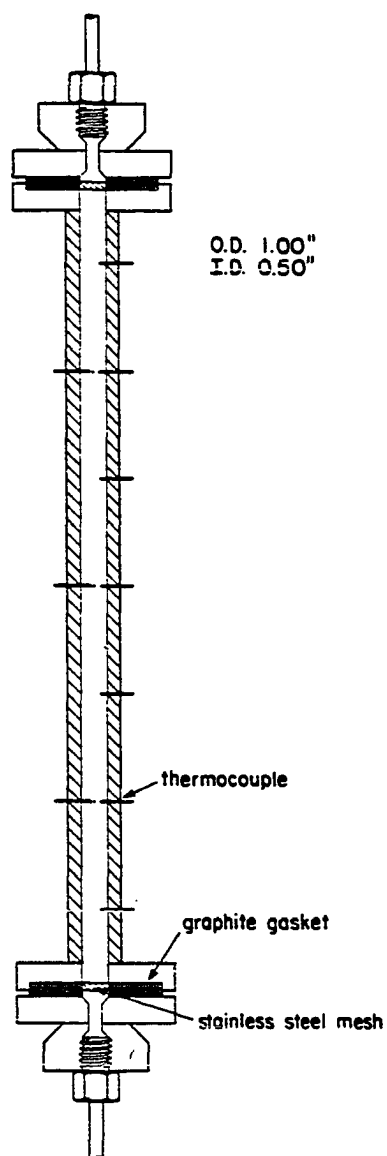
Figure 1.   Integral flow reactor

Tylan Model FC260 mass flow controllers were used to regulate oxygen

and nitrogen gas flow rates. Maleic anhydride delivery was achieved using

a saturator system (Figure 2). The system consisted of a 1 liter Pyrex

vessel with inlet and outlet gas ports, a 50-ft. preheater coil, and an air

convection oven with a built-in air circulation pump. The regulated and

preheated nitrogen-oxygen feed gas was blown just above the surface of

molten maleic anhydride in the saturator vessel. The vessel temperature

was regulated to within ±0.5°C by thermostat control and measured by a

thermocouple probe positioned near the center of the vessel. The saturator

was operated at 50°C (melting point of maleic anhydride ca. 52°C) to obtain

feed concentrations of maleic anhydride of about 0.29% in air. The

stability of maleic anhydride and its concentration in the feed mixture was

analyzed both by gravimetric techniques and by gas chromatography.

Gravimetric measurements were made by condensing the saturator effluent

in a coiled Pyrex tube chilled in an ice bath.

Exit lines from the reactor were heated to 105°C to prevent maleic

anhydride condensation. The composition of both the feed and product gases

was analyzed by gas chromatography. The analytical system consisted of

an Antex 300 gas chromatograph which was equipped with three heated

sampling valves, two flame ionization detectors, and one thermoconductivity

detector. The conversion of maleic anhydride was determined by analysis

of the feed and product gases. The percent conversion reported in this

work was defined as

$$\frac{\text{moles of maleic anhydride consumed}}{\text{moles of maleic anhydride in feed}} \times 100\% \tag{2}$$
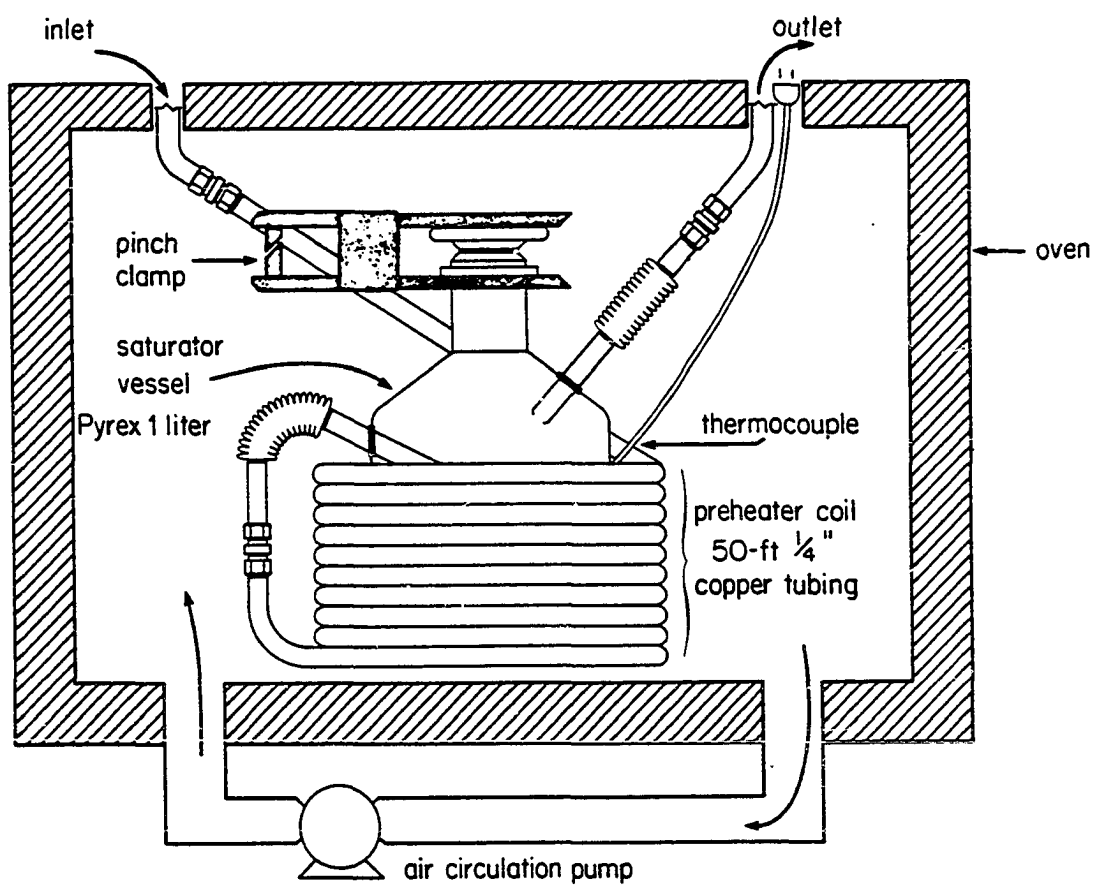
Figure 2. Maleic anhydride delivery system

Rates of maleic anhydride disappearance and $CO_2$ production were normalized to a standard maleic anhydride feed of $1.575 \times 10^{-5}$ g-moles/min/g-cat.

Steady-state kinetic experiments were conducted to examine the effects of reaction temperature and catalyst P-to-V ratio on the conversion of maleic anhydride and the rates of $CO_2$ production and maleic anhydride disappearance. Reaction temperatures of 350, 400, and 450°C were studied for catalysts having P-to-V ratios of 0.9, 1.0, 1.1, and 1.2. The time factor (W/F = 3.11) and oxygen partial pressure ($P_{O_2}$ = 0.22 atm.) were maintained constant during these studies.

## EXPERIMENTAL RESULTS

The conversion of maleic anhydride was studied at 350, 400, and 450°C using V-P-O catalysts having P-to-V ratios of 0.9, 1.0, 1.1, and 1.2. The effect of reaction temperature and catalyst phosphorus loading on maleic anhydride conversion are presented separately.

### Effect of Temperature

Maleic anhydride conversion, the rate of $CO_2$ production, and the rate of maleic anhydride disappearance increased as the reaction temperature increased from 350 to 450°C (Tables 1, 2, and 3, respectively). For the P/V = 0.9 catalyst maleic anhydride conversion was found to increase from 17.1 to 30.8% as reaction temperature increased from 350 to 450°C. Increases in maleic anhydride conversion from 5.5 to 27.8%, from 4.1 to 24.0%, and from 8.3 to 15.0% were observed for the P/V = 1.0, 1.1, and 1.2 catalysts for a temperature increase from 350 to 450°C (Table 1).

### Effect of Catalyst Phosphorus Loading

Maleic anhydride conversion, the rate of $CO_2$ production, and the rate of maleic anhydride disappearance were found to decrease with increasing catalyst phosphorus loading (Tables 1, 2, and 3, respectively). At 350°C maleic anhydride conversion was found to decrease from 17.1 to 8.3% as the catalyst phosphorus loading increased from P/V = 0.9 to P/V = 1.2. At 400 and 450°C the maleic anhydride conversion decreased from 23.2 to 10.8% and from 30.8 to 15.0% with an increase in catalyst P-to-V ratio from 0.9 to 1.2.

Table 1. Conversion of maleic anhydride as a function of catalyst phosphorus loading and reaction temperature (W/F = 3.11; $P_{O_2}$ = 0.22 atm)[a]

| P-to-V ratio | 0.9 | 1.0 | 1.1 | 1.2 |
|---|---|---|---|---|
| 350°C | 17.1 | 5.5 | 4.1 | 8.3 |
| 400°C | 23.2 | 17.6 | 11.8 | 10.8 |
| 450°C | 30.8 | 27.8 | 24.0 | 15.0 |

[a]Rates expressed as g-moles/min/g-catalyst.

Table 2. Rates of $CO_2$ formation as a function of catalyst phosphorus loading and reaction temperature (W/F = 3.11; $P_{O_2}$ = 0.22 atm)[a]

| P-to-V ratio | 0.9 | 1.0 | 1.1 | 1.2 |
|---|---|---|---|---|
| 350°C | 1.88 E-6 | 1.32 E-6 | 7.12 E-7 | 5.88 E-7 |
| 400°C | 3.93 E-6 | 1.76 E-6 | 9.40 E-7 | 8.68 E-7 |
| 450°C | 6.84 E-6 | 5.12 E-6 | 3.69 E-6 | 1.99 E-6 |

[a]Rates expressed as g-moles/min/g-catalyst.

Table 3. Rates of maleic anhydride disappearance as a function of catalyst phosphorus loading and reaction temperature (W/F = 3.11; $P_{O_2}$ = 0.22 atm)[a]

| P-to-V ratio | 0.9 | 1.0 | 1.1 | 1.2 |
|---|---|---|---|---|
| 350°C | 2.69 E-6 | 8.66 E-7 | 6.46 E-7 | 1.31 E-6 |
| 400°C | 3.65 E-6 | 2.77 E-6 | 1.86 E-6 | 1.70 E-6 |
| 450°C | 4.85 E-6 | 4.38 E-6 | 3.78 E-6 | 2.36 E-6 |

[a]Rates expressed as g-moles/min/g-catalyst.

## DISCUSSION OF RESULTS

A decrease in reaction temperature or an increase in catalyst phosphorus content was found to result in lower maleic anhydride combustion activity. Since catalysts having larger P-to-V ratios are more selective for maleic anhydride during n-butane oxidation (3), it appears these selectivity benefits are due in part to lower rates of maleic anhydride combustion. In the previous n-butane oxidation study (3), used V-P-O catalysts having an "excess" of phosphorus were found to possess the selective $(VO)_2P_2O_7$ phase; catalysts deficient in phosphorus contained the nonselective $\alpha$-$VOPO_4$ phase. This study suggests that a primary function of "excess" phosphorus is to inhibit maleic anhydride combustion by stabilizing the $(VO)_2P_2O_7$ phase.

### Conversion of Maleic Anhydride to Maleic Acid

Carbon balances were calculated by comparing the flow rate of maleic anhydride which was fed to the reactor, to the flow rates of unreacted maleic anhydride and carbon dioxide on a $C_4$ basis. Typically, these balances were from 80 to 95%. Analysis of the condensed solids from the reactor effluent by FT-IR spectroscopy indicated that the low material balances could be a result of maleic acid formation. Semi-quantitative FT-IR analysis indicated that 2 to 16% of the condensed solids were maleic acid.

The infrared spectrum of solid maleic anhydride, solid maleic acid, and a representative infrared spectrum of the condensed solids are given in Figure 3. The spectrum of maleic anhydride (spectrum 3[a]) has two intense carbonyl stretching vibrations at 1783 and 1857 $cm^{-1}$ and a =CH
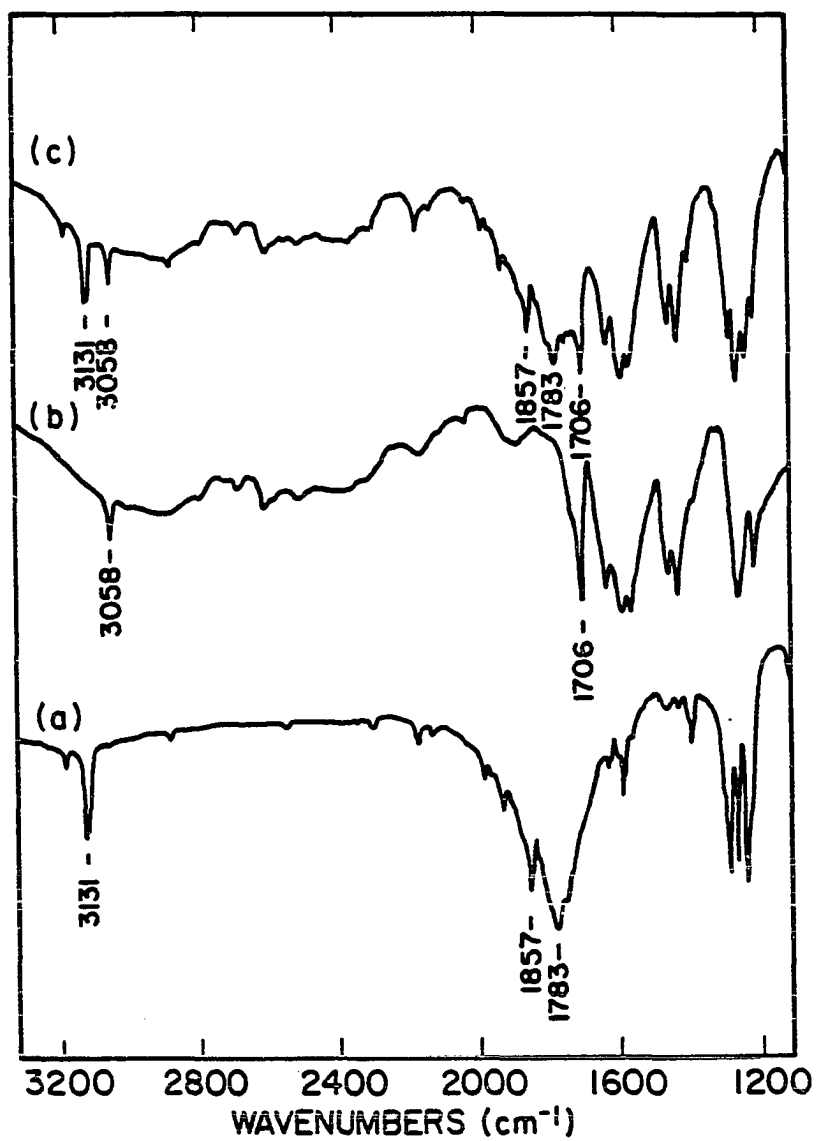
Figure 3. Infrared spectra of:

(a) solid maleic anhydride
(b) solid maleic acid
(c) condensed solids from reactor effluent

stretching vibration at 3131 cm$^{-1}$. Maleic acid (spectrum 3[b]) is characterized by a carbonyl stretching vibration at 1706 cm$^{-1}$ and a =CH stretching vi-ration at 3058 cm$^{-1}$. Infrared bands at 1706, 1783, 1857, 3058, and 3131 cm$^{-1}$ were observed in the condensed solids (spectrum 3[c]) indicating the presence of both maleic anhydride and maleic acid in the reactor effluent. The formation of maleic acid was not unexpected since the low temperature hydrolysis of maleic anhydride has been reported (8).

## CONCLUSIONS

The combustion of maleic anhydride as proposed in the reaction pathway of Escardino et al. (5) has been observed for V-P-O catalysts at 350-450°C. A decrease in maleic anhydride conversion was observed with an increase in catalyst phosphorus loading or by a decrease in reaction temperature. The suppression of maleic anhydride combustion activity by "excess" catalyst phosphorus appears to promote lower maleic anhydride combustion rates by stabilizing the $(VO)_2P_2O_7$ phase.

## ACKNOWLEDGEMENT

REFERENCES

1.  Hodnett, B. K.  Vanadium-phosphorus oxide catalysts for the selective oxidation of $C_4$ hydrocarbons to maleic anhydride.  Catal. Rev.-Sci. Eng. 27(3):  374-424; 1985.

2.  Moser, T. P.; Schrader, G. L.  Selective oxidation of n-butane to maleic anhydride by model V-P-O catalysts.  J. Catal. 92:  216-231; 1985.

3.  Wenig, R. W.; Schrader, G. L.  V-P-O industrial catalysts for n-butane oxidation:  characterization and kinetic measurements.  Ind. Eng. Chem. Fund., accepted.

4.  Wohlfahrt, K.; Hofmann, H.  Kinetik der Synthese von Maleinsäure-anhydrid aus n-Butan.  Chem. Ing. Tech. 52(10):  811-814; 1980.

5.  Escardino, A.; Solá, C.; Ruiz, F.  Oxidacion catalitica de butano a anhidrido maleico.  Anales de Quimica 69:  385-396; 1973.

6.  Centi, G.; Fornasari, G.; Trifiro, F.  Industrial n-butane oxidation to maleic anhydride on vanadium-phosphorus oxides:  kinetic analysis with a tubular flow stacked pellet reactor.  Ind. Eng. Chem. Prod. Res. Dev. 24:  32-37; 1985.

7.  Cavani, F.; Centi, G.; Trifiro, F.  Study of n-butane oxidation to maleic anhydride in a tubular flow stacked-pellet reactor:  influence of phosphorus on the selectivity.  Appl. Catal. 15:  151-160; 1985.

8.  Mount, R. A.  Maleic anhydride, maleic acid, and fumaric acid. Encyclopedia of Chemical Technology.  Vol. 14.  3rd ed.  New York: John Wiley & Sons; 1981.

SECTION III.  IN SITU FTIR STUDY OF n-BUTANE SELECTIVE OXIDATION
TO MALEIC ANHYDRIDE ON V-P-O CATALYSTS

## ABSTRACT

The selective oxidation of n-butane to maleic anhydride using vanadium-phosphorus-oxygen (V-P-O) catalysts having P-to-V ratios of 0.9, 1.0, and 1.1 was studied by transmission infrared spectroscopy. Catalysts were exposed to mixtures of 1.5% n-butane in air at temperatures from 100°C to 500°C. Adsorbed n-butane, maleic anhydride, and carbon oxide species were observed on the catalyst surfaces. In addition, adsorbed maleic acid and highly reactive olefinic species could be detected. The nature of the adsorbed species present on the catalyst surface was dependent on the catalyst phosphorus loading, the reaction temperature, and the time of exposure under reaction conditions.

## INTRODUCTION

The selective oxidation of n-butane by vanadium-phosphorus-oxygen (V-P-O) catalysts is a highly attractive commercial route for producing maleic anhydride. The discovery of this special class of catalysts--which is capable of activating paraffins for partial oxidation--is a significant new development in industrial catalysis.

Much research is documented in the patent literature regarding specific methods for preparing typical industrial V-P-O catalysts (1). Key preparative parameters are apparent from this work. For example, mixed oxides having phosphorus-to-vanadium ratios of 0.9 to 1.2 are identified as having high activity and selectivity. When produced by nonaqueous precipitation methods, these catalysts can also possess high surface areas and significant activity near 350°C. In recent years several research groups have attempted to identify various V-P-O phases which are present in typical industrial catalysts (2, 3). Studies using model catalysts have also been reported, which have permitted the effect of specific aspects of the solid state chemistry of these compounds to be related to catalytic activity, selectivity, and stability (4, 5).

Although industrial V-P-O catalysts are recognized as achieving high conversions to maleic anhydride, much less attention has been focused on the actual mechanism of the selective oxidation catalysis. Paraffin oxidation represents a departure from the dominant olefin oxidation chemistry practiced in industry (used in the production of ethylene oxide and acrylonitrile). V-P-O catalysts are capable of oxidizing both n-butane and butenes to maleic anhydride. Kinetic studies have led to relatively

simple proposals for the possible reaction pathways. However, the mechanisms for olefin (butene) conversions have generally included more reaction intermediates than the corresponding paraffin (n-butane) mechanisms. Considerable speculation concerning the relationships between these reaction pathways has been offered. A brief summary of the status of this literature follows.

The oxidation of 1-butene or the 2-butenes to maleic anhydride over V-P-O catalysts is generally believed to proceed with 1,3-butadiene present as an intermediate (6, 7). Some workers have also included crotonaldehyde (8, 9) or furan (10) as reaction intermediates; generally, however, crotonaldehyde or furan are considered to be side products, together with CO, $CO_2$, acetic acid, and various aldehydes. Brkić and Trifirò conducted kinetic measurements in which 1-butene was converted to 1,3-butadiene (11). Sunderland's investigations using $V_2O_5-P_2O_5$ catalysts for 2-butene oxidation did not explicitly postulate intermediates (12). The reaction network proposed by Varma and Saraf indicated oxidative dehydrogenation of 1-butene to 1,3-butadiene followed by conversion to maleic anhydride; butene isomerization and oxidation of 1,3-butadiene to furan were also included as side reactions (13).

The reaction pathways which have been presented for the oxidation of n-butane to maleic anhydride have been very simple. The models by Escardino et al. (14) and Wohlfahrt and Hofmann (15) have implied the direct conversion of n-butane to maleic anhydride. Hodnett et al. also postulated no production of olefins as part of the oxidation mechanism (16). Observations by Wüstneck et al. were similar in that only a very simple reaction network was proposed (17).

Recently, our research group has reported the results of n-butane oxidation studies in which olefinic species were detected in the reactor effluent stream when model V-P-O compounds were used as catalysts (4). Although this observation does not prove the role of olefins as reaction intermediates, the possible involvement of these compounds in the catalyst surface chemistry merits further investigation. Our current research focuses on the use of in situ spectroscopic techniques for identifying adsorbed species on the surfaces of V-P-O catalysts during n-butane oxidation. Infrared spectroscopy has been demonstrated to be a powerful method for performing such studies (18, 19). In this paper, we report our initial in situ FTIR spectroscopic results for a range of possible reaction pathway intermediates—including species in addition to olefins—which may be involved in n-butane oxidation to maleic anhydride. The spectroscopic studies were performed using typical industrial catalyst materials prepared in a manner consistent with the general industrial practice already summarized. An important goal of this work was to relate the presence of specific adsorbed species to the composition and structure of the catalysts, the reaction temperature, and the time on-stream.

## EXPERIMENTAL PROCEDURE

### Catalyst Preparation

The vanadium-phosphorus-oxide selective oxidation catalysts were prepared according to the precipitation method reported by Katsumoto and Marquis (20) at P-to-V ratios of 0.9, 1.0, and 1.1. The precipitation vessel (1000 ml) consisted of a heated, three neck round bottom flask; a reflux condenser and a water trap were also used. Thirty grams of $V_2O_5$ were suspended by rapid stirring in 60 ml of isobutyl alcohol and 40 ml of benzyl alcohol. The vanadium-oxide-alcohol mixture was heated to 120°C and allowed to reflux for three hours. During this period the suspension changed in color from brown to black, and approximately 2 ml of water was collected and removed. The apparently reduced vanadium suspension was cooled to 40°C prior to the addition of $H_3PO_4$. The suspension was then heated to 120°C and refluxed for an additional three hours. During this time a reduced vanadium phosphate (probably vanadium IV) was formed as indicated by a change in color from black to blue. The resulting catalyst was separated by filtration, dried for twelve hours at 125°C, and calcined in air for three hours at 380°C.

### Catalyst Characterization and Activity Measurements

Extensive catalyst characterization and activity measurements were performed for these alcohol-solution-precipitated catalysts. X-ray diffraction, laser Raman spectroscopy, infrared spectroscopy, X-ray photoelectron spectroscopy, scanning electron microscopy, X-ray energy dispersive spectroscopy, and BET surface area measurements were used to characterize the catalysts. Activity measurements for n-butane selective

oxidation were performed using an integral flow reactor and gas chromatograph analytical system, which has been described previously (4). A more extensive report of these results will be presented elsewhere (21), but here we present a brief summary of our findings since they have an important relation to our investigation of adsorbed species using infrared spectroscopy.

A strong effect of P-to-V synthesis ratio on catalyst morphology, crystal structure, vanadium oxidation state, and stability during activation was revealed. The catalyst having a composition of P/V = 1.1 was found to be unusually stable during activation in air; the block style morphology and $V^{4+}$ oxidation state of $(VO)_2P_2O_7$ was established following n-butane oxidation. Catalysts having compositions of P/V = 0.9 and 1.0 were not stable during activation in air; these catalysts possessed the layered structure and $V^{5+}$ oxidation state of $\alpha$-VOPO$_4$ following n-butane oxidation. The P/V = 1.1 catalyst had a high surface area (33 m$^2$/g) as well as a reduced vanadium surface during n-butane oxidation. In contrast, catalysts with P/V = 0.9 and 1.0 had lower surface areas (12 and 17 m$^2$/g, respectively) and more surface $V^{5+}$ during n-butane oxidation. The P/V = 1.1 catalyst exhibited the lowest specific (per unit surface area) rate of n-butane consumption but the highest selectivity for maleic anhydride. The P/V = 1.0 catalyst produced an intermediate specific rate of n-butane consumption and an intermediate selectivity for maleic anhydride. The P/V = 0.9 catalyst had the highest specific rate of n-butane consumption and the lowest selectivity for maleic anhydride. Consequently, an increase in P-to-V synthesis ratio resulted in lower specific rates of n-butane consumption but led to an increase in

selectivity for maleic anhydride. Only n-butane, maleic anhydride, CO,

$CO_2$, and $H_2O$ were observed in the effluent from the integral reactor using

the industrial-type catalysts prepared for this investigation.

### In Situ FTIR Cell and Gas Delivery System

The in situ FTIR cell (Figure 1) was constructed from a 33 mm OD

quartz tube and was 60 mm in length with two 6 mm OD inlet and outlet gas

ports. A third port in the quartz tube permitted the insertion of a

0.040" thermocouple (Omega Engineering) at a distance of approximately

2 mm from the catalyst surface. Water-cooled, brass window mounts were

cemented to the quartz body. KBr windows (38 mm x 6 mm) were used, and

Viton o-rings were used to seal the windows. An external heater was

constructed from beaded nichrome wire which was tightly wound around the

midsection of the quartz tube. The cell was capable of being evacuated to

pressures of $10^{-5}$ torr and heated to temperatures near 550°C.

Moisture traps consisting of 3 Å molecular sieves were incorporated

in the stainless steel lines used to deliver gases to the quartz inlet

port of the in situ infrared cell. High purity (99.99%) oxygen and

nitrogen gases (Air Products) were mixed with instrument grade (99.5%)

n-butane (Matheson) to form a gas feed consisting of 1.5% n-butane in air.

A flow rate of 75 $cm^3$/min was used in all studies. Rotameters (Matheson)

were employed to establish the flow rates.

### Fourier Transform Infrared Spectrometer

Infrared spectra were recorded using a Nicolet Model 60-SX Fourier

transform infrared spectrometer with single beam optics. Typically 500

scans were accumulated at 2 $cm^{-1}$ resolution with a dry, $N_2$-purged cell
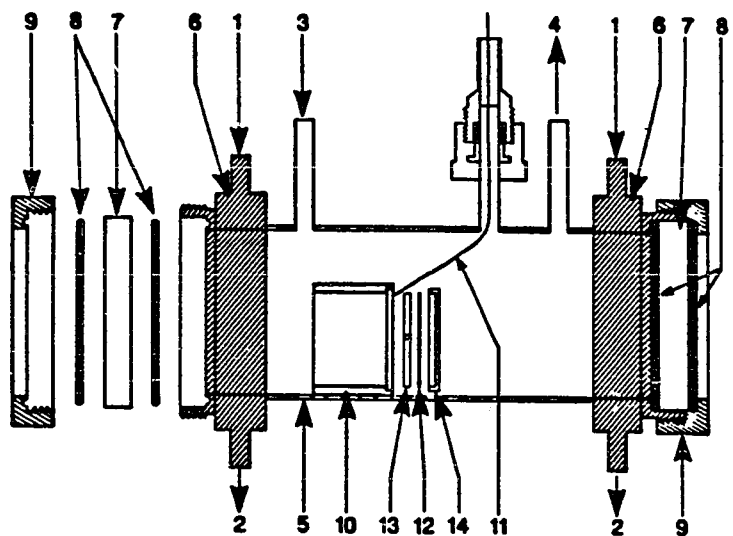
Figure 1. _In situ_ FTIR cell

1 WATER INLET
2 WATER OUTLET
3 GAS INLET
4 GAS OUTLET
5 QUARTZ CELL BODY
6 WATER COOLED BRASS
 FLANGE
7 KBr WINDOW

8 VITON O-RINGS
9 BRASS SCREW CAP
10 RING HOLDER
11 THERMOCOUPLE
12 CATALYST WAFER
13 EXPANDING RING CLAMP
14 SAMPLE HOLDING RING

including the KBr windows. In most cases the spectra recorded in this paper represent a combination of infrared bands due to the adsorbed species, the catalyst, and the gaseous species present in the cell; water bands have been subtracted (as noted) for some spectra to improve the observability of specific adsorbed species.

## Catalyst Preparation for In Situ Spectroscopic Studies

Three precipitated V-P-O catalysts having composition of P/V = 0.9, 1.0, and 1.1 were used for the in situ transmission infrared studies. For each sample, the calcined catalyst powder was pressed between the polished surfaces of a stainless steel dye at a load of 15,000 lbs; "ultra-thin" catalyst disks were formed of dimension 15 mm by 0.10 mm. The catalyst wafer was transferred to a two piece ring assembly and placed in a stainless steel holder within the quartz cavity of the infrared cell. Pretreatment of the catalyst prior to the in situ studies consisted of raising the cell temperature to 300°C for 2 hours in a flowing stream of air (75 $cm^3$/min). The goal of this pretreatment was to remove vibrational bands due to water (1620-1640 and 3100-3600 $cm^{-1}$) and residual solvent (1650-1900 $cm^{-1}$).

## RESULTS

The infrared spectra of the species adsorbed on the catalytic surfaces were found to be highly dependent on the composition of the catalysts, specifically the P-to-V ratio. For this reason the spectra will be presented with respect to the nominal (preparative) catalyst composition; "excess" phosphorus is also apparently important for industrial V-P-O catalysts. Two additional factors which affected the adsorption properties of the catalyst were reaction temperature and time of exposure under reaction conditions. For typical industrial processes involving the selective oxidation of n-butane, reactors would be operated in the range of 400-475°C (22). Somewhat lower temperatures were investigated in our in situ studies in order to stabilize specific surface species and to assist in the identification of reaction pathways. Time of exposure to the n-butane-air mixture was observed to influence the relative concentrations of adsorbed species. At 400°C steady state conversions were observed after approximately three to four hours, based on integral reactor and in situ infrared results.

Our discussion of vibrational assignments involves species in both gaseous and adsorbed phases. The assignment of infrared bands to gaseous CO and $CO_2$ were made on the basis of rotational splitting of vibrational energy levels at 2143 $cm^{-1}$ and 2350 $cm^{-1}$. Adsorbed $CO_2$ was identified by two bands at 2338 and 2361 $cm^{-1}$. Gaseous water was identified by weak bands in the region 1400-1800 $cm^{-1}$. Adsorbed waters were clearly identified by a sharp band in the region 1620-1640 $cm^{-1}$ and a broad band from 3100-3600 $cm^{-1}$. Both gaseous and adsorbed n-butane were observed in the

in situ infrared spectra at 100°C, although the contribution of gaseous

n-butane was small especially at 400°C. Adsorbed maleic anhydride, maleic

acid and olefins were identified by strong C=O and C=C vibrations (1570-

1850 cm$^{-1}$) which were found to remain following a nitrogen purge at 400°C.

## Catalyst with P/V = 0.9

The in situ infrared spectra associated with the P/V = 0.9 catalyst

are presented in Figures 2 and 3. Catalyst vibrational bands are observed

below 1300 cm$^{-1}$; the spectral region above 1300 cm$^{-1}$ includes infrared

bands from adsorbed and gaseous species. Spectrum 2[a] was observed for

the unpretreated catalyst at 100°C. Surface hydroxyl species (free -OH

groups) were observed in the 3590-3650 cm$^{-1}$ region, adsorbed waters were

apparent at 1620 (sharp) cm$^{-1}$ and at 3100-3600 cm$^{-1}$ (broad). Subsequent

spectra (Figures 2b-3d) were collected following the 300°C air pretreatment

described previously and during the flow of the 1.5% n-butane-in-air

mixture. Spectrum 2[b] was obtained at 100°C for the pretreated catalyst

one hour after the start of reactive gas flow. Gaseous and adsorbed

n-butane was assigned to the -CH$_2$ and -CH$_3$ bending vibrations at 1380 cm$^{-1}$

and 1462 cm$^{-1}$ while -CH$_2$ and -CH$_3$ stretching bands were indicated at 2850-

3000 cm$^{-1}$. The band at 1380 cm$^{-1}$ was assigned to symmetric -CH$_3$

deformation of n-butane; bands near 1462 cm$^{-1}$ were assigned to the -CH$_2$ and

-CH$_3$ deformation of n-butane. Vibrational bands at 2858, 2878, 2933, and

2966 cm$^{-1}$ were assigned to the symmetric -CH$_2$, symmetric -CH$_3$, and

asymmetric -CH$_2$ stretching vibrations of n-butane (23). The 2979 cm$^{-1}$

shoulder band can be attributed to the symmetric =CH$_2$ stretching vibration

Figure 2. Adsorption of n-butane on P/V = 0.9 V-P-O catalyst:

    (a) catalyst at 100°C
    (b) pretreated catalyst in n-butane flow at 100°C
    (c) 200°C
    (d) 300°C
    (e) 400°C

Figure 3. Reaction of n-butane on P/V = 0.9 V-P-O catalyst at 400°C:

(a) 1 hour reaction
(b) 2 hour reaction
(c) 3 hour reaction
(d) 4 hour reaction
(e) 4 hour reaction and $N_2$ purge

of an adsorbed olefinic species. A single infrared band at 2338 $cm^{-1}$ was assigned to adsorbed $CO_2$.

At 200°C (spectrum 2[c]), a second band at 2361 $cm^{-1}$ was observed due to adsorbed $CO_2$. The 2338 and 2361 $cm^{-1}$ bands were assigned to the symmetric and asymmetric stretching vibrations of $CO_2$. At 300°C and 400°C three additional bands emerged as the cell temperature was increased at a rate of 100°C/hr (spectra 2[d] and 2[e]). The single band at 1725 $cm^{-1}$ was assigned to the carbonyl stretch of maleic acid (24) and was observed to intensify at higher temperatures. The two bands present at 1779 and 1848 $cm^{-1}$ were assigned to the asymmetric and symmetric carbonyl stretches of maleic anhydride (24).

At 400°C the cell temperature was stabilized, the infrared spectra were collected at one hour intervals. This series of spectra is shown in Figure 3. After one hour of reaction at 400°C (spectrum 3[a]) the vibrational-rotational bands of gaseous CO (near 2143 $cm^{-1}$) and gaseous $CO_2$ (near 2350 $cm^{-1}$) were observed. Spectra obtained at 400°C revealed that the activity of the catalyst had increased, as also indicated by integral reactor experiments. Vibrational bands corresponding to maleic acid (1720 $cm^{-1}$), maleic anhydride (1779 and 1848 $cm^{-1}$), CO (2143 $cm^{-1}$), and $CO_2$ (2350 $cm^{-1}$) were observed to rapidly intensify. During four hours of reaction at this temperature (spectrum 3[b] - 3[d]), a shoulder band at 1650 $cm^{-1}$ and a weak band at 3081 $cm^{-1}$ appeared. These bands were assigned to the =$CH_2$ stretch and C=C stretch of an adsorbed olefin, perhaps resembling 1-butene. These bands were not assigned to maleic acid since the C=C stretch and =CH stretch of this acid are found at 1570, 1590, and 1636 $cm^{-1}$ (several C=C bands) and at 3058 $cm^{-1}$, respectively. A broad

infrared band in the region 1385-1462 $cm^{-1}$ (spectrum 3[d]) was suggestive

of the $-CH_2$ and $-CH_3$ deformation of n-butane.

Spectrum 3[e] was collected after four hours of reaction at 400°C

and following a 30 minute $N_2$ purge. Infrared bands corresponding to

gaseous CO (2143 $cm^{-1}$), gaseous $CO_2$ (2350 $cm^{-1}$), and gaseous or physically

adsorbed n-butane (2858-2966 $cm^{-1}$) were removed. Vibrational bands

assigned to adsorbed surface species persisted at 1430 and 1720 $cm^{-1}$

(broad) for maleic acid, at 1779 and 1848 $cm^{-1}$ for maleic anhydride, and

2858-2966 $cm^{-1}$ for n-butane. An adsorbed olefinic species was suggested

by infrared bands at 1650 (shoulder) and 3081 $cm^{-1}$ (weak). Adsorbed $CO_2$

was also indicated by stretching vibrations at 2338 and 2361 $cm^{-1}$.

## Catalyst with P/V = 1.0

The *in situ* infrared spectra obtained for the P/V = 1.0 catalyst are

presented in Figures 4 and 5. Spectrum 4[a] was observed for the catalyst

at 100°C prior to pretreatment. This spectrum possessed a sharp -OH

bending band at 1640 $cm^{-1}$ and a broad -OH stretching band in the region

3100-3600 $cm^{-1}$. In addition residual solvent bands at 1690 and 1857 $cm^{-1}$

and adsorbed $CO_2$ at 2340 $cm^{-1}$ were observed. Spectrum 4[b] was obtained

following high temperature catalyst pretreatment; as a result infrared

bands corresponding to adsorbed water and residual solvent were removed.

Spectrum 4[c] was observed after catalyst pretreatment following the flow

of a 1.5% n-butane-in-air mixture for one hour. Vibrational bands

corresponding to n-butane were observed at 1460, 2858 (weak), 2878, 2933,

and 2966 $cm^{-1}$. As before these bands were assigned to $-CH_3$ and $-CH_2$

stretching and bending vibrations of an n-butane species. An additional

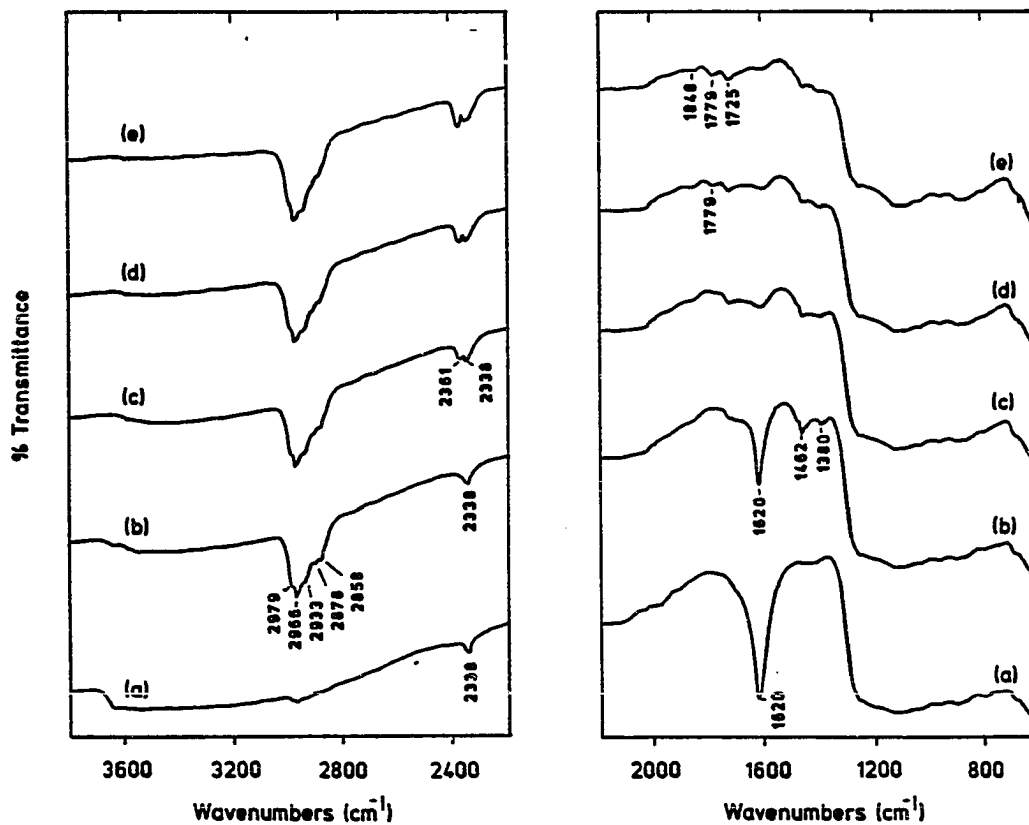Figure 4. Adsorption of n-butane on P/V = 1.0 V-P-O catalyst:

(a) catalyst at 100°C
(b) pretreated catalyst at 100°C
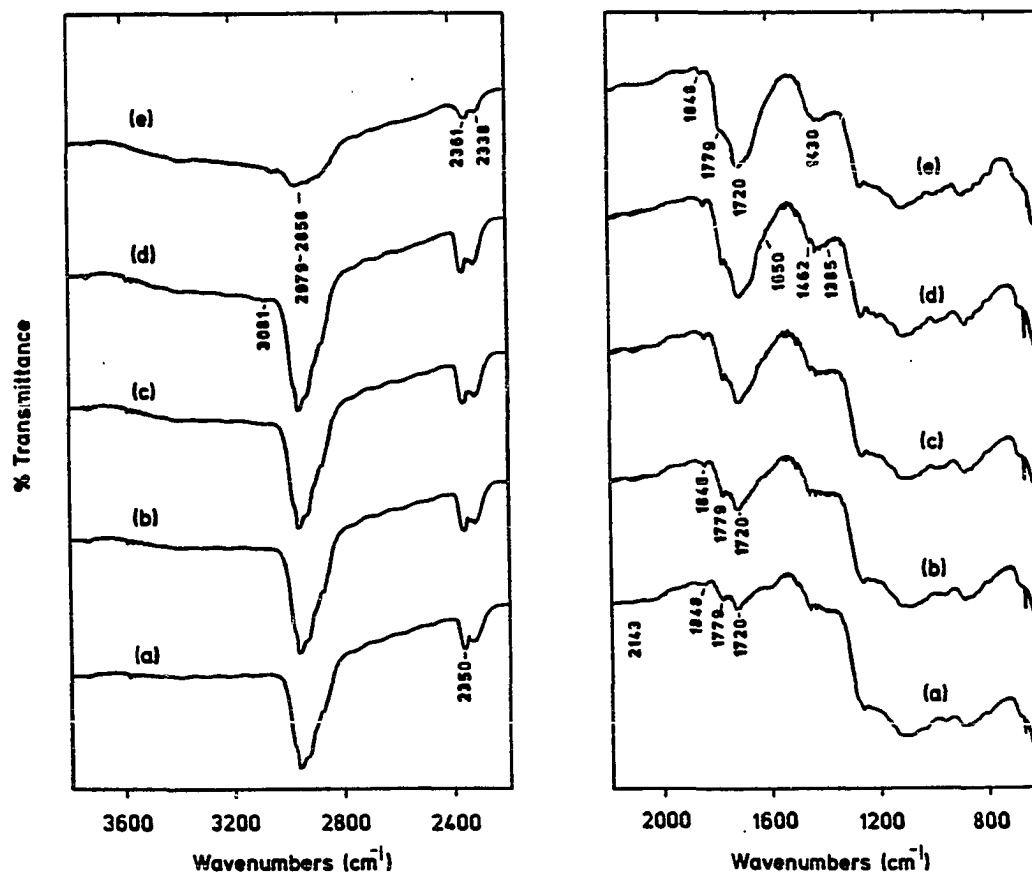(c) catalyst in n-butane flow at 100°C
(d) 200°C
(e) 300°C
(f) 400°C
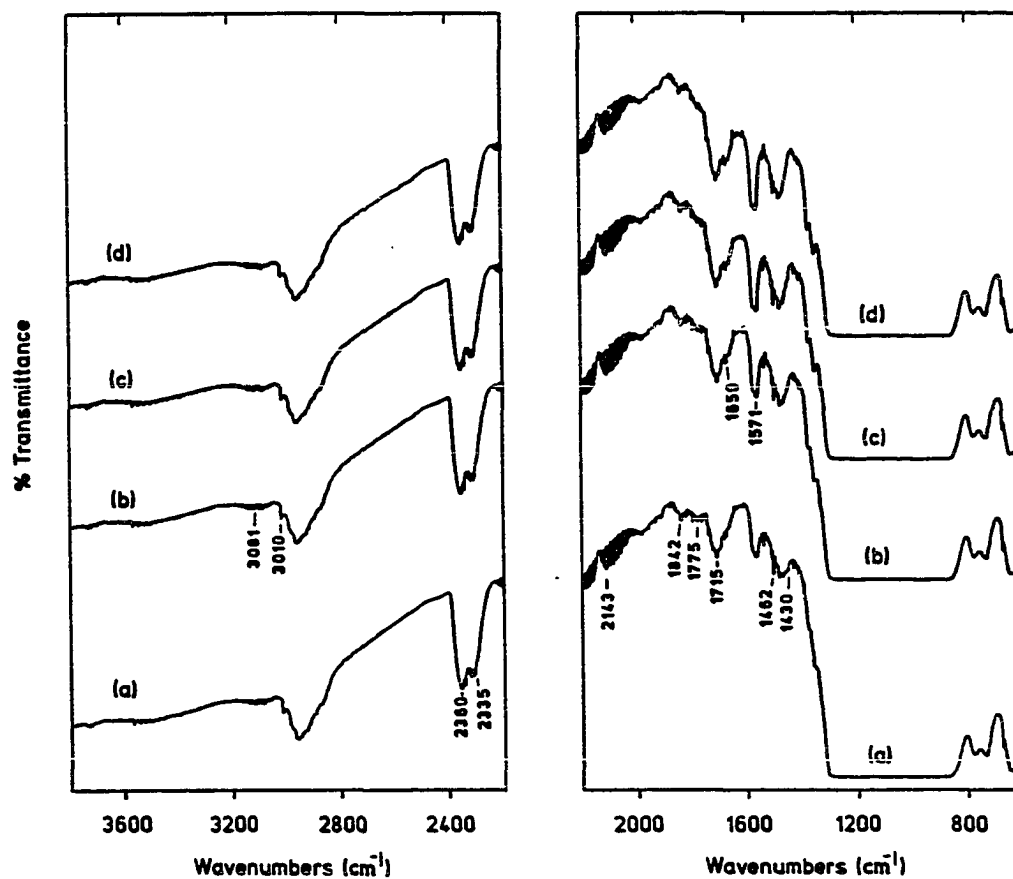
Figure 5. Reaction of n-butane on P/V = 1.0 V-P-O catalyst at 400°C:

(a) 1 hour reaction
(b) 2 hour reaction
(c) 3 hour reaction
(d) 4 hour reaction

shoulder band at 2979 $cm^{-1}$ was suggestive of the symmetric $=CH_2$ stretching

vibration of an olefinic species. At 200°C (spectrum 4[d]), adsorbed $CO_2$

was identified by stretching vibrations at 2335 and 2360 $cm^{-1}$. At 300°C

(spectrum 4[e]), gaseous CO and gaseous $CO_2$ were identified by vibrational-

rotational bands near 2143 and 2350 $cm^{-1}$ respectively. The vibrational-

rotational bands of gaseous CO and $CO_2$ were found to intensify greatly

at 400°C (spectrum 4[f]). At this temperature the carbonyl stretching

vibration of maleic acid was observed at 1715 $cm^{-1}$. Similarly, maleic

anhydride bands at 1775 and 1842 $cm^{-1}$ became more intense. A sharp band

at 3010 $cm^{-1}$ which appeared at 400°C was assigned to a =CH stretch of an

adsorbed olefinic species.

During four hours of reaction at 400°C (see Figure 5), the vibrational

bands corresponding to maleic anhydride, maleic acid, CO, and $CO_2$ were

observed to intensify (spectra 5[a]-5[d]). Gas phase $H_2O$ bands have been

subtracted from these spectra to improve the observability of other bands.

In addition, the vibrational bands due to n-butane appeared to diminish in

intensity while bands at 1571 and 3010 $cm^{-1}$ became more intense. Infrared

bands at 1571 and 3010 $cm^{-1}$ were suggestive of =CH and C=C stretching

vibrations shifted by substituent groups, by strain, or by conjugation (24).

The 1571 $cm^{-1}$ band could be ascribed to the C=C stretch of maleic acid

(three bands at 1569, 1589 and 1626 $cm^{-1}$), to cyclobutene (1566 $cm^{-1}$), or

to the C=C stretch of a conjugated olefin (24). Assignment of the 1571

$cm^{-1}$ band to maleic acid would not appear to be reasonable since no bands

were observed at 1589 or 1636 $cm^{-1}$. This band might possibly be assigned

to either a cyclic $C_4$ olefin resembling cyclobutene (24) or a strongly

conjugated π-allyl surface complex (16, 25). The sharp C=H band at 3010

$cm^{-1}$ was suggestive of either a =CH stretch or a $-CH_2$ stretch shifted by conjugation or strain.

## Catalyst with P/V = 1.1

The in situ infrared spectra for the P/V = 1.1 catalyst are presented in Figures 6 and 7. Spectrum 6[a] was obtained for the catalyst at 100°C prior to pretreatment. This spectrum includes a sharp -OH bending vibration at 1620 $cm^{-1}$ and a broad -OH stretching band in the region 3100-3600 $cm^{-1}$. In addition, residual solvent bands from 1680 to 1857 $cm^{-1}$ and adsorbed $CO_2$ at 2338 $cm^{-1}$ were observed. Spectrum 6[b] was obtained following high temperature catalyst pretreatment. As a result, infrared bands corresponding to adsorbed water and residual solvent were removed. Spectrum 6[c] was observed after catalyst pretreatment and following the flow of a 1.5% n-butane-in-air mixture for one hour. n-Butane was distinguished by very weak $-CH_3$ and $-CH_2$ stretching vibrations at 2858, 2879, 2933, and 2966 $cm^{-1}$. A weak shoulder band at 2979 was suggestive of a symmetric $=CH_2$ stretching vibration of an olefinic species. Additional spectra were collected at one hour intervals as the cell temperature was increased at a rate of 100°C/hr. At 200°C (spectrum 6[d]) adsorbed $CO_2$ was identified by two bands at 2335 and 2360 $cm^{-1}$. At 400°C (spectrum 6[f]) gaseous CO and gaseous $CO_2$ were assigned to the vibrational-rotational bands at 2143 and 2350 $cm^{-1}$; gas phase $H_2O$ bands have been subtracted from this spectrum. A weak olefinic =CH stretch at 3010 $cm^{-1}$ was also observed at 400°C.

During three hours of reactions at 400°C (Figure 7), the carbonyl stretching vibrations of maleic acid (1705 $cm^{-1}$) and maleic anhydride
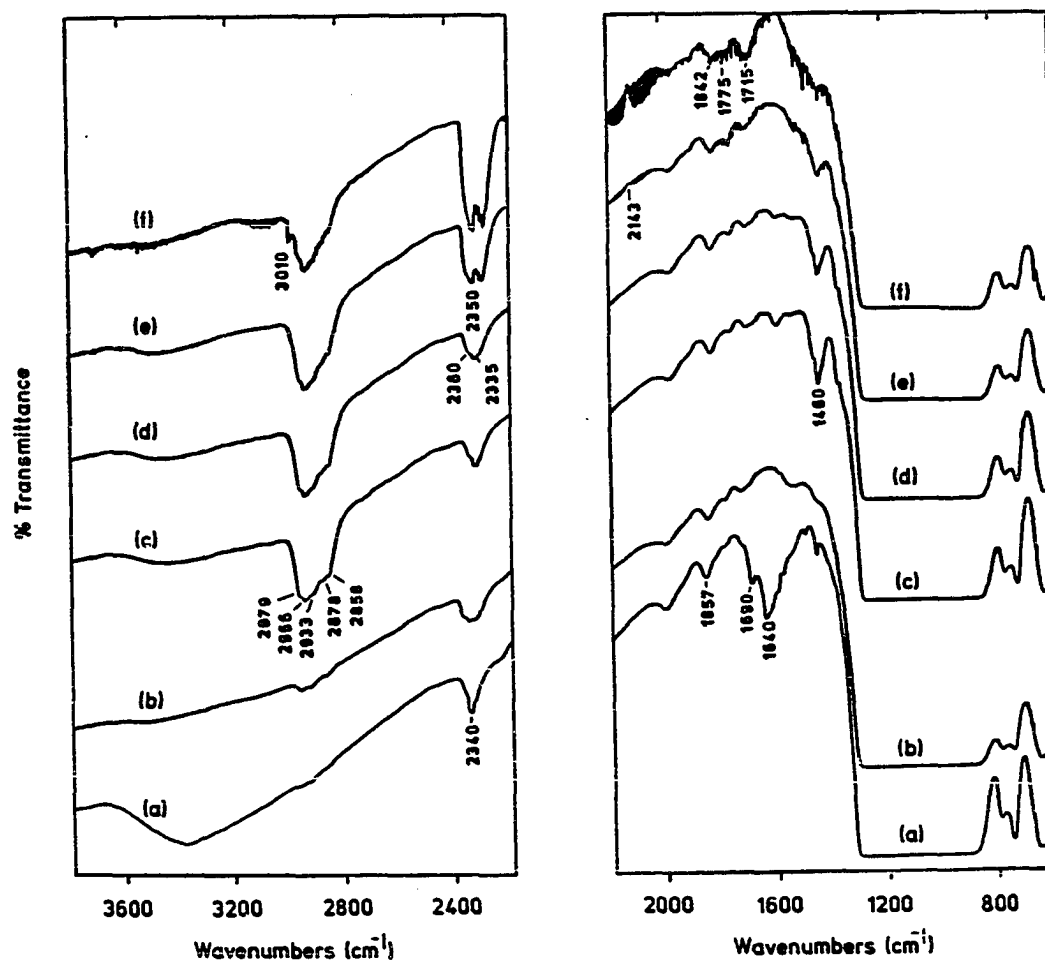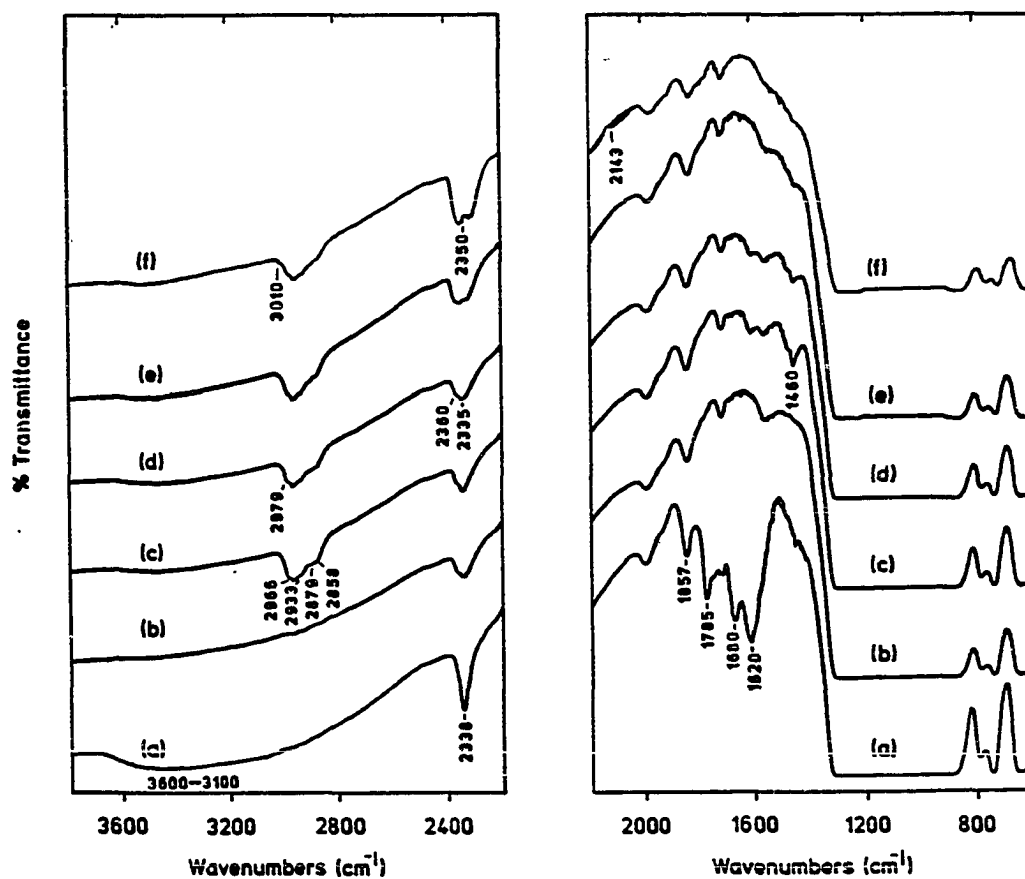
Figure 6. Adsorption of n-butane on P/V = 1.1 V-P-O catalyst:

    (a) catalyst at 100°C
    (b) pretreated catalyst at 100°C
    (c) catalyst in n-butane flow at 100°C
    (d) 200°C
    (e) 300°C
    (f) 400°C
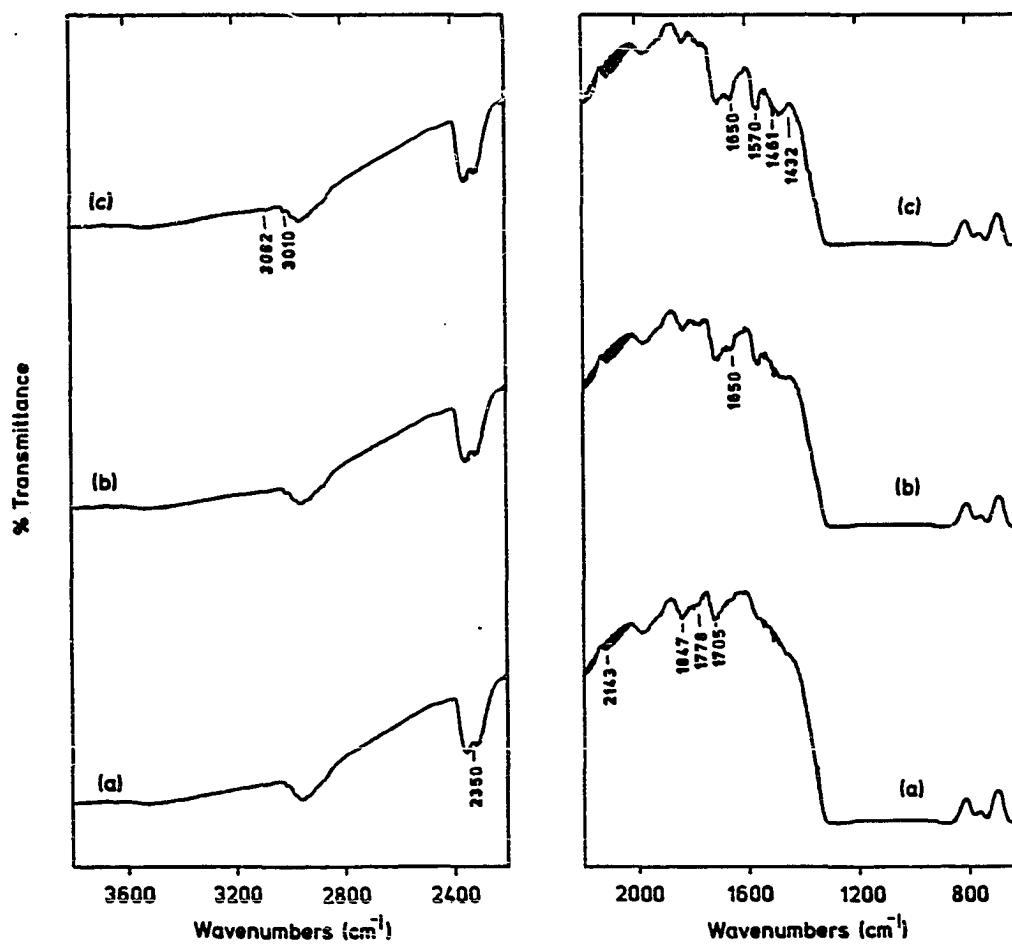
Figure 7. Reaction of n-butane on P/V = 1.1 V-P-O catalyst at 400°C:

    (a) 1 hour reaction
    (b) 2 hour reaction
    (c) 3 hour reaction

(1778 and 1847 $cm^{-1}$) were observed. Gas phase $H_2O$ bands have been subtracted from all spectra. The vibrational bands due to $CO_2$, CO, and maleic acid were found to intensify during this period while the carbonyl bands of maleic acid appeared unchanged in intensity. After three hours of reaction at 400°C (spectrum 7[c]) additional bands at 1570, 1650, 3010 (sharp), and 3082 (weak) $cm^{-1}$ were observed. The 1650 and 3082 $cm^{-1}$ bands are suggestive of an adsorbed 1-butene surface species. The 1570 and 3010 $cm^{-1}$ bands could indicate =CH stretching and C=C stretching for an adsorbed cyclobutene species or a π-allyl surface complex.

## DISCUSSION

The identification of specific gaseous and adsorbed species for n-butane oxidation by V-P-O catalysts by Fourier transform infrared spectroscopy has led to useful insights concerning the mechanism for this catalytic reaction. The reaction pathway proposed by Escardino et al. (14) is relatively simple:

$$\text{n-butane} \longrightarrow \text{maleic anhydride } (H_2O)$$
$$\searrow \qquad\qquad \nearrow$$
$$CO, CO_2 \ (H_2O)$$
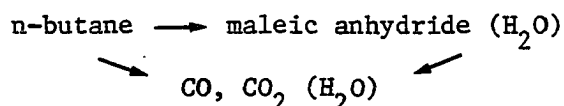
Maleic anhydride and carbon oxides are formed directly from n-butane; subsequently, maleic anhydride can be combusted to carbon oxides. Water is included in this reaction network as a product of both butane and maleic anhydride oxidation. The in situ infrared experiments have clearly identified n-butane, maleic anhydride, CO, $CO_2$, and $H_2O$ during n-butane selective oxidation to maleic anhydride. The vibrational bands of these five species were observed for studies involving each catalyst. However, the concentrations of these species were found to vary with catalyst phosphorus loading, reaction temperature, and time of exposure of the catalyst to reaction conditions. These reaction parameters are believed to affect catalyst activity and selectivity by modifying the relative rates of the competing heterogeneous reactions.

The assignment of vibrational bands for n-butane species under in situ conditions relied on a comparison with the infrared spectrum of gaseous n-butane (spectrum 8[a]). C-H bending vibrations are assigned to the 1465 $cm^{-1}$ band; C-H stretching vibrations are assigned to the 2858, 2879, 2933,
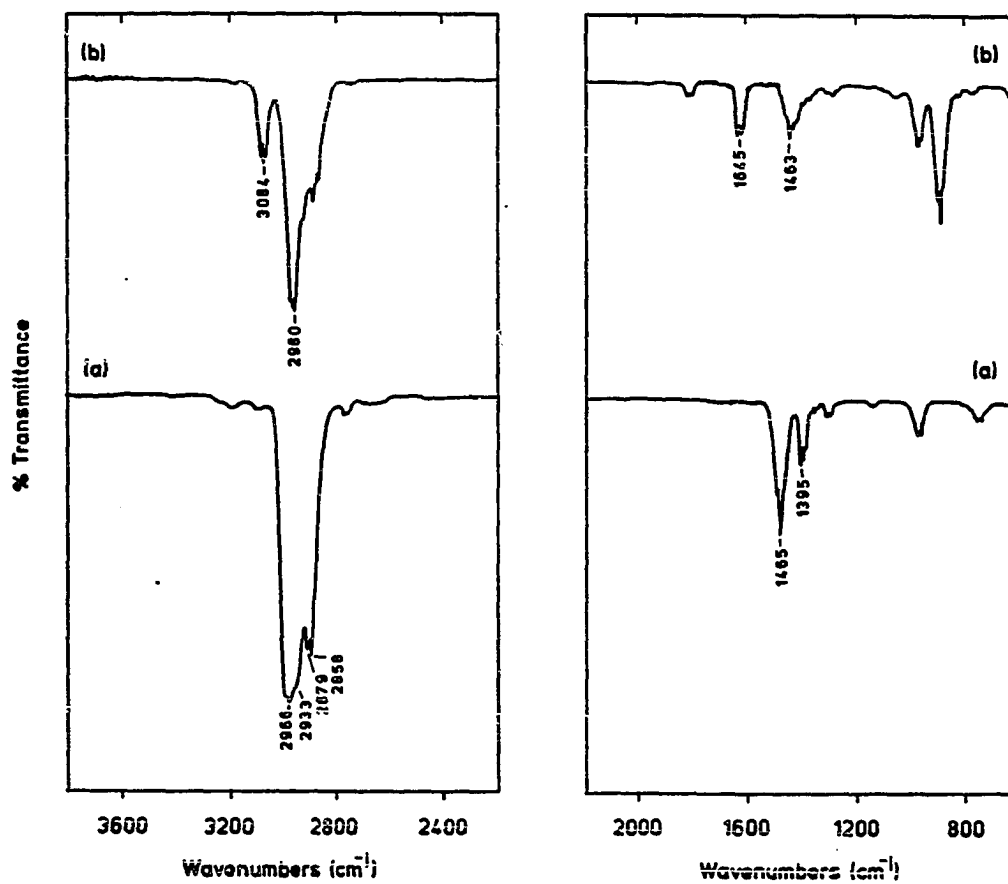
Figure 8. Infrared spectra of:

    (a) n-butane (gas)
    (b) 1-butene (gas)

and 2966 $cm^{-1}$ bands. Infrared bands at these frequencies observed under in situ conditions were assigned to gaseous and adsorbed n-butane. The C-H stretching bands of n-butane were found to decrease in intensity either with an increase in catalyst phosphorus loading or with an increase in reaction temperature. The decrease in n-butane adsorption with increasing catalyst phosphorus loading suggests high phosphorus catalysts may have fewer sites for paraffin adsorption. Integral reactor studies confirm that catalysts with excess phosphorus are less active (but more selective) for maleic anhydride (21). This could be a result of decreasing the rate of n-butane selective oxidation to maleic anhydride slightly, while decreasing the nonselective reaction rates greatly. The decrease in the intensity of the n-butane bands with increasing temperature is a result of increasing rates of conversion of the paraffin to maleic anhydride or to complete combustion products.

The assignment of the in situ spectra for maleic anhydride species was based on the infrared spectrum of solid maleic anhydride (spectrum 9[a]). Two bands at 1783 and 1857 $cm^{-1}$ are assigned to C=O stretching vibrations; =CH stretching vibrations are assigned to the 3131 $cm^{-1}$ band. A C=C stretching vibration is assigned to a weak band at 1593 $cm^{-1}$. The in situ catalysis spectra revealed bands at 1775 and 1845 $cm^{-1}$ which were assigned to the carbonyl stretching vibrations of maleic anhydride. These C=O bands first appeared at 400°C and intensified at near-equal rates (per gram catalyst) for the P/V = 0.9, P/V = 1.0, and P/V = 1.1 catalysts. Since catalyst surface area increases significantly with P-to-V ratio, excess catalyst phosphorus appears to decrease the specific rate of maleic anhydride formation. An intensification of these 1775 and 1845 $cm^{-1}$ bands
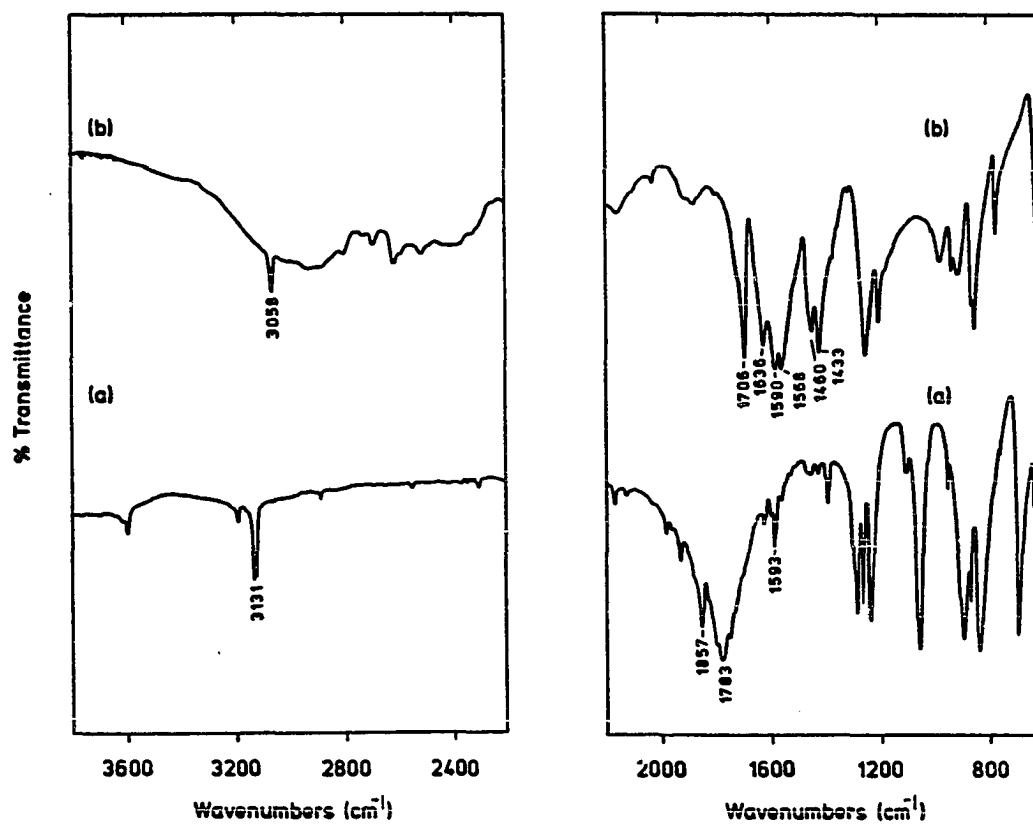
Figure 9.   Infrared spectra of:

(a) maleic anhydride (solid)
(b) maleic acid (solid)

at 400°C indicated increased rates of maleic anhydride formation at

elevated reaction temperatures. The relatively weak =CH stretch at 3131

$cm^{-1}$ and the C=C stretch at 1593 $cm^{-1}$ were not observed for maleic

anhydride under in situ conditions.

The assignment of in situ spectral features to $H_2O$, $CO_2$, and CO is

readily accomplished (26). Adsorbed water is identified by a sharp O-H

bending band at 1620-1640 $cm^{-1}$ and by broad O-H stretching bands from

3100-3600 $cm^{-1}$. Gaseous CO and $CO_2$ are identified by intense vibrational-

rotational bands at 2143 and 2350 $cm^{-1}$ respectively. Adsorbed $CO_2$ is

indicated by two bands at 2335 and 2360 $cm^{-1}$. The infrared bands assigned

to these nonselective oxidation products were found to be more intense

for the P/V = 1.0 and 1.1 catalysts. However, integral reactor studies

indicate lower specific (per square meter catalyst) rates of n-butane and

maleic anhydride combustion for catalysts incorporating "excess"

phosphorus (21, 27). The apparent intensity of bands in the infrared

spectra is not simply a function of relative reaction rates, but is also

dependent on surface area, sample thickness, and beam area.

In addition to n-butane, maleic anhydride, $H_2O$, $CO_2$, and CO (the major

components of simplified reaction pathways), three additional adsorbed

species were observed in these in situ infrared experiments at 400°C.

Both adsorbed maleic acid and adsorbed olefinic species were identified

on the surfaces of the catalysts. These adsorbed species were not detected

during integral reactor studies using these catalysts and may exist as

reactive intermediates for n-butane conversion to maleic anhydride. The

concentration of these adsorbed species was found to vary with catalyst

phosphorus loading and time of exposure of the catalyst to reaction conditions at 400°C.

The assignment of _in situ_ vibrational bands to maleic acid is assisted by the infrared spectrum of solid maleic acid (spectrum 9[b]). Three C=C vibrations are observed at 1568, 1590, and 1636 $cm^{-1}$, a single carbonyl stretching vibration is found at 1706 $cm^{-1}$, and olefinic =CH stretching vibrations are observed at 3058 $cm^{-1}$. O-H bending vibrations are observed at 1433 $cm^{-1}$; the C-H bending vibrations are found at 1460 $cm^{-1}$. _In situ_ studies revealed infrared bands near 1710 $cm^{-1}$ with a weaker band at 1433 $cm^{-1}$. These bands are assigned to the carbonyl stretch and O-H bending vibrations of maleic acid. The weak =CH stretch at 3058 $cm^{-1}$ and the more intense C=C vibrations at 1590 and 1636 $cm^{-1}$ of maleic acid were not observed in the _in situ_ FTIR studies. The intensity of the 1710 $cm^{-1}$ C=O stretch of maleic acid was found to increase rapidly during three hours of reaction at 400°C; after three hours, a steady state concentration of this species was achieved. The intensity of the C=O stretch of maleic acid was also found to increase with catalyst phosphorus loading. This suggests that the more selective pathway from n-butane to maleic anhydride (as indicated by reactivity studies (21)) involves higher surface concentrations of maleic acid.

The assignment of _in situ_ vibrational bands to 1-butene is assisted by the infrared spectrum of gaseous 1-butene (spectrum 8[b]). Symmetric =$CH_2$ stretching vibrations are observed as 2980 $cm^{-1}$, whereas asymmetric =$CH_2$ stretching vibrations are observed at 3084 $cm^{-1}$. The remaining C-H stretching vibrations and the C=H bending vibrations (1463 $cm^{-1}$) of 1-butene occur at frequencies which can be obscured by the C-H vibrations

of n-butane (spectrum 8[a]). The C=C stretching vibration of 1-butene

is assigned to the 1645 $cm^{-1}$ band. In situ catalytic experiments resulted

in the observation of infrared bands at 1650 (shoulder) and 3081 (weak)

$cm^{-1}$; these bands were assigned to the C=C stretching vibration and

asymmetric =$CH_2$ stretching vibration of an adsorbed 1-butene species. The

intensity of the 1650 $cm^{-1}$ C=C stretch was observed at near equal strength

for each catalyst studied and was found to intensify until a steady state

was reached after three hours of reaction at 400°C. An in situ FTIR study

of 1-butene selective oxidation to maleic anhydride will be presented in

a future publication (28).

Additional infrared bands perhaps indicative of another adsorbed

reactive species was observed on the P/V = 1.0 and P/V = 1.1 catalysts.

Sharp bands at 1571 and 3012 $cm^{-1}$ were observed at 400°C and were assigned

to the C=C and =CH stretching vibrations of an adsorbed olefin resembling

cyclobutene or a strongly conjugated π-allyl surface complex. The 1571

$cm^{-1}$ band was not assigned to the C=C vibration of maleic acid since maleic

acid has three C=C bands at 1569, 1590, and 1637 $cm^{-1}$ (spectrum 9[b]).

The possibility that furan and 1,3-butadiene are reaction intermediates

for n-butane selective oxidation was discussed earlier. However, this

study can offer no evidence for the existence of these species on the

catalyst surface. Infrared spectra of furan and 1,3-butadiene are reported

in the literature (28). During these in situ oxidation studies, no

observation was made of the intense C=C stretching bands of furan at 1380,

1486, and 1593 $cm^{-1}$, or of butadiene at 1588 and 1606 $cm^{-1}$. Furthermore

the =CH bands of furan at 3121 and 3150 $cm^{-1}$, and butadiene at 3110 $cm^{-1}$

were not observed.  An _in situ_ FTIR study of 1,3-butadiene selective oxidation to maleic anhydride will be presented in a future publication (29).

Table 1 summarizes the infrared band assignments at 400°C for n-butane selective oxidation to maleic anhydride by V-P-O catalysts.

Table 1. Vibrational assignments at 400°C

| P/V = 0.9 | P/V = 1.0 | P/V = 1.1 | Assignment | Species |
|-----------|-----------|-----------|------------|---------|
| 1430 | 1430 | 1432 | $\delta-OH$ | maleic acid |
| 1462 | 1462 | 1461 | $\delta-CH_2$, $\delta-CH_3$ | n-butane |
| 1650 | 1650 | 1650 | $\nu$ C=C | 1-butene |
| | 1571 | 1570 | $\nu$ C=C | |
| 1720 | 1715 | 1705 | $\nu$ C=O | maleic acid |
| 1779 | 1775 | 1778 | $\nu$ C=O | maleic anhydride |
| 1848 | 1842 | 1847 | $\nu$ C=O | maleic anhydride |
| 2143 | 2143 | 2143 | $\nu$ C≡O | CO |
| 2350 | 2350 | 2350 | $\nu$ O=C=O | $CO_2$ |
| 2879 | 2877 | 2879 | $\nu-CH_2$ | n-butane |
| 2933 | 2934 | 2933 | $\nu-CH_2$ | n-butane |
| 2966 | 2965 | 2966 | $\nu-CH_3$ | n-butane |
| | 3010 | 3010 | $\nu=CH$ | |
| 3081 | 3081 | 3082 | $\nu-CH_2$ | 1-butene |

## CONCLUSIONS

In situ Fourier transform infrared spectroscopy is a highly useful
technique for examining the nature of adsorbed species on V-P-O catalysts
used for n-butane oxidation. The presence of reactants (n-butane),
partially oxidized products (maleic anhydride), and combustion products
($CO$, $CO_2$, $H_2O$) could be confirmed on the surfaces of the catalysts.
Maleic acid and olefins were detected as reactive surface species. How-
ever, other possible reaction intermediates such as furan and 1,3-butadiene
were not observed. The adsorptive properties of the catalyst were found
to depend on the catalyst P-to-V ratio, the reaction temperature, and the
time on-stream.

## ACKNOWLEDGEMENT

REFERENCES

1. Mount, R. A. Maleic anhydride, maleic acid, and fumaric acid. Encyclopedia of Chemical Technology. Vol. 14. 3rd ed. New York: John Wiley & Sons; 1981.

2. Cavani, F.; Centi, G.; Trifirò, F. Study of n-butane oxidation to maleic anhydride in a tubular flow stacked-pellet reactor: influence of phosphorus on the selectivity. Appl. Catal. 15: 151-160; 1985.

3. Hodnett, B. K.; Delmon, B. Influence of the phosphorus to vanadium ratio on the solid state chemistry and redox properties of vanadium phosphate-based catalysts. J. Catal. 88: 43-53; 1984.

4. Moser, T. P.; Schrader, G. L. Selective oxidation of n-butane to maleic anhydride by model V-P-O catalysts. J. Catal. 92: 216-231; 1985.

5. Shimoda, T.; Okahara, T.; Misono, M. Preparation of vanadium-phosphorus mixed oxide (P/V = 1) catalysts and their application in butane oxidation to maleic anhydride. Bull. Chem. Soc. Jpn. 58: 2163-2171; 1985.

6. Ostroushko, V. I.; Kernos, Yu. D.; Ioffe, I. I. Oxidation of butenes with a vanadium-phosphorus catalysts. Neftekhimiya 12(3): 362-369; 1972.

7. Morselli, L.; Riva, A.; Trifirò, F.; Zucchi, M.; Emig, G. The chemistry of V and P oxides based oxidation catalysts. I - relationship between structure and activity for the oxidation of 1-butene to maleic anhydride. La Chimica E L'Industria 60(10): 791-797; 1978.

8. Ai, M.; Boutry, P.; Montarnal, R. Kinetics of the oxidation of butene to maleic anhydride on vanadium pentoxide-phosphorus pentoxide. I. Experimental kinetics. Bull. Soc. Chim. Fr. 8-9: 2775-2782; 1970.

9. Ai, M. A study of the partial catalytic oxidation of hydrocarbons. V. The effect of phosphorus addition to the vanadium catalyst on the oxidation of butene, butadiene, and furan. Bull. Chem. Soc. Jpn. 43(11): 3490-3495; 1970.

10. Ai, M.; Suzuki, S. Oxidation activity and acidity of $V_2O_5-P_2O_5$ catalyst. Bull. Chem. Soc. Jpn. 47(12): 3074-3077; 1974.

11. Brkíc, D.; Trifirò, F. Kinetic analysis of 1-butene oxidation to maleic anhydride with a polyfunctional catalyst. Ind. Eng. Chem. Prod. Res. Dev. 18(4): 333-339; 1979.

12. Sunderland, P. Butene-2 oxidation to maleic anhydride. Ind. Eng. Chem. Prod. Res. Dev. 15(2): 90–99; 1976.

13. Varma, R. L.; Saraf, D. N. Oxidation of butene to maleic anhydride. I. Kinetics and mechanism. Journal of Catalysis 55: 361–372; 1978.

14. Escardino, A.; Solá, C.; Ruiz, F. Oxidacion catalitica de butano a anhidrido maleico. Anales de Quimica 69: 385–396; 1973.

15. Wohlfahrt, K.; Hofmann, H. Kinetik der synthese von maleinsäure-anhydrid aus n-butan. Chem. Ing. Tech. 52(10): 811–814; 1980.

16. Hodnett, B. K.; Permanne, Ph.; Delmon, B. Influence of P/V ratio on the phase composition and catalytic activity of vanadium phosphate based catalysts. Applied Catalysis 6: 231–244; 1983.

17. Wüstneck, N.; Wolf, H.; Seeboth, H. Role of vanadyl pyrophosphate in mild oxidation of hydrocarbons. React. Kinet. Catal. Lett. 21(4): 497–503; 1982.

18. Dent, A. L.; Kokes, R. J. The nature of adsorbed propylene on zinc oxide: formation of π-allyl species. J. Am. Chem. Soc. 92(23): 6709–6718; 1970.

19. Dent, A. L.; Kokes, R. J. The nature of adsorbed propylene on zinc oxide: reactions of π-allyl species. J. Am. Chem. Soc. 92: 6718–6725; 1970.

20. Katsumoto, K.; Marquis, D. U.S. Patent 4 132 670; 1979.

21. Wenig, R. W.; Schrader, G. L. V–P–O industrial catalysts for n–butane oxidation: characterization and kinetic measurements. Ind. Eng. Chem. Fund., accepted.

22. Hodnett, B. K. Vanadium–phosphorus–oxide catalysts for the selective oxidation of $C_4$ hydrocarbons to maleic anhydride. Catal. Rev.-Sci. Eng. 27(3): 374–424; 1985.

23. Sheppard, N. The assignment of the vibrational spectra of the $C_4$ hydrocarbons butyne-1, butene-1, and vinyl acetylene, to the normal modes of vibration of these molecules. J. Chem. Phys. 17(1): 74–79; 1949.

24. Bellamy, L. J. The infrared spectra of complex molecules. New York: Chapman and Hall; 1980.

25. Chang, C. C.; Conner, W. C.; Kokes, R. J. Isomerization of 1-butene on ZnO. J. Phys. Chem. 77: 1957–1971; 1973.

26. Hill, R. R.; Rendell, D. A. The interpretation of infrared spectra. London: Heyden; 1975.

27. Moser, T. P.; Wenig, R. W.; Schrader, G. L. Conversion of maleic anhydride by V-P-O catalysts. Appl. Catal., submitted.

28. Pouchert, C. The Aldrich library of infrared spectra. Milwaukee: Aldrich; 1981.

29. Wenig, R. W.; Schrader, G. L. In situ FTIR study of 1-butene and 1,3-butadiene selective oxidation by V-P-O catalysts. J. Phys. Chem., submitted.

SECTION IV.  IN SITU FTIR SPECTROSCOPY OF 1-BUTENE AND 1,3-BUTADIENE
            SELECTIVE OXIDATION TO MALEIC ANHYDRIDE ON V-P-O CATALYSTS

## ABSTRACT

The selective oxidation of 1-butene and 1,3-butadiene was studied by transmission infrared spectroscopy. Vanadium-phosphorus-oxygen catalysts prepared by the reaction of $V_2O_5$ with $H_3PO_4$ in alcohol solution were used. Infrared spectra were collected _in situ_ during the flow of 75 ccm of 1.5% hydrocarbon-in-air mixtures over catalysts having P-to-V ratios of 0.9, 1.0, and 1.1. Reaction temperatures from 300°C to 400°C were investigated with 1-butene feeds, whereas the highly reactive 1,3-butadiene was studied only at 300°C.

An adsorbed butadiene species, maleic acid, and maleic anhydride were observed during both olefin partial oxidation studies. Evidence was obtained for a second olefin species which had been previously observed for _in situ_ n-butane selective oxidation studies. Concentrations of adsorbed species were found to vary with catalyst phosphorus loading, reaction temperature, and time of exposure to reaction conditions.

## INTRODUCTION

Vanadium-phosphorus oxides have been used successfully for the industrial production of maleic anhydride from $C_4$ hydrocarbons. Despite the commercial importance of this catalytic process, there remains much uncertainty concerning the mechanism of the selective oxidation catalysis. Of particular interest is the ability of V-P-O catalysts to activate paraffin feedstocks such as n-butane. In previous investigations of n-butane oxidation to maleic anhydride we observed the presence of olefins in the reactor effluent (1) and on the surfaces of V-P-O catalysts (2). In this paper we report further use of in situ Fourier transform infrared spectroscopy to examine adsorbed species on the surfaces of catalysts during 1-butene and 1,3-butadiene oxidation.

The reaction pathway for 1-butene selective oxidation to maleic anhydride is generally believed to involve 1,3-butadiene (3, 4) or crotonaldehyde (5) and furan (6) as reaction intermediates. Varma and Saraf (7) describe 1,3-butadiene and possibly furan as reaction intermediates; a pathway for the complete combustion of 1-butene, butadiene, and maleic anhydride to carbon oxides and water was also proposed. In contrast, the proposed reaction pathways for n-butane oxidation have been much simpler. The models by Escardino et al. (8) and Wohlfahrt and Hofmann (9) have implied the direct conversion of n-butane to maleic anhydride and the possible combustion of maleic anhydride to carbon oxides and water. The reaction pathways described by Hodnett et al. (10) and Wüstneck et al. (11) are very similar and do not postulate the involvement of olefins in the paraffin oxidation mechanism.

In a previous paper (2), we reported an *in situ* infrared study of n-butane adsorbed on industrial V-P-O catalysts with different P-to-V ratios. In these studies an adsorbed 1-butene species, a conjugated (or possibly strained) olefin species, and maleic acid were observed on the surfaces of V-P-O catalysts. The present study has used *in situ* infrared spectroscopy to investigate the reactivity of adsorbed olefin species such as 1-butene and 1,3-butadiene; further understanding of the mechanism of paraffin (n-butane) oxidation has been achieved.

# EXPERIMENTAL PROCEDURE

## Catalyst Synthesis and Characterization

Vanadium-phosphorus mixed oxide catalysts having P-to-V ratios of 0.9, 1.0, and 1.1 were prepared by the addition of $H_3PO_4$ to reduced $V_2O_5$ (12). Characterization of the precipitated, air-calcined, and used V-P-O catalysts was performed using X-ray diffraction, laser Raman spectroscopy, infrared spectroscopy, and X-ray photoelectron spectroscopy. The synthesis procedure and characterization results are reported elsewhere (12).

## Kinetic Measurements

Kinetic measurements for n-butane selective oxidation were performed using an integral flow reactor and gas chromatograph analytical system. Catalyst activity, selectivity, and specific rates of oxidation as a function of catalyst P-to-V ratio are reported elsewhere (12).

## Catalyst Wafer Preparation

"Ultra-thin" 0.1 mm catalyst disks were prepared from calcined catalyst powder. Highly polished stainless steel dies were used to compress the catalyst under a load of 15,000 lbs. The catalyst wafer was transferred to a stainless steel sample holder within the quartz cavity of the infrared cell (2). Catalyst pretreatment was accomplished by increasing the cell temperature to 300°C for 3 hours in a flowing stream of air (75 $cm^3$/min). Vibrational bands due to residual solvent (1650-1900 $cm^{-1}$) and adsorbed waters (1620-1640 and 3100-3600 $cm^{-1}$) were usually removed.

## In Situ FTIR Cell and Gas Delivery System

The in situ infrared cell and gas delivery system has been described previously (2). For this study a feed gas consisting of 1.5% hydrocarbon-in-air was obtained by high accuracy rotameters. Total flow rates of 75 $cm^3$/min were used for the n-butene and 1,3-butadiene studies. Moisture removal was provided by 3 Å molecular sieves.

## Fourier Transform Infrared Spectrometer

A Nicolet Model 60-SX FTIR was used to obtain the infrared spectra. Typically 600 scans were accumulated at 2 $cm^{-1}$ resolution. All spectra were ratioed against single beam spectra of a dry $N_2$ purged cell with KBr windows. Consequently, the spectra recorded in this paper contain infrared bands due to adsorbed species, the catalyst, and gaseous species present in the cell.

## RESULTS

Industrial reactors for olefin oxidation typically operate in the range of 350°C to 450°C. In this study somewhat lower temperatures were used to stabilize specific surface species and to assist in understanding the mechanism of olefin partial oxidation. Reaction temperatures from 300°C to 400°C were investigated for 1-butene-air feeds while the highly reactive 1,3-butadiene-air feeds were studied only at 300°C.

The infrared spectra of adsorbed species were found to vary with catalyst P-to-V ratio, reaction temperature, and time of exposure to olefin-air feeds. The results are presented separately for 1-butene and 1,3-butadiene selective oxidation as a function of catalyst P-to-V ratio.

### 1-Butene Studies

The _in situ_ infrared spectra for the selective oxidation of 1-butene by V-P-O catalysts having P-to-V ratio 0.9, 1.0, and 1.1 are presented in Figures 1, 2, and 3, respectively. Infrared spectra are provided for the pretreated catalyst at 300°C and the functioning catalyst with 1-butene-air flow at 300°C and 400°C.

#### Catalysts with P/V = 0.9

Figure 1 presents the _in situ_ infrared spectra for the P/V = 0.9 catalyst. Spectrum 1[a] was observed for the pretreated catalyst at 300°C prior to 1-butene-air flow. As a result of air pretreatment waters of crystallization (1620, 3100-3600 $cm^{-1}$) and residual solvent bands (1680-1857 $cm^{-1}$) were largely removed. Infrared spectra of fresh and pretreated catalysts have been described previously (2).

Figure 1.   Reaction of 1-butene on P/V = 0.9 V-P-O catalyst

        (a) pretreated catalyst at 300°C
        (b) 1 hour reaction at 300°C
        (c) 2 hour reaction at 300°C
        (d) 3 hour reaction at 400°C
        (e) 4 hour reaction at 400°C

Spectra 1[b]-1[e] were collected during the flow of a 1.5% 1-butene-in-air mixture. Spectrum 1[b] was obtained for the pretreated catalyst at 300°C after one hour of reactive gas flow. A broad infrared band (1570-1615 $cm^{-1}$) with a peak at 1605 $cm^{-1}$ was observed. This band could not be assigned to the O-H bending vibrations of adsorbed water since such bands are not stable at 300°C (2) and O-H stretching vibrations were not observed. This band was assigned to the C=C stretching vibrations of a conjugated $C_4$ olefin resembling butadiene, or butadiene and a second conjugated olefinic species. The infrared band at 1729 $cm^{-1}$ was assigned to a residual solvent band which was not removed during air pretreatment. Infrared bands at 1779 and 1847 $cm^{-1}$ were assigned to the symmetric and asymmetric carbonyl stretching vibrations of adsorbed maleic anhydride. Vibrational-rotational bands centered at 2143 $cm^{-1}$ were assigned to gaseous CO; infrared bands at 2322 and 2358 $cm^{-1}$ were assigned to gaseous $CO_2$. Stretching vibrations at 2961 $cm^{-1}$ and 3085 $cm^{-1}$ were assigned to $-CH_2$ and $=CH_2$ vibrations of 1-butene. Spectrum 1[c] was collected following two hours of reaction at 300°C. An intensification of the carbonyl stretching vibrations of maleic anhydride at 1779 and 1847 $cm^{-1}$ was observed. A new band at 1725 $cm^{-1}$ (superimposed upon the 1729 $cm^{-1}$ solvent band) was assigned to the carbonyl stretch of maleic acid.

At 400°C infrared spectra were collected at one hour intervals (spectra 1[d], 1[e]). The broad infrared band found earlier at 1570-1615 $cm^{-1}$ was observed as a shoulder band from 1570 to 1640 $cm^{-1}$. The width and asymmetry of this band suggests two species such as butadiene (1605 $cm^{-1}$) and a second conjugated olefin (closer to 1570 $cm^{-1}$) could be present. At 400°C the activity of the catalyst increased as indicated by

growth in the bands corresponding to maleic acid (1725 $cm^{-1}$), maleic

anhydride (1775 and 1845 $cm^{-1}$), CO (2143 $cm^{-1}$) and $CO_2$ (2330 $cm^{-1}$). A

decrease in intensity of the 2958 and 3085 $cm^{-1}$ ($\nu_{-CH_2}$ and $\nu_{=CH_2}$) infrared

bands indicated lower surface concentrations of 1-butene. An additional

adsorbed olefin was suggested by a 3010 $cm^{-1}$ $=CH_2$ stretching vibration.

Strong O-H stretching vibrations at 3100-3600 $cm^{-1}$ were assigned to

adsorbed water.

## Catalysts with P/V = 1.0

The in situ infrared spectra for the P/V = 1.0 catalyst are presented

in Figure 2. Spectrum 2[a] was observed for the pretreated V-P-O catalyst

at 300°C. Spectrum 2[b] was collected after 1 hour of 1-butene-air flow.

A wide infrared band was observed in the region 1550-1615 $cm^{-1}$ and

assigned to the C=C stretching vibrations of conjugated $C_4$ olefin(s). The

infrared band at 1722 $cm^{-1}$ was assigned to the C=O stretching vibration of

adsorbed maleic acid. Infrared bands at 1775 and 1845 $cm^{-1}$ were assigned

to the two carbonyl stretching vibrations of adsorbed maleic anhydride.

Vibrational-rotational bands at 2143 $cm^{-1}$ and 2330 $cm^{-1}$ were assigned to

gaseous CO and gaseous $CO_2$, respectively. Adsorbed olefin species were

assigned to a broad C-H stretching band centered at 2958 $cm^{-1}$. After two

hours of reaction at 300°C (spectrum 2[c]) the C=O stretching vibrations

of maleic acid (1722 $cm^{-1}$) and maleic anhydride (1775 and 1845 $cm^{-1}$) were

found to intensify. The band assigned to a C=C stretch of a conjugated

olefinic species was observed at 1750-1615 $cm^{-1}$ After one hour of reaction

at 400°C an intensification of the infrared bands corresponding to each
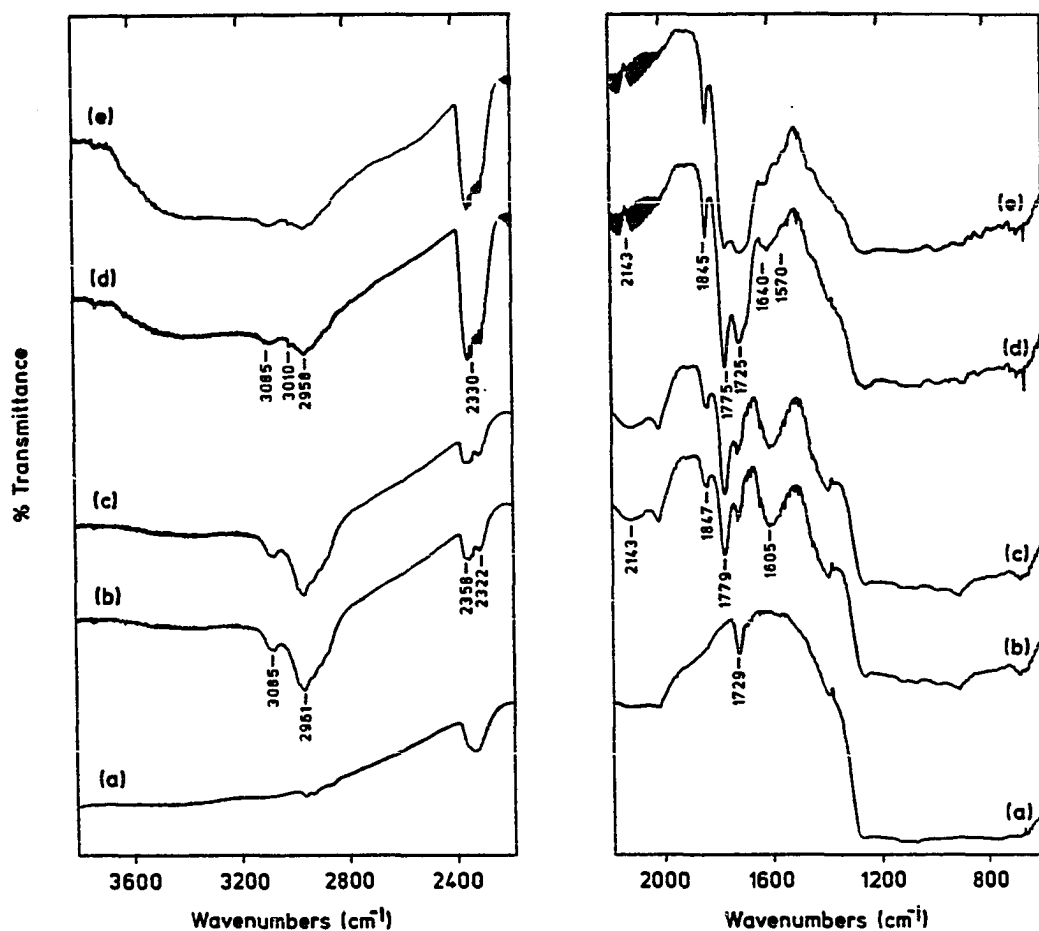
Figure 2.  Reaction of 1-butene on P/V = 1.0 V-P-O catalyst

.(a)  pretreated catalyst at 300°C
(b)  1 hour reaction at 300°C
(c)  2 hour reaction at 300°C
(d)  3 hour reaction at 400°C

adsorbed and gaseous species was observed. Adsorbed water was indicated by weak O-H stretching vibrations from 3100-3600 $cm^{-1}$.

## Catalysts with P/V = 1.1

The in situ infrared spectra for the P/V = 1.1 catalyst are presented in Figure 3. Spectrum 3[a] was obtained for the P/V = 1.1 catalyst at 300°C following air pretreatment. Spectrum 3[b] was collected after one hour of 1-butene-air flow. Infrared bands at 1460 and 1650 $cm^{-1}$ (shoulder) were assigned to the $CH_2$ bending and C=C stretching vibrations of 1-butene. The infrared band centered at 1615 $cm^{-1}$ was assigned to the C=C stretching vibration of a conjugated $C_4$ olefin (probably adsorbed 1,3-butadiene). The C=O stretching vibrations of maleic acid (1727 $cm^{-1}$) and maleic anhydride (1777 and 1845 $cm^{-1}$) were also identified. Gaseous $CO_2$ was assigned to the band at 2336 $cm^{-1}$; adsorbed 1-butene was assigned to the weak C-H stretching band at 2963 $cm^{-1}$. After two hours of reaction at 300°C (spectrum 3[c]) the carbonyl stretching vibrations of maleic acid and maleic anhydride were found to intensify; little change in intensity was observed for the 1615 $cm^{-1}$ band assigned to a conjugated olefin species.

At 400°C infrared spectra were collected at 1 hour intervals (spectra 3[d], 3[e]). The 1615 $cm^{-1}$ C=C stretching vibration assigned to adsorbed 1,3-butadiene was observed at 1595-1615 $cm^{-1}$. The activity of the catalyst was found to increase as indicated by growth in the bands corresponding to maleic acid (1727 $cm^{-1}$), maleic anhydride (1777 and 1845 $cm^{-1}$), CO (2143 $cm^{-1}$), and $CO_2$ (2336 $cm^{-1}$). Decreased intensities of C-H bending (1460 $cm^{-1}$) and C-H stretching (2963 $cm^{-1}$) vibrations indicated lower surface concentrations of 1-butene at 400°C.
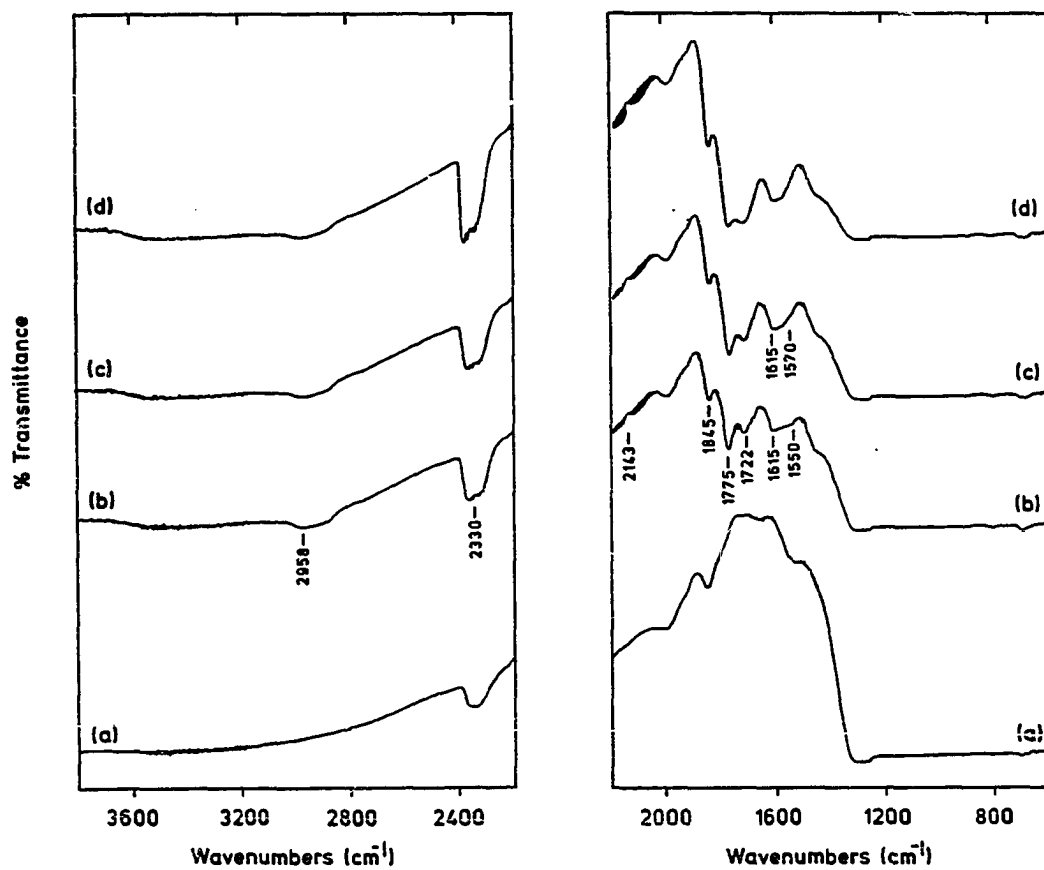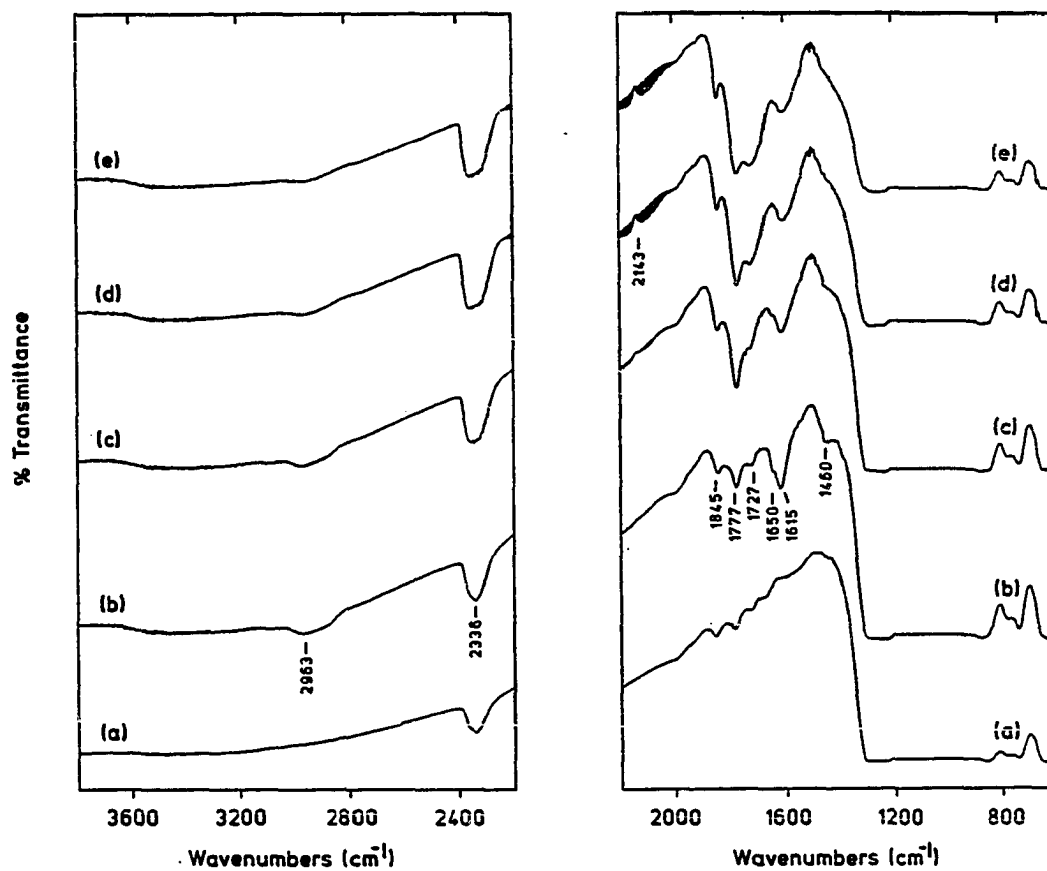
Figure 3. Reaction of 1-butene on P/V - 1.1 V-P-O catalyst

(a) pretreated catalyst at 300°C
(b) 1 hour reaction at 300°C
(c) 2 hour reaction at 300°C
(d) 3 hour reaction at 400°C
(e) 4 hour reaction at 400°C

## 1,3-Butadiene Studies

The _in situ_ infrared spectra for the reaction of 1,3-butadiene on the

P/V = 0.9, 1.0, and 1.1 catalysts are presented in Figures 4, 5, and 6.

The infrared spectrum of the pretreated catalysts are shown at 300°C;

_in situ_ spectra of the functioning V-P-O catalysts are displayed after 20,

40, and 60 minutes of 1,3-butadiene-air flow at 300°C.

### Catalysts with P/V = 0.9

The _in situ_ infrared spectra for the P/V = 0.9 catalyst are presented

in Figure 4. Spectrum 4[a] was observed for the pretreated catalyst at

300°C. Spectrum 4[b] was observed after 20 minutes of 1,3-butadiene-air

flow at 300°C. A broad infrared band (1570–1620 $cm^{-1}$) with a minimum at

1600 $cm^{-1}$ was observed and assigned to adsorbed butadiene and possibly a

second adsorbed olefin species. A 1690 $cm^{-1}$ band was also observed and

suggests an adsorbed trans-2-butene species. The infrared band at 1721

$cm^{-1}$ was assigned to the C=O stretching vibration of maleic acid, two bands

at 1777 and 1847 $cm^{-1}$ were assigned to the C=O stretching vibrations of

maleic anhydride. Gaseous CO and $CO_2$ were indicated by vibrational-

rotational bands centered at 2143 and 2333 $cm^{-1}$. A broad band at 2965

$cm^{-1}$ and a weak band at 3081 $cm^{-1}$ were assigned to the =CH and $=CH_2$

stretching vibrations of adsorbed olefin species. After 40 minutes of

reaction (spectrum 4[c]) the carbonyl vibrations of maleic acid (1721 $cm^{-1}$)

and maleic anhydride (1777 and 1847 $cm^{-1}$) were observed to intensify.

Growth in the 1690 $cm^{-1}$ C=C stretching vibration of trans-2-butene was also

observed. Following 60 minutes of butadiene-air flow (spectrum 4[d])

steady state was reached.
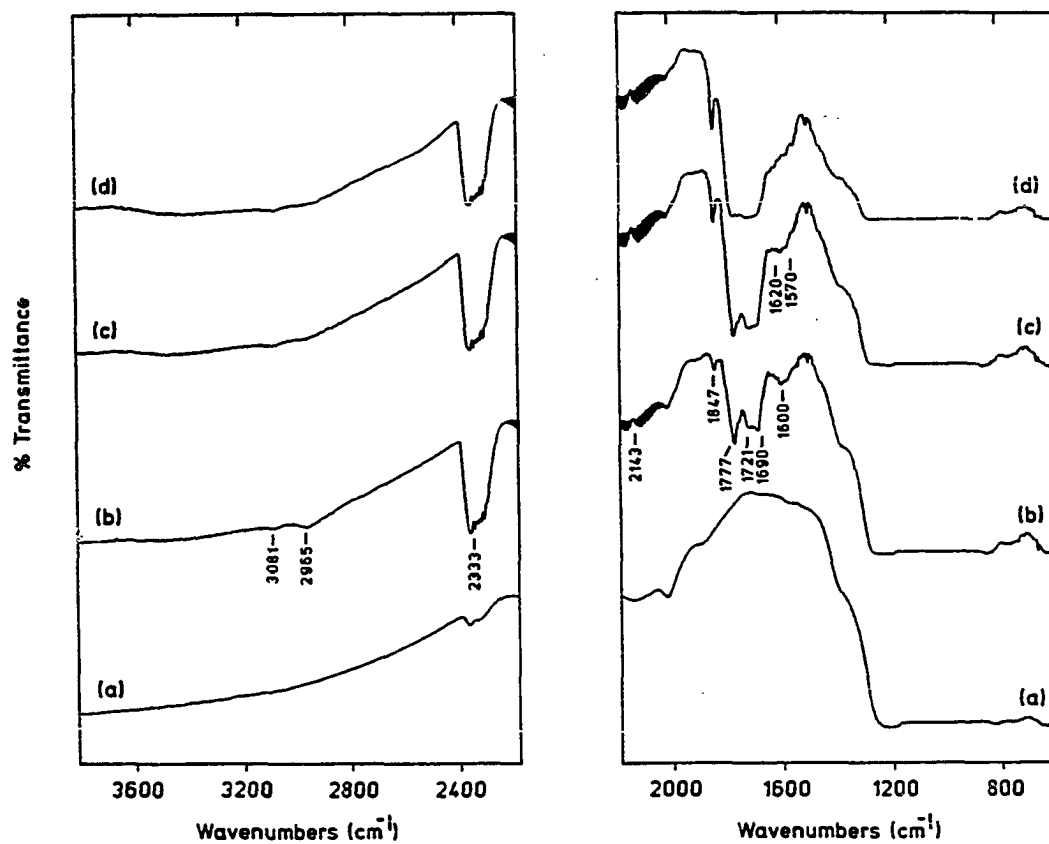
Figure 4. Reaction of 1,3-butadiene on P/V = 0.9 V-P-O catalyst

(a) pretreated catalyst at 300°C
(b) 20 minutes reaction at 300°C
(c) 40 minutes reaction at 300°C
(d) 60 minutes reaction at 300°C

## Catalysts with P/V = 1.0

The _in situ_ infrared spectra for the P/V = 1.0 catalyst are presented in Figure 5. Spectrum 5[a] was observed for the pretreated catalyst at 300°C. Spectrum 5[b] was observed after 20 minutes of 1,3-butadiene air flow at 300°C. An adsorbed butadiene species was assigned to the infrared band (1580-1605 $cm^{-1}$) centered at 1595 $cm^{-1}$. A 1690 $cm^{-1}$ band suggested the C=C stretch of a trans-2-butene species or possibly the C=O stretch of an adsorbed acid species. The infrared band at 1722 $cm^{-1}$ was assigned to the C=O stretching vibration of maleic acid; infrared bands at 1733 and 1843 $cm^{-1}$ were assigned to the C=O stretching vibrations of maleic anhydride. Gaseous CO was assigned to vibrational-rotational bands at 2143 $cm^{-1}$; two bands at 2330 $cm^{-1}$ and 2358 $cm^{-1}$ were assigned to gaseous $CO_2$. Adsorbed water was indicated by O-H stretching vibrations at 3100-3600 $cm^{-1}$. After 40 minutes of reaction at 300°C (spectrum 5[c]) the vibrational bands assigned to adsorbed trans-2-butene (1690 $cm^{-1}$), maleic acid (1722 $cm^{-1}$); and maleic anhydride (1773 and 1843 $cm^{-1}$) were observed to intensify. Spectrum 5[d] indicated that steady state was reached after 60 minutes of butadiene-air flow at 300°C.

## Catalysts with P/V = 1.1

The _in situ_ infrared spectra for the P/V = 1.1 catalyst are presented in Figure 6. Spectrum 6[a] was observed for the pretreated catalyst at 300°C. Spectrum 6[b] was observed following 20 minutes of butadiene-air flow at 300°C. An adsorbed butadiene species was assigned to the infrared band (1580-1605) with a minimum at 1600 $cm^{-1}$. An additional adsorbed species was again indicated by a 1687 $cm^{-1}$ band. The infrared band
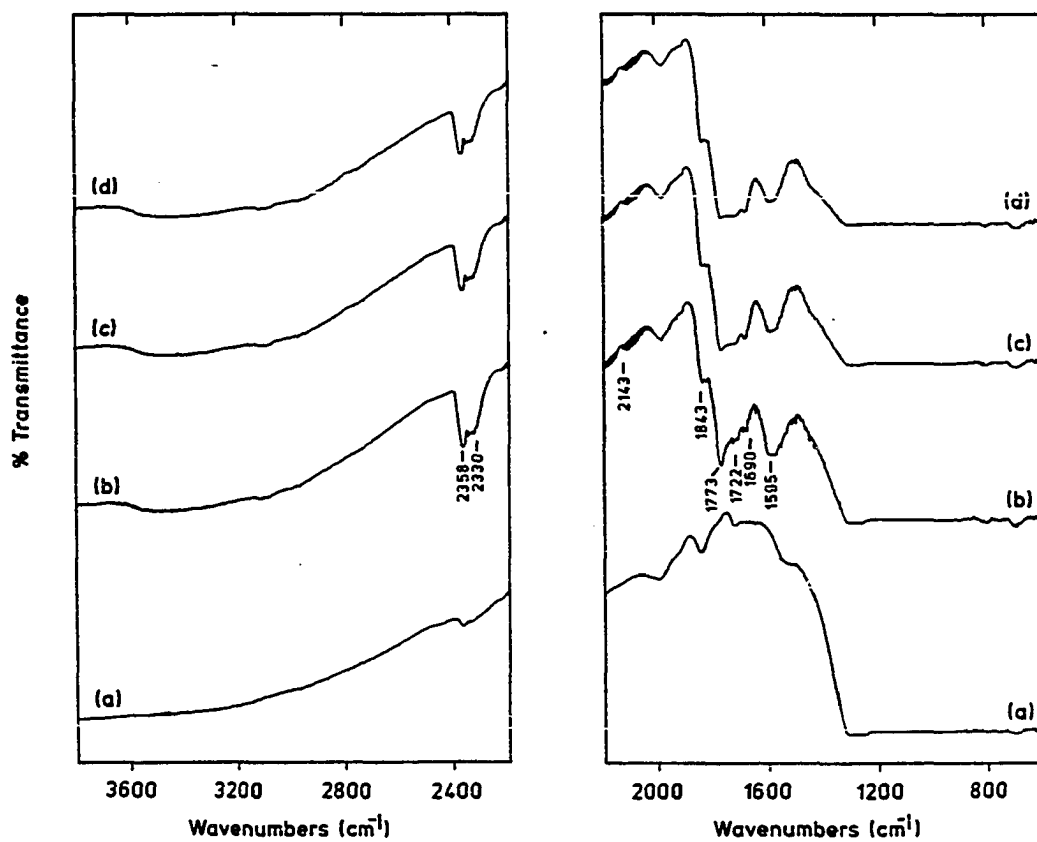
Figure 5. Reaction of 1,3-butadiene on P/V = 1.0 V-P-O catalyst

       (a) pretreated catalyst at 300°C
       (b) 20 minutes reaction at 300°C
       (c) 40 minutes reaction at 300°C
       (d) 60 minutes reaction at 300°C
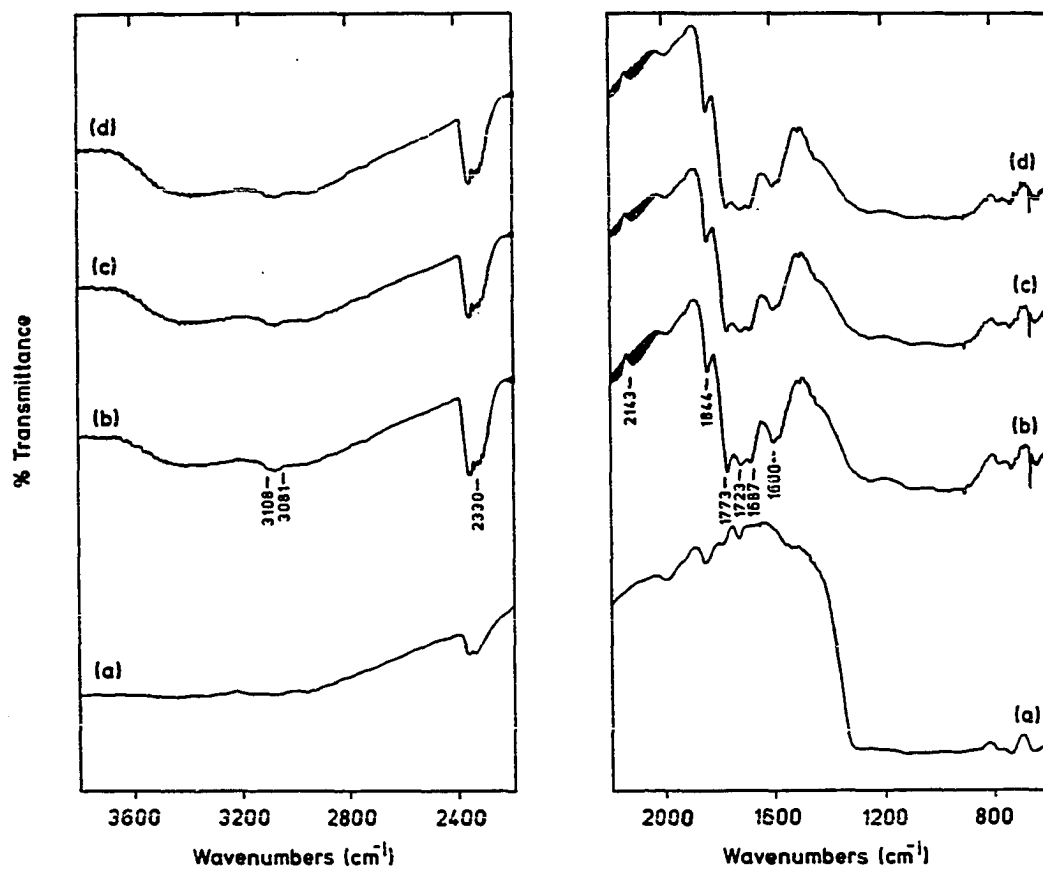
Figure 6. Reaction of 1,3-butadiene on P/V = 1.1 V-P-O catalyst

      (a) pretreated catalyst at 300°C
      (b) 20 minutes reaction at 300°C
      (c) 40 minutes reaction at 300°C
      (d) 60 minutes reaction at 300°C

at 1723 cm$^{-1}$ was assigned to the C=O stretching vibration of maleic acid; two infrared bands at 1773 and 1844 cm$^{-1}$ were assigned to the C=O stretching vibrations of maleic anhydride. The vibrational-rotational bands observed at 2143 cm$^{-1}$ and 2330 cm$^{-1}$ were assigned to gaseous CO and gaseous $CO_2$, respectively. Infrared bands at 3081 and 3108 cm$^{-1}$ were assigned to the =CH stretching vibrations of butadiene. Adsorbed water was indicated by O-H stretching vibrations from 3100-3600 cm$^{-1}$. During the next 40 minutes of reaction at 300°C (spectra 6[c] and 6[d]) the concentration of adsorbed species increased to steady state values.

## DISCUSSION

The mechanism of 1-butene selective oxidation is generally believed to proceed with 1,3-butadiene (4) and furan (6) as reaction intermediates. Crotonaldehyde and 2-butenes are usually considered to be side products. The reaction pathway proposed by Varma and Saraf (7) involves the selective oxidation of 1-butene to maleic anhydride via a 1,3-butadiene surface intermediate (furan is described as a "secondary" intermediate). The combustion of 1-butene, butadiene, and maleic anhydride to carbon oxides and water is proposed in parallel reactions. The reaction scheme follows:

1-butene ⟶ butadiene ⟶ maleic anhydride

$CO_x$, $H_2O$
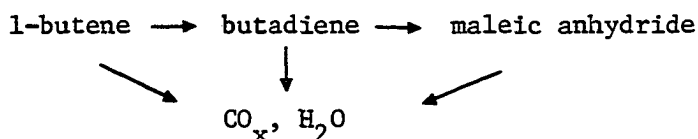
The *in situ* infrared olefin oxidation experiments have identified 1-butene, butadiene, maleic anhydride, CO, $CO_2$, and $H_2O$ during the 1-butene studies and butadiene, maleic anhydride, CO, $CO_2$, and $H_2O$ during the butadiene studies. The concentration of the adsorbed species was found to vary with catalyst phosphorus loading, reaction temperature, and time of reaction.

An increase in catalyst phosphorus loading was found to reduce catalyst activity and to increase selectivity for maleic anhydride with 1-butene-air feeds; little effect was observed on the *in situ* infrared spectra with the highly reactive 1,3-butadiene feeds. The decrease in concentration of 1-butene species with "excess" catalyst phosphorus suggests that higher phosphorus catalysts may have fewer sites for olefin adsorption. An increase in reaction temperature from 300°C to 400°C

(1-butene studies) was found to increase catalyst activity (intensity of $CO_x$, $H_2O$, and maleic anhydride bands), while decreasing catalyst selectivity (ratio of $CO_x$ to maleic anhydride band intensities). Steady state band intensities were observed in two hours with 1-butene-air feeds and one hour with butadiene-air feeds.

The assignment of infrared bands for 1-butene species, 1,3-butadiene species, and maleic anhydride under in situ conditions relied on a comparison with pure compound spectra; assignments to adsorbed water and gaseous carbon oxides were readily accomplished (13). Pure compound reference spectra and assignments for 1-butene and maleic anhydride are discussed elsewhere (2). The gas phase spectrum of 1,3-butadiene (spectrum 7[a]) is presented in Figure 7. Infrared bands at 1371 and 1390 $cm^{-1}$ are assigned to C-H bending modes; two intense bands at 1588 and 1606 $cm^{-1}$ are assigned to C=C stretching vibrations of 1,3-butadiene. Olefinic $=CH_2$ stretching vibrations are observed at 3110 and 3090 $cm^{-1}$ with additional =CH vibrations near 3000 $cm^{-1}$. The strong infrared band observed near 1600 $cm^{-1}$, and the weak 3081 and 3108 $cm^{-1}$ bands which were observed during the in situ olefin studies were assigned to the C=C and $=CH_2$ stretching vibrations of an adsorbed 1,3-butadiene species.

In addition to 1-butene, conjugated olefin species, maleic anhydride, $H_2O$, and carbon oxides (the major components of simplified reaction pathways) one more adsorbed specie was observed during the in situ 1-butene studies, and two additional adsorbed species were observed during the in situ 1,3-butadiene studies. Adsorbed maleic acid was observed on the catalyst surface during both olefin oxidation reactions; a surface olefin
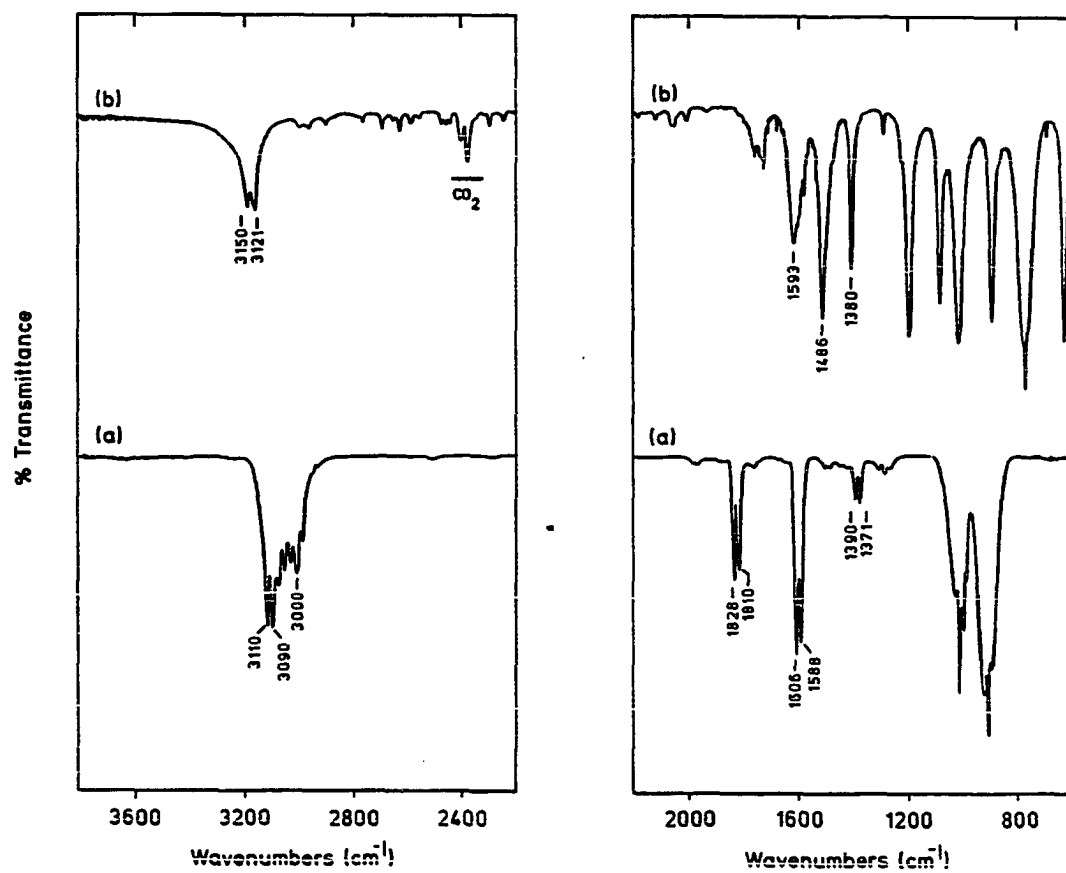
Figure 7. Infrared spectra of

(a) gaseous 1,3-butadiene
(b) liquid furan

species resembling trans-2-butene was observed during the in situ 1,3-butadiene studies.

The assignment of infrared bands to maleic acid and possibly trans-2-butene required a comparison with pure compound spectra. The assignment of a 1725 $cm^{-1}$ band to the C=O stretch of maleic acid has been made (2). The 1687-1690 $cm^{-1}$ band observed in these studies was attributed to either an adsorbed trans-2-butene species (C=C stretch at 1681 $cm^{-1}$ (14)) or to a C=O stretch of an adsorbed acid species on the catalyst surface. A future study will investigate the oxidation of crotonic acid species (15).

The simplified reaction network proposed by Varma and Saraf (7) describes butadiene and possibly furan as reaction intermediates in 1-butene selective oxidation to maleic anhydride. The in situ infrared study of 1-butene oxidation has identified olefin species (including butadiene) and maleic acid on the surface of V-P-O catalysts. It appears that an adsorbed butadiene species would be a reaction intermediate in 1-butene partial oxidation; however the in situ infrared spectra cannot provide any evidence for a furan species on the catalyst surface. The intense C=C bands at 1380, 1486, and 1593 $cm^{-1}$ which characterize furan (spectrum 7[b]) were not observed under in situ conditions. This study indicates that maleic acid and not furan is an important surface species in olefin selective oxidation. Tables 1 and 2 summarize the vibrational band assignments for the in situ infrared spectra of 1-butene oxidation at 400°C and 1,3-butadiene oxidation at 300°C.

In a previous in situ study of n-butane selective oxidation to maleic anhydride (2), adsorbed 1-butene, a strongly conjugated or strained $C_4$

Table 1. Vibrational band assignments during 1-butene selective oxidation at 400°C

| P/V = 0.9 | P/V = 1.0 | P/V = 1.1 | Assignment | Species |
|-----------|-----------|-----------|------------|---------|
| 1605 | 1610 | 1615 | $\nu_{C=C}$ | 1,3-butadiene |
| 1725 | 1722 | 1727 | $\nu_{C=O}$ | maleic acid |
| 1775 | 1775 | 1777 | $\nu_{C=O}$ | maleic anhydride |
| 1845 | 1845 | 1845 | $\nu_{C=O}$ | maleic anhydride |
| 2143 | 2143 | 2143 | $\nu_{C=O}$ | CO |
| 2330 | 2330 | 2330 | $\nu_{O=C=O}$ | $CO_2$ |
| 2958 | 2958 | 2963 | $\nu_{CH}$ | --- |
| 3010 | --- | -- | $\nu_{=CH}$ | --- |
| 3085 | --- | -- | $\nu_{=CH_2}$ | 1-butene |

Table 2. Vibrational band assignments during 1,3-butadiene selective oxidation at 300°C

| P/V = 0.9 | P/V = 1.0 | P/V = 1.1 | Assignment | Species |
|-----------|-----------|-----------|------------|---------|
| 1600 | 1595 | 1600 | $\nu_{C=C}$ | 1,3-butadiene |
| 1690 | 1690 | 1687 | $\nu_{C=C}$ | ---- |
| 1721 | 1722 | 1723 | $\nu_{C=O}$ | maleic acid |
| 1777 | 1773 | 1773 | $\nu_{C=O}$ | maleic anhydride |
| 1847 | 1843 | 1844 | $\nu_{C=O}$ | |
| 2143 | 2143 | 2143 | $\nu_{C\equiv O}$ | CO |
| 2333 | 2330 | 2330 | $\nu_{O=C=O}$ | $CO_2$ |
| 2965 | -- | -- | $\nu_{CH}$ | ---- |
| 3081 | 3081 | 3081 | $\nu_{=CH}$ | 1,3-butadiene |
| -- | 3108 | 3108 | $\nu_{=CH_2}$ | 1,3-butadiene |

olefin, and maleic acid were observed on the surface of V-P-O catalysts. Since these species were observed in high concentrations on the catalyst surface and were not observed in the reactor effluent (12), the possibility exists that olefins and maleic acid could be reaction intermediates in paraffin selective oxidation.

Figure 8 presents the C=O stretching, C=C stretching, and C-H bending region (1400-2600 cm$^{-1}$) of the infrared spectrum for in situ studies involving the P/V = 1.0 catalyst. Spectrum 8[a] presents the infrared spectrum of the pretreated P/V = 1.0 catalyst as a reference. The in situ infrared spectrum for the P/V = 1.0 catalyst after 1 hour of 1-butene-air flow at 300°C is presented in spectrum 8[b]. A broad infrared band was observed from 1550 to 1615 cm$^{-1}$. Adsorbed butadiene was assigned to the band near 1600 cm$^{-1}$; the width and shape of the 1550-1615 cm$^{-1}$ band indicated additional conjugated or possibly strained olefin species could be present. Spectrum 8[c] presents the in situ infrared spectrum of adsorbed species observed for the P/V = 1.0 catalyst following three hours of n-butane-air flow at 400°C (6). (The 1462 cm$^{-1}$ infrared band was assigned to C-H bending vibrations of adsorbed n-butane.) The intense infrared band at 1571 cm$^{-1}$ was assigned to the C=C stretching vibration of a highly conjugated (possibly π-allyl) or strained (possibly cyclo-butene) adsorbed olefin species. Following one hour of butadiene-air flow at 300°C (spectrum 7[d]) an infrared band centered at 1595 cm$^{-1}$ was observed and assigned to the C=C stretching vibrations (1585-1605 cm$^{-1}$) of adsorbed butadiene.

It appears the unusual width and asymmetry of the broad 1570-1615 cm$^{-1}$ infrared band observed in the 1-butene oxidation studies could be
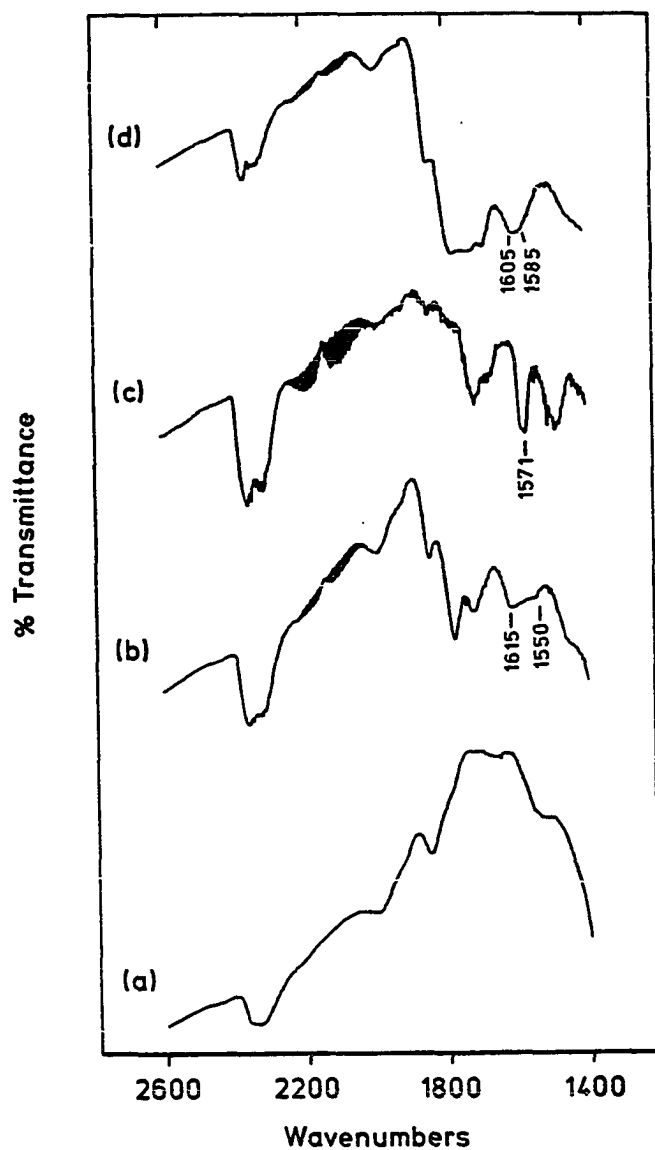
Figure 8. In situ infrared spectra for the P/V = 1.0 V-P-O catalyst

    (a) pretreated catalyst at 300°C
    (b) 1 hour 1-butene-air flow at 300°C
    (c) 3 hour n-butane-air flow at 400°C
    (d) 1 hour 1,3-butadiene-air flow at 300°C

due to the presence of two conjugated or strained olefin species; possibly butadiene and the olefin species observed earlier (2). Since 1-butene, conjugated olefin species, and maleic acid were observed on the catalyst surface during n-butane oxidation, and both conjugated olefins and maleic acid were observed during 1-butene oxidation, this study suggests that olefins and maleic acid could be intermediates in paraffin selective oxidation. Temperature and compositional effects appear to determine the relative concentration of adsorbed olefin species.

## CONCLUSIONS

Adsorbed species have been identified on the surfaces of V-P-O catalysts during olefin selective oxidation. The presence of reactants (1-butene or 1,3-butadiene), partially oxidized products (maleic anhydride), and complete oxidation products ($CO_x$, $H_2O$) was observed by in situ infrared spectroscopy. In addition, reactive surface species including butadiene and maleic acid were detected. It appears that butadiene and maleic acid could be reaction intermediates in 1-butene selective oxidation; further evidence has been gathered in support of olefin and maleic acid intermediates in paraffin oxidation. Other possible reaction intermediates such as furan were not observed. The adsorptive properties of the catalyst were dependent on P-to-V ratio, the reaction temperature, and the time on stream.

146

## ACKNOWLEDGEMENT

## REFERENCES

1. Moser, T. P.; Schrader, G. L.   Selective oxidation of n-butane to maleic anhydride by model V-P-O catalysts.   J. Catal. 92:   216-231; 1985.

2. Wenig, R. W.; Schrader, G. L.   In situ FTIR study of n-butane selective oxidation to maleic anhydride by V-P-O catalysts.   J. Phys. Chem., accepted.

3. Ostroushko, V. I.; Kernos, Yu. D.; Ioffe, I. I.   Oxidation of butenes with a vanadium-phosphorus catalysts.   Neftekhimiya 12(3):   362-369; 1972.

4. Morselli, L.; Riva, A.; Trifirò, F.; Zucchi, M.; Emig, G.   The chemistry of V and P oxides based oxidation catalysts.   I - relationship between structure and activity for the oxidation of 1-butene to maleic anhydride.   La Chimica E L'Industria 60(10):   791-797; 1978.

5. Ai, M.; Boutry, P.; Montarnal, R.   Kinetics of the oxidation of butene to maleic anhydride on vanadium pentoxide-phosphorus pentoxide. I.   Experimental kinetics.   Bull. Soc. Chim. Fr. 8-9:   2775-2782; 1970.

6. Ai, M.   A study of the partial catalytic oxidation of hydrocarbons. V.   The effect of phosphorus addition to the vanadium catalyst on the oxidation of butene, butadiene, and furan.   Bull. Chem. Soc. Jpn. 43(11):   3490-3495; 1970.

7. Varma, R. L.; Saraf, D. N.   Oxidation of butene to maleic anhydride. I.   Kinetics and mechanism.   Journal of Catalysis 55:   361-372; 1978.

8. Escardino, A.; Solá, C.; Ruiz, F.   Oxidacion catalitica de butano a anhidrido maleico.   Anales de Quimica 69:   385-396; 1973.

9. Wohlfahrt, K.; Hofmann, H.   Kinetik der Synthese von Maleinsäureanhydride aus n-Butan.   Chem. Ing. Tech. 52(10):   811-814; 1980.

10. Hodnett, B. K.; Permanne, Ph.; Delmon, B.   Influence of P/V ratio on the phase composition and catalytic activity of vanadium phosphate based catalysts.   Appl. Catal. 6:   231-244; 1983.

11. Wüstneck, N.; Wolf, H.; Seeboth, H.   Role of vanadyl pyrophosphate in mild oxidation of hydrocarbons.   React. Kinet. Catal. Lett. 21(4):   497-503; 1982.

12. Wenig, R. W.; Schrader, G. L.   V-P-O industrial catalysts for n-butane oxidation:   characterization and kinetic measurements.   Ind. Eng. Chem. Fund., accepted.

13. Hill, R. R.; Rendell, D. A.  The interpretation of infrared spectra. London:  Heyden; 1975.

14. Bellamy, L. F.  The infrared spectra of complex molecules.  New York: Chapman and Hall; 1980.

15. Wenig, R. W.; Schrader, G. L.  In situ FTIR study of crotyl alcohol, maleic acid, crotonic acid, and maleic anhydride oxidation on V-P-O catalysts.  J. Phys. Chem.; submitted.

SECTION V.  IN SITU FTIR STUDY OF CROTYL ALCOHOL, MALEIC
            ACID, CROTONIC ACID, AND MALEIC ANHYDRIDE
            OXIDATION ON A V-P-O INDUSTRIAL CATALYST

ABSTRACT

Vaporized crotyl alcohol, maleic acid, crotonic acid, and maleic anhydride were fed by syringe injection to an _in situ_ infrared cell at 300°C. A P/V = 1.1 V-P-O catalyst containing the patented B-phase was used for these studies. Crotyl alcohol was used as a mechanistic probe for the formation of conjugated and possibly strained olefin species observed during the previous n-butane selective oxidation studies. Crotonic acid and maleic acid were fed as probes for adsorbed acid species which were observed during the _in situ_ n-butane studies. Maleic anhydride oxidation by V-P-O catalysts was studied with vaporized maleic anhydride feeds. This study indicates that olefin species and maleic acid, but not crotonic acid could be reaction intermediates in n-butane selective oxidation to maleic anhydride. The possible involvement of peroxide species in the transformation of butadiene to maleic acid is discussed.

## INTRODUCTION

Vanadium-phosphorus-oxygen (V-P-O) catalysts are used commercially for the selective oxidation of n-butane to maleic anhydride. Industrial V-P-O catalysts are prepared in alcohol solution (1) and typically contain the active and selective B-phase (2, 3). This study employs in situ infrared spectroscopy to investigate the mechanism of paraffin selective oxidation on a V-P-O industrial catalyst containing the B-phase (4).

In the past, reaction pathways for the conversion of n-butane to maleic anhydride have been very simple. The reaction schemes offered by Escardino et al. (5) and Wohlfahrt and Hofmann (6) propose the direct formation of maleic anhydride from n-butane without the involvement of reaction intermediates. The combustion of n-butane and maleic anhydride to carbon oxides and water was proposed in parallel reactions. In contrast, the reaction pathway for 1-butene selective oxidation is rather complex. The reaction scheme is generally believed to involve 1,3-butadiene (7, 8) or crotonaldehyde (9) and furan (10) as reaction intermediates. Some researchers have also included crotonic acid (7) or peroxide species (11, 12) as possible intermediates.

In previous studies (13, 14) this research group has used in situ infrared spectroscopy to investigate the mechanism for n-butane selective oxidation to maleic anhydride. Adsorbed olefins including a methyl-allyl species and maleic acid were observed on the surfaces of functioning V-P-O catalysts. In this study, crotyl alcohol, maleic acid, and crotonic acid vapor were adsorbed on a V-P-O catalyst to probe the involvement of

olefin and carboxylic acid intermediates in the selective oxidation of
n-butane to maleic anhydride. Escardino's (5) maleic anhydride oxidation
scheme was studied with gaseous maleic anhydride feeds.

EXPERIMENTAL PROCEDURE

Characterization and Kinetic Measurements

A vanadium-phosphorus mixed oxide catalyst having a P-to-V ratio of 1.1 was prepared by the addition of $H_3PO_4$ to reduced $V_2O_5$ in alcohol solution. The characterization results and kinetic measurements for industrial type V-P-O catalysts varying in P-to-V ratio are presented elsewhere (2).

## In Situ FTIR Cell

The in situ infrared cell has been described previously (13). Thin catalyst wafers were formed between stainless steel dies at high pressures and transferred to a sample holder within the infrared cell for study. Catalyst pretreatment was accomplished by heating the wafer to 300°C in a flowing stream of air (75 $cm^3$/min). Infrared bands due to residual solvent (1650–1900 $cm^{-1}$) and adsorbed waters (1620–1640 and 3100–3600 $cm^{-1}$) were usually removed.

## Vapor Delivery System

Gaseous crotyl alcohol (b.p. 121°C), maleic acid (b.p. 140°C), maleic anhydride (b.p. 202°C), and crotonic acid (b.p. 185°C) were fed to the in situ infrared cell. This was accomplished by placing approximately 1 cc of the solid compound into a gas sampling bulb evacuated to 1 x $10^{-4}$ torr (1 cc of crotyl alcohol liquid was injected by syringe into an evacuated sampling vessel). The organic compounds were vaporized by placing the vessel into a thermostatically controlled oven at temperatures close to the boiling point. Vaporized species were fed to the in situ infrared cell

at 300°C with a heated syringe. Evacuation of the infrared cell was required to promote injection of the vaporized feed and to prevent the rapid oxidation of the hydrocarbon on the catalyst surface. Air was later fed to selected adsorbates in order to study the ultimate formation of reaction products. Consequently, the vibrational spectrum of both adsorbed and reacted species could be independently observed.

## Vacuum System

A Welsh Model 1402 vacuum pump and Edwards Model E 02 air cooled diffusion pump were used for the evacuation studies. Typically a brief (5 minutes) evacuation of the infrared cell to pressures of $10^{-4}$ torr was needed to remove gaseous and weakly adsorbed oxidation products.

## Fourier Transform Infrared Spectrometer

A Nicolet Model 60-SX FTIR was used to collect spectra of adsorbed and reacting species at 300°C. Each infrared spectrum represents an accumulation of 600 scans at 2 $cm^{-1}$ resolution. All spectra presented in this paper were ratiod against a single beam spectrum of an evacuated cell at 300°C with KBr windows. The infrared spectra collected after the syringe injection of gaseous feedstocks were found to have vibrational bands due to adsorbed species, the catalyst, and gaseous species present in the cell. In situ infrared spectra obtained after a brief evacuation contain vibrational bands due only to adsorbed species and the V-P-O catalyst.

RESULTS

During the previous in situ studies of n-butane selective oxidation (13) olefins, maleic acid, and maleic anhydride were observed on the catalyst surface at 400°C. Reaction temperatures of 300°C were used in these adsorption studies in order to stabilize surface species which were found to be very reactive—especially at higher temperatures. The in situ infrared spectra for crotyl alcohol, maleic acid, crotonic acid, and maleic anhydride adsorption and reaction on an industrial type V-P-O catalyst are presented separately.

Crotyl Alcohol

The in situ infrared spectra following a 10 cc injection of crotyl alcohol vapor into the evacuated infrared cell are presented in Figure 1. Spectrum 1[a] was observed for the pretreated P/V = 1.1 catalyst at 300°C. Spectrum 1[b] was collected 20 minutes after the injection of crotyl alcohol vapor into the infrared cell. A comparison of spectrum 1[b] with a reference spectrum of gaseous crotyl alcohol at 300°C (spectrum 2[a]) reveals the nearly complete conversion of crotyl alcohol to butadiene. The formation of butadiene was indicated by C=C stretching vibrations at 1584 and 1603 $cm^{-1}$, and combination bands at 1816 and 1829 $cm^{-1}$ (14). Carboxylic acid species were suggested by C=O stretching vibrations at 1709 and 1722 $cm^{-1}$. Vibrational-rotational bands at 2143 and 2350 $cm^{-1}$ were assigned to CO and $CO_2$, respectively. C-H stretching vibrations at 2995, 3030, 3081, and 3105 $cm^{-1}$ were assigned to butadiene. After 40 minutes of reaction (spectrum 1[c]) additional C-H vibrations due to butadiene were observed at 2864, 2927, and 2970 $cm^{-1}$.

Figure 1.  Crotyl alcohol reaction on P/V = 1.1 V-P-O catalyst at 300°C

        (a) pretreated catalyst at 300°C
        (b) 20 minutes reaction
        (c) 40 minutes reaction
        (d) evacuation
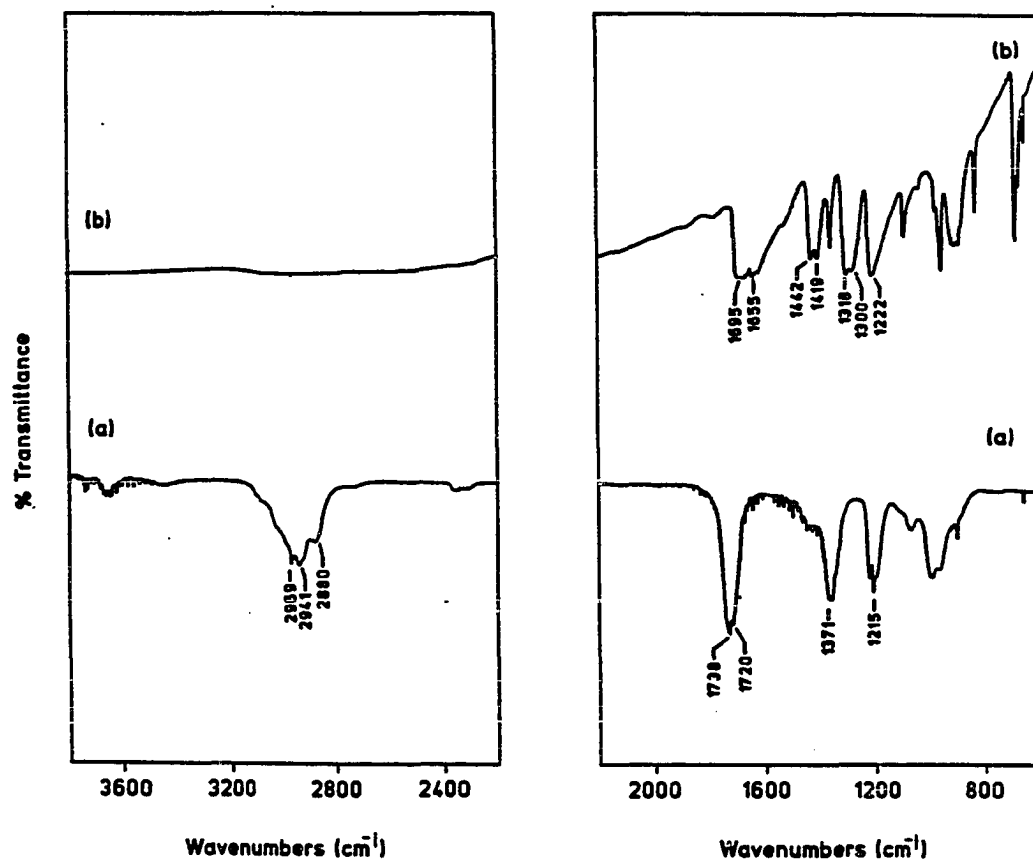
Figure 2.  Infrared spectra of

(a)  gaseous crotyl alcohol
(b)  gaseous crotonic acid

Spectrum 1[d] was collected following a mild evacuation of the in situ infrared cell. As a result the infrared bands of gaseous and weakly adsorbed species were removed. A broad C=C stretching vibration from 1570 to 1615 $cm^{-1}$ was suggestive of the conjugated olefin species observed in n-butane (13) and 1-butene (14) oxidation. The C=O stretching vibrations of maleic acid (1719 $cm^{-1}$) and maleic anhydride (1773 $cm^{-1}$) were assigned to the broad infrared band in the region 1719-1773 $cm^{-1}$.

Figure 3 displays the in situ infrared spectra following the introduction of 75 $cm^3$/min of air into the infrared cell. Spectra 3[a], 3[b], and 3[c] were collected after 20, 40, and 60 minutes (respectively) of air flow. The transformation of adsorbed olefin species to maleic anhydride was indicated by a decrease in the 1570-1615 $cm^{-1}$ ($\nu_{C=C}$) olefin band intensity and the appearance of 1778 and 1847 $cm^{-1}$ ($\nu_{C=O}$) infrared bands of maleic anhydride. Maleic acid was indicated by a weak infrared band at 1720 $cm^{-1}$; adsorbed $CO_2$ was assigned to C=O stretching vibrations at 2334 and 2362 $cm^{-1}$.

## Maleic Acid

The in situ infrared spectra following a 10 cc injection of maleic acid vapor are presented in Figure 4. Spectrum 4[a] was observed for the pretreated P/V = 1.1 catalyst at 300°C. Residual alcohols were assigned to the 1840 $cm^{-1}$ band; adsorbed $CO_2$ was assigned to two bands at 2334 and 2360 $cm^{-1}$. Spectrum 4[b] was collected following 10 minutes of maleic acid reaction. Maleic anhydride was assigned to carbonyl stretching vibrations at 1777 $cm^{-1}$ and 1849 $cm^{-1}$, and by =CH stretching vibrations at 3125 $cm^{-1}$. Gaseous $CO_2$ was indicated by vibrational-rotational bands near
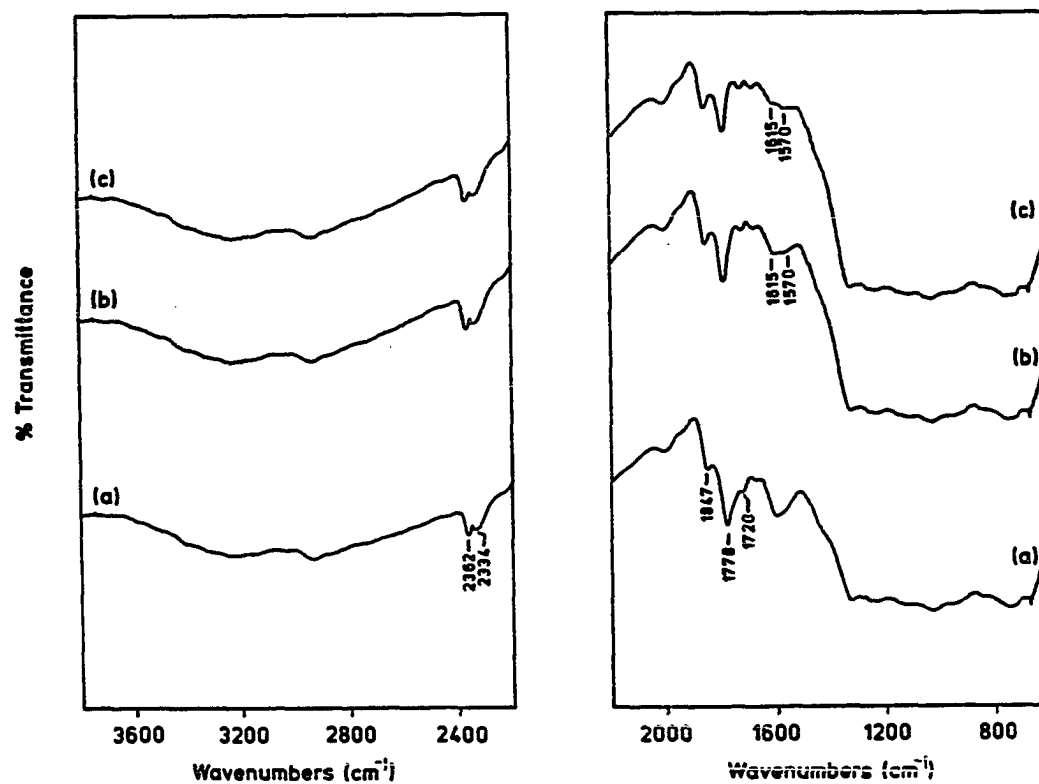
Figure 3. Crotyl alcohol reaction on P/V = 1.1 V-P-O catalyst in air at
300°C

(a) 20 minutes reaction
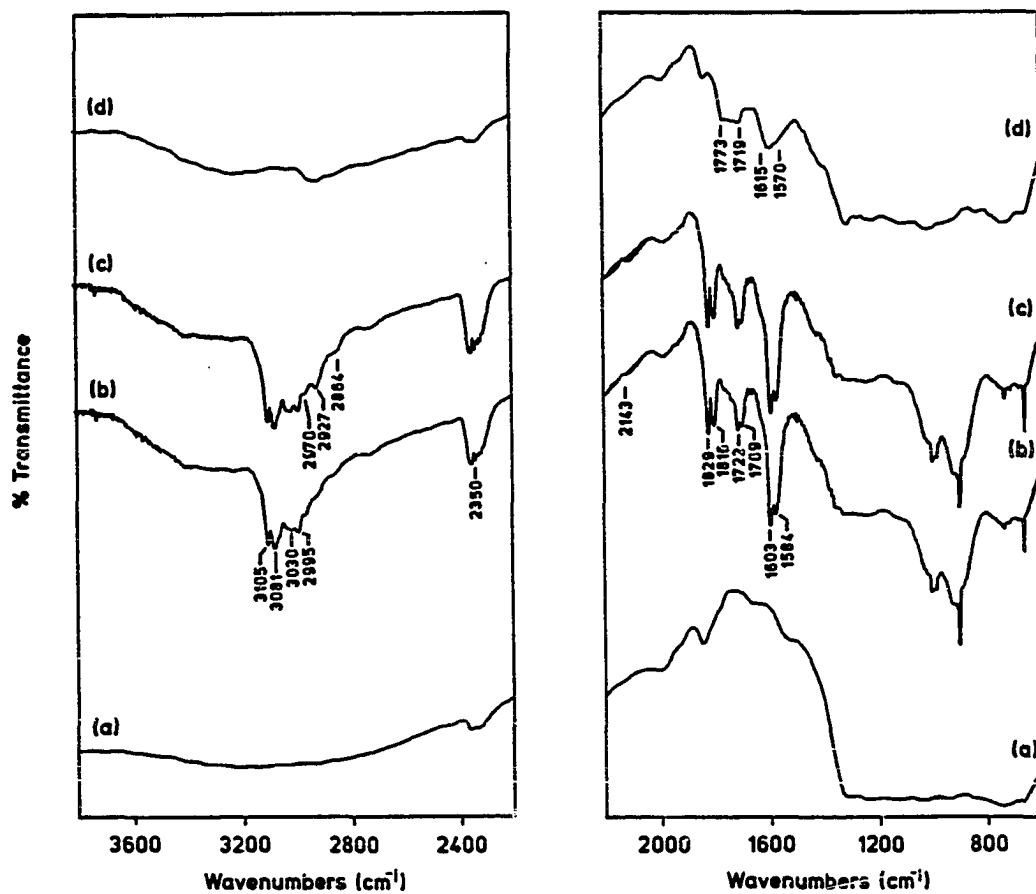(b) 40 minutes reaction
(c) 60 minutes reaction

Figure 4. Maleic acid reaction on P/V = 1.1 V-P-O catalyst at 300°C

　　　　　(a) pretreated catalyst at 300°C
　　　　　(b) 10 minutes reaction
　　　　　(c) 20 minutes reaction
　　　　　(d) 30 minutes reaction
　　　　　(e) evacuation

$2350 \text{ cm}^{-1}$. Spectrum 4[c] was collected following 20 minutes of maleic

acid reaction with the P/V = 1.1 V-P-O catalyst. A decrease in intensity

of the 1777 and 1849 $\text{cm}^{-1}$ maleic anhydride bands, and an increase in the

intensity of the 2350 $\text{cm}^{-1}$ $CO_2$ bands suggested the complete oxidation of

maleic anhydride to $CO_2$. After 30 minutes of reaction (spectrum 4[d]),

the further oxidation of maleic anhydride to $CO_2$ was indicated by very

weak C=O stretching vibrations of maleic anhydride and intense $CO_2$ bands.

Weak infrared bands at 1628 and 1715 $\text{cm}^{-1}$ were assigned to the C=C

stretching vibration of maleic anhydride and to the C=O stretching vibra-

tion of maleic acid, respectively.

Spectrum 4[e] was collected following a mild evacuation of the infra-

red cell. As a result the infrared bands of gaseous CO and $CO_2$ were

removed. Adsorbed maleic acid (1715 $\text{cm}^{-1}$), adsorbed maleic anhydride

(1777, 1849 $\text{cm}^{-1}$), and adsorbed $CO_2$ (2350 $\text{cm}^{-1}$) were observed.

## Crotonic Acid

The in situ infrared spectra for the crotonic acid studies with the

P/V = 1.1 catalyst are presented in Figure 5. Spectrum 5[a] was observed

for the pretreated V-P-O catalyst at 300°C. Spectrum 5[b] was collected

20 minutes after the injection of crotonic acid vapor into the infrared

cell. Infrared bands at 1416, 1441, 1625, 1640, 1681, and 1698 were

assigned to crotonic acid by comparison to a reference spectrum of gaseous

crotonic acid at 300°C (spectrum 2[b]). The C-H bending vibrations of

crotonic acid were assigned to the 1416 and 1441 $\text{cm}^{-1}$ bands; the 1625 and

1640 $\text{cm}^{-1}$ bands were assigned to C=C vibrations of crotonic acid; the

1681 and 1698 $\text{cm}^{-1}$ bands were assigned to C=O stretching vibrations of

crotonic acid. The infrared band observed at 1779 $cm^{-1}$ (spectrum 5[b])

was assigned to the asymmetric carbonyl stretching vibration of maleic

anhydride. (The symmetric C=O vibration of maleic anhydride seems to be

obscured by a residual solvent band at 1842 $cm^{-1}$.) Gaseous CO and $CO_2$

were identified by bands at 2143 and 2350 $cm^{-1}$, respectively.

After 40 minutes of reaction (spectrum 5[c]) the infrared bands

assigned to crotonic acid diminished in intensity while the bands assigned

to maleic anhydride (1779 $cm^{-1}$) and carbon oxides (2143, 2350 $cm^{-1}$)

intensified. In addition, new infrared bands were observed at 1725 and

1760 $cm^{-1}$. The 1725 $cm^{-1}$ band was assigned to the C=O stretching vibration

of a second carboxylic acid species—possibly maleic acid. The 1760 $cm^{-1}$

shoulder band was not observed during previous in situ studies and suggests

the presence of an additional oxidation product. After 60 minutes of

reaction (spectrum 5[d]) the crotonic acid bands continued to lose

intensity while the infrared bands due to carbon oxides increased in

intensity.

Spectrum 5[e] was collected after a mild evacuation of the infrared

cell. Adsorbed crotonic acid was assigned to C=C and C=O stretching

vibrations at 1620 and 1692 $cm^{-1}$, respectively. Adsorbed maleic acid and

adsorbed maleic anhydride were assigned to C=O stretching vibrations at

1720 and 1780 $cm^{-1}$. The 1760 $cm^{-1}$ infrared band indicated the C=O

stretching vibration of a previously unobserved oxidation product.

## Maleic Anhydride

The in situ infrared spectra following a 10 cc injection of maleic

anhydride vapor are presented in Figure 6. Spectrum 6[a] was observed for
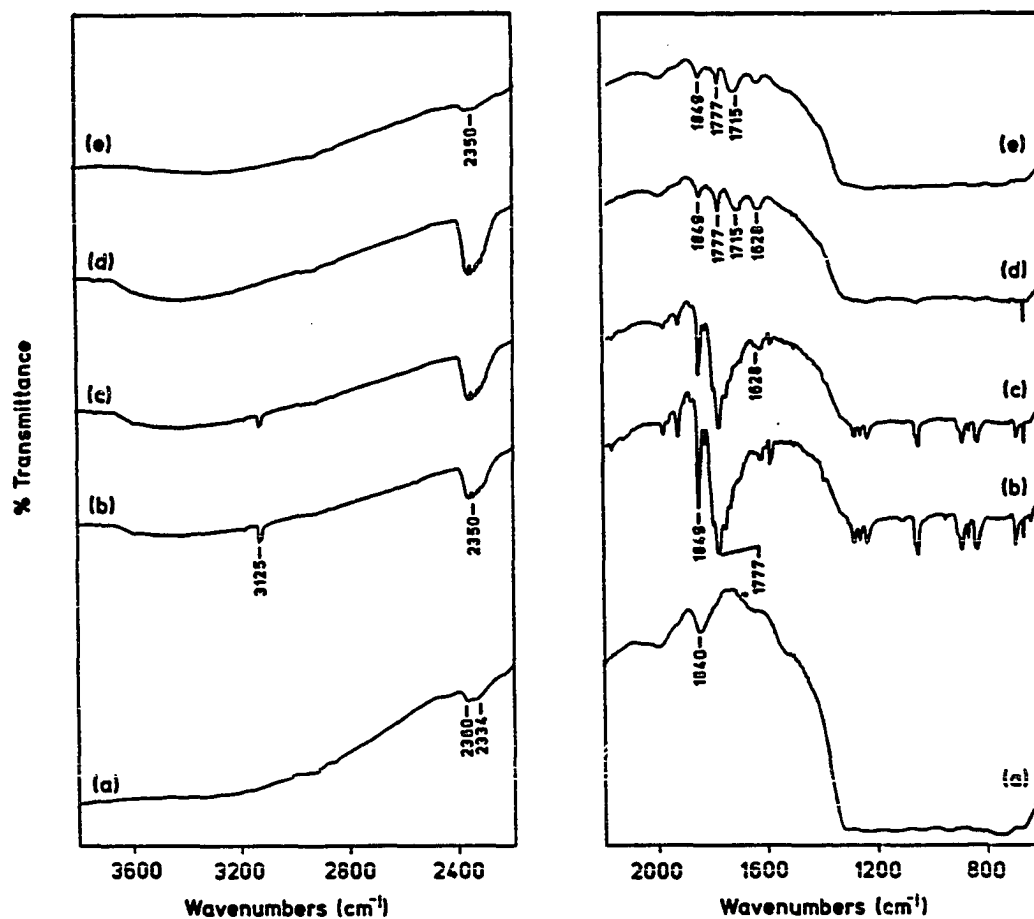
Figure 5. Crotonic acid reaction on P/V = 1.1 V-P-O catalyst at 300°C

(a) pretreated catalyst at 300°C
(b) 20 minutes reaction
(c) 40 minutes reaction
(d) 60 minutes reaction
(e) evacuation

the pretreated P/V = 1.1 V–P–O catalyst at 300°C.  A residual solvent

band was observed at 1842 $cm^{-1}$; two weak bands at 2334 and 2359 $cm^{-1}$ were

assigned to adsorbed $CO_2$.  Spectrum 6[b] was observed 20 minutes after the

introduction of maleic anhydride vapor into the evacuated 300°C cell.

Maleic anhydride was identified by C=O stretching vibrations at 1777

(shoulder at 1793 $cm^{-1}$) and 1847 $cm^{-1}$.  Gaseous CO and $CO_2$ were assigned

to infrared bands at 2143 and 2350 $cm^{-1}$, respectively.  A combination band

of maleic anhydride was observed at 3587 $cm^{-1}$.  Spectra 6[c] and 6[d] were

observed after 40 and 60 minutes of maleic anhydride reaction, respectively.

These spectra indicate the oxidation of maleic anhydride to CO and $CO_2$ on

the surface of the V–P–O catalyst.

In spectrum 6[e] the vibrational-rotational bands of gaseous carbon

oxides were removed by an evacuation of the _in situ_ infrared cell.

Adsorbed maleic anhydride was assigned to a 1774 $cm^{-1}$ C=O stretching

vibration; the 1847 C=O vibration of maleic anhydride was obscured by a

residual solvent band at 1842 $cm^{-1}$.  Adsorbed $CO_2$ was indicated by two
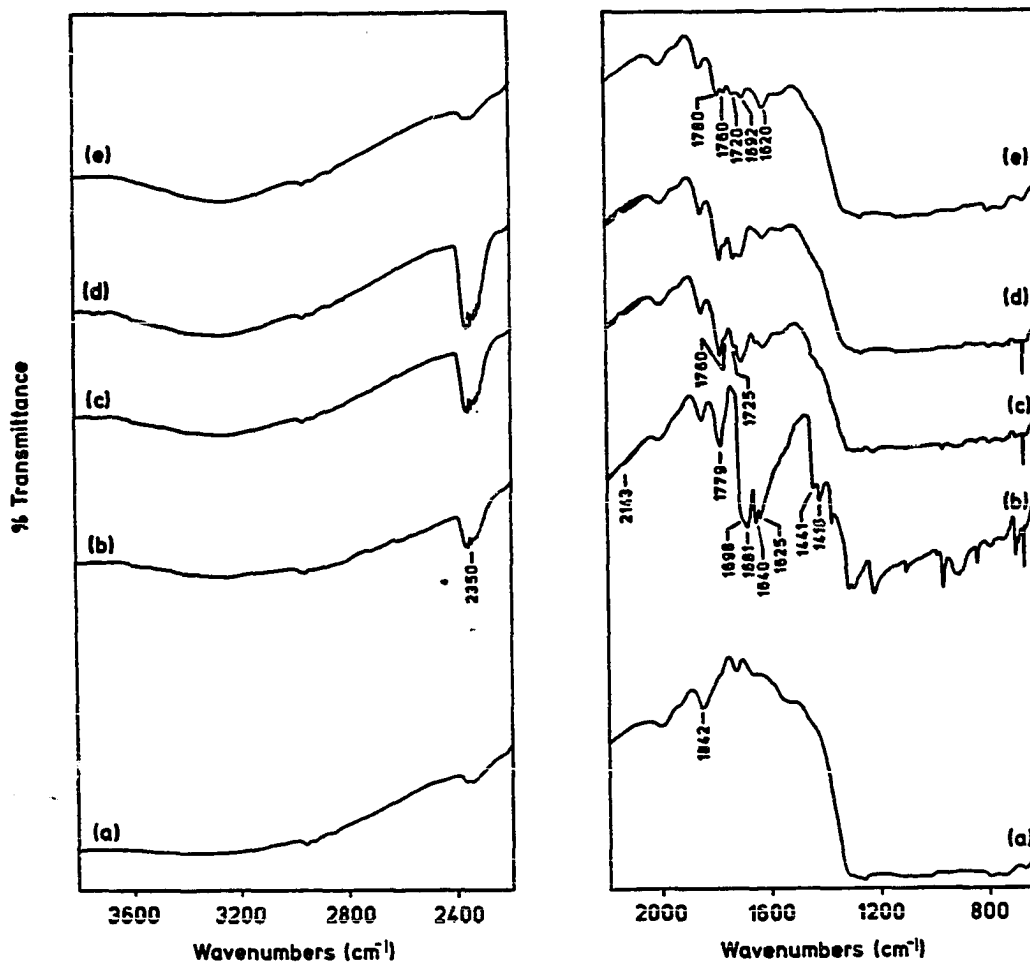
weak bands near 2350 $cm^{-1}$.
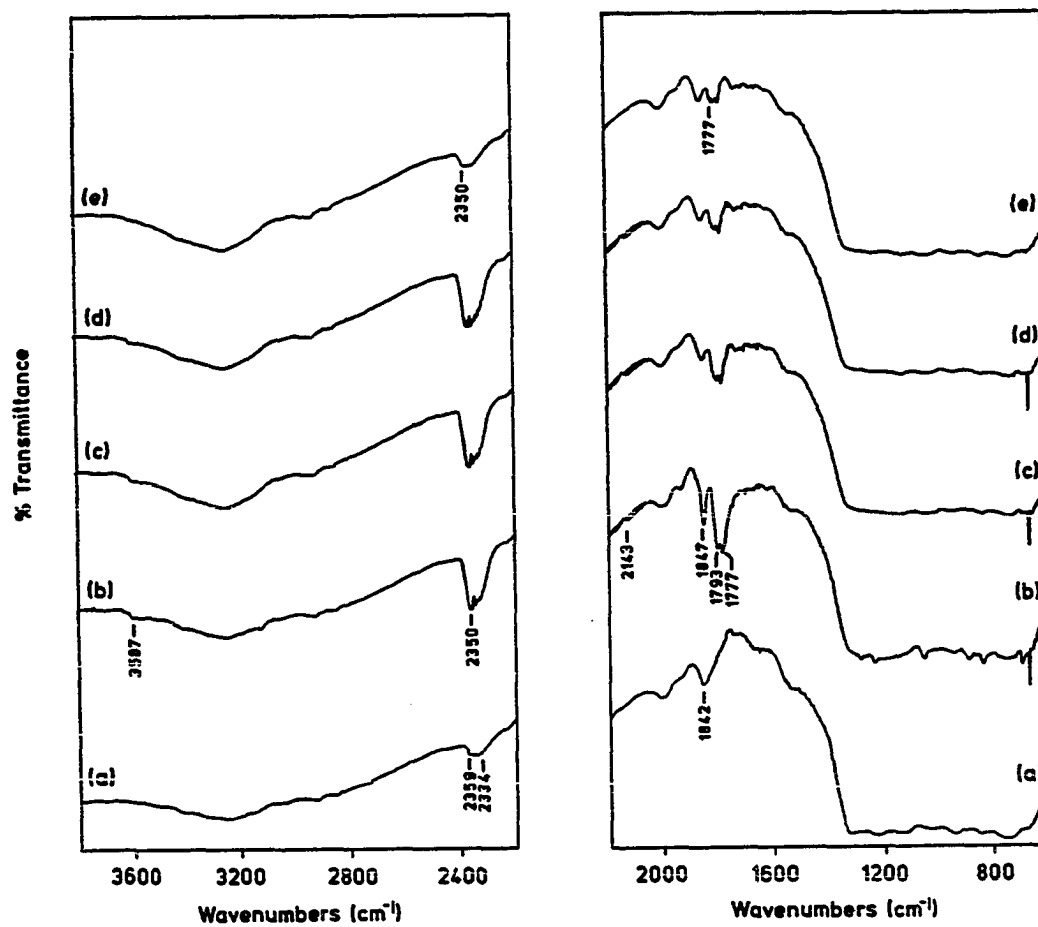
Figure 6. Maleic anhydride reaction on P/V = 1.1 V-P-O catalysts at 300°C

(a) pretreated catalyst at 300°C
(b) 20 minutes reaction
(c) 40 minutes reaction
(d) 60 minutes reaction
(e) evacuation

## DISCUSSION

The adsorption and reaction of specific surface species which were observed during the in situ n-butane oxidation allows us to explore the mechanism of maleic anhydride formation. Escardino's (5) reaction scheme postulates the direct conversion of n-butane to maleic anhydride with the combustion of n-butane and maleic anhydride to carbon oxides.

n-butane ⟶ maleic anhydride

CO, $CO_2$, $H_2O$
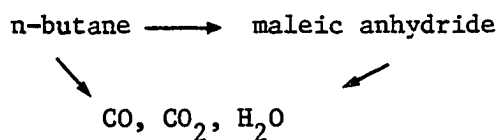
In this study, specific adsorbates were introduced into the infrared cell in order to explore the participation of reaction intermediates and the possible oxidation of maleic anhydride. Crotyl alcohol was used as a mechanistic probe for the formation of conjugated or possibly strained adsorbed olefin species. Since adsorbed acid species were observed during the in situ n-butane studies, maleic acid and crotonic acid were adsorbed onto the V-P-O catalyst. Maleic anhydride vapor was introduced as a probe for Escardino's (5) proposed combustion scheme. The discussion of results for crotyl alcohol, maleic acid, crotonic acid, and maleic anhydride adsorbates is made separately.

### Crotyl Alcohol

During the in situ n-butane studies (13) a 1571 $cm^{-1}$ infrared band was observed and assigned to the C=C stretching vibration of a methyl-allyl species (or possibly cyclobutene). A broader 1570-1615 $cm^{-1}$ infrared band was observed during 1-butene oxidation (14) and assigned to adsorbed

butadiene (and other olefin species). Crotyl alcohol was used in this study as a mechanistic probe for the formation of these highly reactive olefin species.

In a similar study, Burrington et al. (15) found allyl alcohol to be a suitable probe specie for allylic intermediates on bismuth-molybdate catalysts. This study uses crotyl alcohol (trans-2-butenoic acid) as a probe for the formation of reactive olefin species (including methyl-allyl intermediates) on the surface of an industrial-type V-P-O catalyst.

The formation of adsorbed olefin species from crotyl alcohol may occur at a Lewis acid site (anion vacancy) on the catalyst surface. Such active sites are believed to involve local structural modifications of the $(VO)_2P_2O_7$ structure (16). The transfer of a hydroxide ion to an anion vacancy on the catalyst surface could lead to the formation of a methyl-allyl cation. The subsequent abstraction of a proton by a V=O center would form a butadiene species.



The 1571 cm$^{-1}$ band observed during the _in situ_ n-butane studies suggests the possible rearrangement of butadiene to cyclobutene on the catalyst surface.
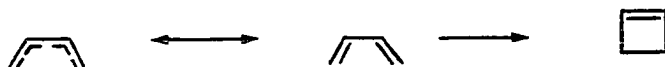


During the _in situ_ crotyl alcohol studies gaseous butadiene was identified by C=C stretching vibrations at 1584 and 1603 cm$^{-1}$, and by combination bands at 1816 and 1829 cm$^{-1}$. In addition, highly reactive

adsorbed olefin species were identified by C=C stretching vibrations in the 1570-1615 $cm^{-1}$ region. This study indicates that crotyl alcohol adsorbs to form butadiene (1605-1585 $cm^{-1}$) and possibly methyl-allyl or cyclo-butene (1571 $cm^{-1}$) species. In the presence of oxygen these highly reactive adsorbed olefin species were found to form maleic acid (1720 $cm^{-1}$) and maleic anhydride (1847, 1778 $cm^{-1}$).

## Maleic Acid

During the _in situ_ n-butane studies (13) an infrared band was observed at 1705-1715 $cm^{-1}$ and assigned to the C=O stretching vibration of an adsorbed maleic acid species. In this study an adsorbed maleic acid specie was again indicated by a 1715 $cm^{-1}$ infrared band; maleic anhydride (1777, 1849 $cm^{-1}$) and water (3100-3600 $cm^{-1}$) were observed as further oxidation products. This study indicates that maleic acid is readily dehydrated on the catalyst surface to form maleic anhydride. The catalytic oxidation of maleic acid and maleic anhydride to carbon oxides and water was also observed.

## Crotonic Acid

The crotyl alcohol and maleic acid adsorption studies indicate that conjugated olefin species and maleic acid could be intermediates in n-butane selective oxidation to maleic anhydride. Crotonic acid adsorption studies at 300°C were used to investigate the possible involvement of 2-butenoic acid species in the stepwise oxidation of allyl-butadiene species to maleic acid.

Figure 7 provides a comparison of the _in situ_ infrared spectra for the n-butane (13) and crotonic acid studies. Spectrum 7[a] was collected after three hours of n-butane flow at 400°C; spectrum 7[b] was observed after 40 minutes of crotonic acid reaction at 300°C. An adsorbed crotonic acid species was identified by C=C stretching vibrations at 1620 and 1640 $cm^{-1}$, and by C=O stretching vibrations at 1692 $cm^{-1}$ (spectrum 7[b]). Infrared spectra collected during the _in situ_ n-butane studies (spectrum 7[a]) revealed C=C stretching vibrations at 1570 and 1655 $cm^{-1}$, and C=O stretching vibrations at 1710, 1778, and 1848 $cm^{-1}$. (The 1461 $cm^{-1}$ band was assigned to C-H bending vibrations of n-butane.) Since the 1620, 1640, and 1692 $cm^{-1}$ infrared bands of adsorbed crotonic acid were not observed in the _in situ_ n-butane studies, crotonic acid does not appear to be an intermediate in paraffin oxidation to maleic anhydride. However, 2-butenoic acid species do appear to form maleic acid (1710-1715 $cm^{-1}$) and maleic anhydride (1778, 1848 $cm^{-1}$) on the surface of V-P-O catalysts.

The transformation of allyl-butadiene species to maleic acid without the participation of 2-butenoic acid species makes monoperoxide species unlikely reaction intermediates. However, diperoxide species can be formed by the addition of two oxygen molecules to butadiene; the formation of hydroperoxides and di-acids would follow. The addition of oxygen to butadiene might also lead to intramolecular peroxide formation across a double bond. The transformation of cyclic peroxide species to maleic acid and maleic anhydride has been proposed (11, 12).
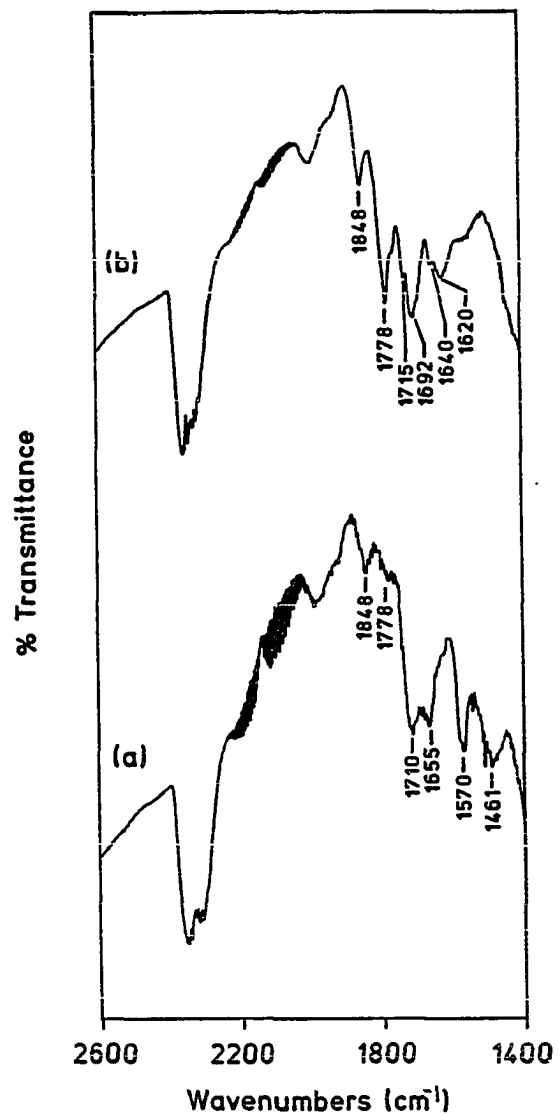
Figure 7. In situ infrared spectra for the P/V = 1.1 catalyst

    (a) three hours n-butane-air flow at 400°C

    (b) one hour crotonic acid reaction at 300°C

## Maleic Anhydride

During the _in situ_ n-butane studies, infrared bands at 1778 and 1847 $cm^{-1}$ were observed on the surfaces of functioning V-P-O catalysts and assigned to adsorbed maleic anhydride. In this study, maleic anhydride vapor was adsorbed onto the surface of a V-P-O catalyst at 300°C and the carbonyl stretching vibrations of maleic anhydride were observed at 1777 and 1847 $cm^{-1}$. Furthermore, this _in situ_ study of maleic anhydride reaction identified the catalytic oxidation of maleic anhydride to carbon oxides and water on the V-P-O catalyst surface.

CONCLUSIONS

Crotyl alcohol, maleic acid, crotonic acid, and maleic anhydride were found to be reactive species when adsorbed on a V-P-O catalyst at 300°C. Crotyl alcohol was observed to form conjugated olefin species on the catalyst surface--possibly by interaction with catalyst Lewis acid sites. These adsorbed olefins were identified by C=C stretching vibrations (1605-1570 $cm^{-1}$) assigned to methyl-allyl, butadiene, or possibly cyclobutene species which were previously observed on the catalyst surface (7, 8). Maleic acid was observed to readily form maleic anhydride and water; furthermore, adsorbed maleic acid was identified by a 1715 $cm^{-1}$ C=O stretching vibration which was also observed during the in situ n-butane studies (13). Crotonic acid was observed to form maleic acid and maleic anhydride on the catalyst surface; however, the C=C (1620-1640 $cm^{-1}$) and the C=O (1680-1692 $cm^{-1}$) stretching vibrations of crotonic acid were not observed during n-butane oxidation. The non-stepwise formation of acid groups suggests the possible involvement of cyclic peroxide intermediates in the transformation of conjugated olefin species to maleic acid. Adsorbed maleic anhydride was identified by two C=O vibrations at 1778 and 1848 $cm^{-1}$, and was readily oxidized to CO and $CO_2$ at 300°C.

Since the adsorbed olefin species and maleic acid were identified by the same vibrational frequencies observed for the earlier studies, it seems that olefins and maleic acid could be reaction intermediates in paraffin oxidation. Although crotonic acid did form maleic acid and maleic anhydride, no evidence for 2-butenoic acid participation in the mechanism for n-butane selective oxidation was gathered.

## ACKNOWLEDGEMENT

## REFERENCES

1. Hodnett, B. K. Vanadium-phosphorus oxide catalysts for the selective oxidation of $C_4$ hydrocarbons to maleic anhydride. Catal. Rev.-Sci. Eng. 27(3): 374-424; 1985.

2. Wenig, R. W.; Schrader, G. L. V-P-O industrial catalysts for n-butane oxidation: characterization and kinetic measurements. Ind. Eng. Chem. Fund.; accepted.

3. Cavani, F.; Centi, G.; Trifiro, F. Study of n-butane oxidation to maleic anhydride in a tubular flow stacked-pellet reactor: influence of phosphorus on the selectivity. Appl. Catal. 15: 151-160; 1985.

4. Schneider, R. U.S. Patent 3 864 280; 1970.

5. Escardino, A.; Sola, C.; Ruiz, F. Oxidacion catalitica de butano a anhidrido maleico. Anales de Quimica 69: 385-396; 1973.

6. Wohlfahrt, K.; Hofmann, H. Kinetik der Synthese von Maleinsäureanhydrid aus n-Butan. Chem. Ing. Tech. 52(10): 811-814; 1980.

7. Ostroushko, V. I.; Kernos, Yu. D.; Ioffe, I. I. Oxidation of butene with a vanadium-phosphorus catalyst. Neftekhimiya 12(3): 362-369; 1972.

8. Morselli, L.; Riva, A.; Trifiro, F.; Zucchi, M.; Emig, G. The chemistry of V and P oxides based oxidation catalysts. I - relationship between structure and activity for the oxidation of 1-butene to maleic anhydride. La Chimica E L'Industria 60(10): 791-797; 1978.

9. Ai, M.; Boutry, P.; Montarnal, R. Kinetics of the oxidation of butene to maleic anhydride on vanadium pentoxide-phosphorus pentoxide. I. Experimental kinetics. Bull. Soc. Chim. Fr. 8-9: 2775-2782; 1970.

10. Ai, M. A study of the partial catalytic oxidation of hydrocarbons. V. The effect of phosphorus addition to the vanadium catalyst on the oxidation of butene, butadiene, and furan. Bull. Chem. Soc. Jpn. 43(11): 3490-3495; 1970.

11. Trimm, D. L. Design of industrial catalysts. New York: Elsevier Scientific Publishing Company; 1980.

12. Margolis, L. Y. Present state of ideas on the mechanism of catalytic hydrocarbon oxidation. Catalysis Reviews 9: 241-267; 1973.

13. Wenig, R. W.; Schrader, G. L. In situ FTIR study of n-butane selective oxidation to maleic anhydride on V-P-O catalysts. J. Phys. Chem.; accepted.

14. Wenig, R. W.; Schrader, G. L. In situ FTIR study of 1-butene and 1,3-butadiene selective oxidation by V-P-O catalysts. J. Phys. Chem.; submitted.

15. Burrington, J. D.; Kartisek, C. T.; Grasselli, R. K. Aspects of selective oxidation and ammoxidation mechanisms over bismuth molybdate catalysts: allyl alcohol as a probe for the allylic intermediate. J. Catal. 63: 235-254; 1980.

16. Cavani, F.; Centi, G.; Trifiro, F. Structure sensitivity of the catalytic oxidation of n-butane to maleic anhydride. J. Chem. Soc., Chem. Commun. No. 1591: 492-494; 1985.

SECTION VI. V-P-O INDUSTRIAL CATALYSTS FOR $C_4$ HYDROCARBON
OXIDATION: REACTION MECHANISM

## ABSTRACT

A reaction mechanism for $C_4$ hydrocarbon selective oxidation to maleic anhydride on V-P-O industrial catalysts is proposed. In situ infrared studies for the oxidation of maleic anhydride, maleic acid, 1,3-butadiene, 1-butene, n-butane, 2-butenoic acid, and 2-buten-1-ol have led to the development of a reaction scheme for paraffin and olefin selective oxidation. The participation of reactive olefin and maleic acid intermediates in n-butane selective oxidation to maleic anhydride is postulated. No evidence was gathered in support of furan or crotonic acid reaction intermediates.

## INTRODUCTION

Selective oxidation reactions with transition metal oxide catalysts have found wide commercial application for the synthesis of partially oxygenated hydrocarbons. The selective oxidation of propylene to acrolein, ethylene to ethylene oxide, naphthalene to phthalic anhydride, and n-butane oxidation to maleic anhydride are current examples of industrial selective oxidation processes. Only in the case of propylene selective oxidation to acrolein (and ammoxidation to acrylonitrile) on bismuth molybdate catalysts has a nearly complete picture of the reaction mechanism emerged (1). In this paper, a reaction network for $C_4$ hydrocarbon selective oxidation to maleic anhydride on vanadium-phosphorus-oxygen (V-P-O) industrial catalysts is proposed.

The discovery of V-P-O catalysts which are able to activate paraffins for selective oxidation is an important recent advance in catalysis. However, the actual mechanism for paraffin, as well as olefin selective oxidation, is not yet fully understood. Kinetic measurements have led to simplistic proposals for n-butane oxidation while the corresponding 1-butene oxidation mechanisms are more complex. A brief summary of the literature follows.

Escardino et al. (2), Wohlfahrt and Hofmann (3), and Wüstneck et al. (4) have each proposed the direct conversion of n-butane to maleic anhydride with the simultaneous combustion of n-butane and maleic anhydride to carbon oxides and water. In contrast, the reaction network for 1-butane oxidation often includes 1,3-butadiene (5, 6), crotonaldehyde (7, 8), furan (9), and possibly maleic acid (10) as reaction intermediates. The 1-butene

oxidation network proposed by Ostroushko et al. (11) describes parallel reaction schemes for maleic anhydride synthesis from either butadiene or crotonaldehyde intermediates (Figure 1). Trimm (12) postulates the formation of monoperoxides, diperoxides, or possibly cycloperoxy species in the oxidation of 1,3-butadiene to maleic acid and maleic anhydride.

In previous investigations this research group has reported the synthesis, characterization, and reactivity of V-P-O industrial catalysts having variable P-to-V ratio (13). A fixed bed integral flow reactor system was used to obtain kinetic measurements for n-butane selective oxidation (13) and maleic anhydride combustion experiments (14). V-P-O catalysts incorporating a slight "excess" of phosphorus (P/V = 1.1) were found to contain $(VO)_2P_2O_7$, displayed low rates of maleic anhydride combustion, and were both active and selective in paraffin oxidation. In situ infrared spectroscopy was also used to investigate the mechanism for $C_4$ hydrocarbon selective oxidation to maleic anhydride. The partial oxidation of n-butane (15), 1-butene and 1,3-butadiene (16), and the oxidation of crotyl alcohol, maleic acid, and maleic anhydride (17) was studied on the surfaces of ultra-thin V-P-O catalyst wafers. Adsorbed 1-butene, a methyl-allyl species (possibly cyclobutene), and 1,3-butadiene were observed during paraffin oxidation; reactive olefin species and maleic acid were also identified during the in situ olefin oxidation studies.

This paper explores the results of the previous reactor studies (13, 14), and the in situ infrared studies (15, 16, 17), and proposes a reaction network for $C_4$ hydrocarbon oxidation which includes the partial oxidation of n-butane to maleic anhydride. Vibrational assignments are
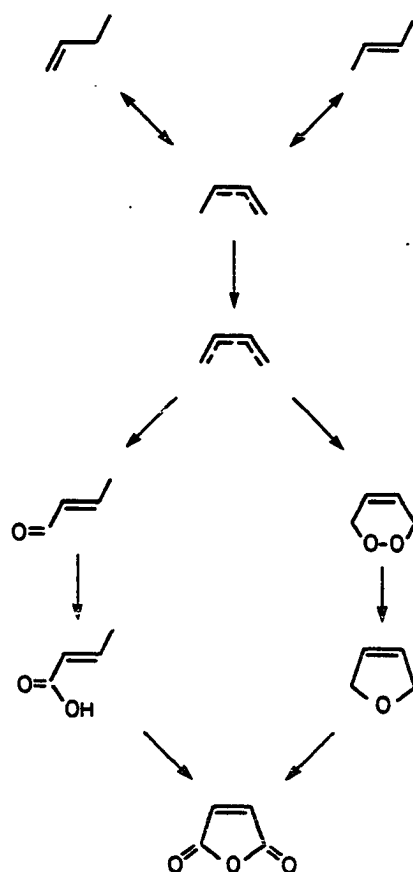
Figure 1. Reaction network for 1-butene selective oxidation

tabulated for the P/V = 0.9, 1.0, and 1.1 catalysts; the effects of catalyst composition and reaction temperature on the proposed mechanism are discussed.

## DISCUSSION OF RESULTS

### Maleic Anhydride Oxidation

The combustion of maleic anhydride to carbon oxides and water was studied using V-P-O industrial catalysts in a fixed bed integral flow reactor at 350-450°C (14). Kinetic measurements were obtained for the rates of maleic anhydride disappearance and carbon oxide formation for catalysts having P-to-V ratios of 0.9, 1.0, 1.1, and 1.2. Both an increase in reaction temperature or a decrease in catalyst phosphorus content were found to result in higher rates of maleic anhydride disappearance. The incorporation of "excess" catalyst phosphorus was found to stabilize a $(VO)_2P_2O_7$ phase with especially low rates of maleic anhydride combustion (14). The high activity and selectivity of the P/V = 1.1 catalyst in n-butane selective oxidation studies (13) was attributed to a strong suppression of maleic anhydride combustion activity by "excess" catalyst phosphorus, while n-butane partial oxidation reactions were largely uneffected.

The in situ infrared spectra collected during the maleic anhydride oxidation studies at 300°C confirmed the oxidation of maleic anhydride on the surface of the P/V = 1.1 V-P-O catalyst (17). Adsorbed maleic anhydride was distinguished by carbonyl stretching vibrations at 1777 and 1847 $cm^{-1}$, while gaseous CO and $CO_2$ were indicated by vibrational-rotational bands at 2143 and 2350 $cm^{-1}$, respectively. Adsorbed waters were also indicated by a broad O-H stretching band from 3100-3600 $cm^{-1}$. Table 1 provides a summary of vibrational assignments for maleic anhydride

Table 1. Vibrational assignments for maleic anhydride oxidation at 300°C

| Frequency $(cm^{-1})$ | Assignment | Species |
|---|---|---|
| 1777 | $\nu_{C=O}$ | maleic anhydride |
| 1847 | $\nu_{C=O}$ | maleic anhydride |
| 2143 | $\nu_{C\equiv O}$ | carbon monoxide |
| 2350 | $\nu_{O=C=O}$ | carbon dioxide |
| 3100–3600 | $\nu_{O=H}$ | water |

oxidation at 300°C. Since maleic anhydride was readily oxidized to CO, $CO_2$, and $H_2O$, the following reaction scheme is proposed.

 $\longrightarrow$ $CO, CO_2, (H_2O)$
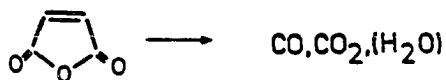
## Maleic Acid Oxidation

The _in situ_ infrared spectra collected during the maleic acid oxidation studies at 300°C identified the rapid formation of maleic anhydride and carbon oxides from maleic acid (17). Maleic acid adsorbed on the P/V = 1.1 V-P-O catalyst surface was identified by a C=O stretching vibration at 1715 $cm^{-1}$. Adsorbed maleic anhydride was again identified by carbonyl stretching vibrations at 1777 and 1849 $cm^{-1}$, while CO, $CO_2$, and water were observed at 2143, 2350, and 3100–3600 $cm^{-1}$, respectively. Table 2 provides a summary of vibrational assignments for maleic acid oxidation at 300°C. Since maleic acid was observed to form maleic

Table 2. Vibrational assignments for maleic acid oxidation at 300°C

| Frequency $(cm^{-1})$ | Assignment | Species |
|---|---|---|
| 1715 | $\nu_{C=O}$ | maleic acid |
| 1777 | $\nu_{C=O}$ | maleic anhydride |
| 1849 | $\nu_{C=O}$ | maleic anhydride |
| 2143 | $\nu_{C\equiv O}$ | carbon monoxide |
| 2350 | $\nu_{O=C=O}$ | carbon dioxide |
| 3100–3600 | $\nu_{O-H}$ | water |

anhydride, which in turn was readily oxidized to CO, $CO_2$, and water, the following reaction scheme is proposed.
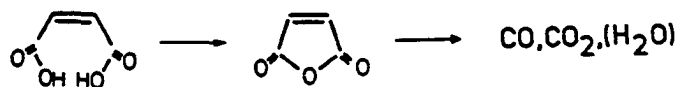


## 1,3-Butadiene Oxidation

The reaction pathway for 1,3-butadiene selective oxidation to maleic anhydride is generally believed to involve the addition of oxygen to form very reactive peroxide species on the catalyst surface (12). The addition of a single oxygen molecule to butadiene could lead to the formation of monoperoxides and 2-butenoic acid species, before a second addition of oxygen to give maleic acid. The dehydration of maleic acid to maleic anhydride would follow.

$$CH_2=CH-CH=CH_2 + O_2 \longrightarrow \cdot H_2C-CH=CH-CH_2OO\cdot$$

$$\cdot H_2C-CH=CH-CH_2OO\cdot + RH \longrightarrow \cdot H_2C-CH=CH-CH_2OOH + R\cdot$$

$$\cdot H_2C-CH=CH-CH_2OH \xrightarrow[O_2]{-H_2O} \cdot H_2C-CH=CH-C\underset{OH}{\overset{O}{\diagup}}$$

$$\cdot H_2C-CH=CH-C\underset{OH}{\overset{O}{\diagup}} + RH \xrightarrow{O_2} \underset{HO}{\overset{O}{\diagdown}}C-CH=CH-C\underset{OH}{\overset{O}{\diagup}} + R\cdot$$

$$\underset{HO}{\overset{O}{\diagdown}}C-CH=CH-C\underset{OH}{\overset{O}{\diagup}} \xrightarrow{-H_2O} \text{(cyclic anhydride structure)}$$
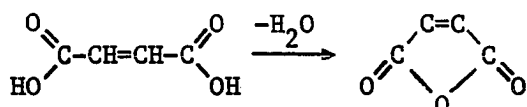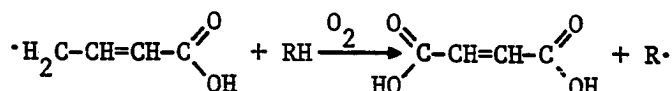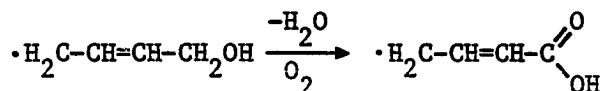
The addition of oxygen to butadiene could also lead to intramolecular peroxide formation across the double bond (10, 12). Further reaction of the cycloperoxide species to furan and maleic anhydride was proposed (10).
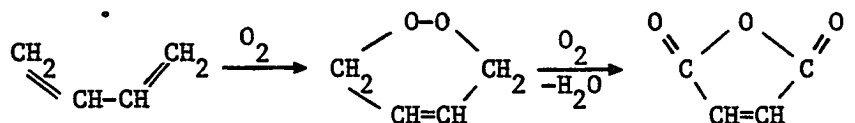


The *in situ* infrared spectra collected during 1,3-butadiene selective oxidation at 300°C revealed adsorbed 1,3-butadiene, maleic acid, maleic anhydride, CO, and $CO_2$ on the catalyst surface. Evidence was not gathered for adsorbed furan species on either the P/V = 0.9, 1.0, or 1.1 V-P-O catalysts. These studies (15, 16, 17) indicate that adsorbed maleic acid and not furan is an intermediate in $C_4$ hydrocarbon oxidation.

Table 3 provides a summary of vibrational assignments for butadiene oxidation on the P/V = 0.9, 1.0, and 1.1 catalysts at 300°C. Infrared frequencies and band assignments are given for the P/V = 1.1 catalyst.

Table 3. Vibrational assignments for 1,3-butadiene oxidation at 300°C

| Frequency ($cm^{-1}$) | Assignment | Species |
|---|---|---|
| (1595-1600) | $\nu_{C=C}$ | 1,3-butadiene |
| 1687[a] | — | — |
| 1723 | $\nu_{C=O}$ | maleic acid |
| 1773 | $\nu_{C=O}$ | maleic anhydride |
| 1844 | $\nu_{C=O}$ | maleic anhydride |
| 2143 | $\nu_{C\equiv O}$ | carbon monoxide |
| 2350 | $\nu_{O=C=O}$ | carbon dioxide |
| 3081 | $\nu_{=CH}$ | 1,3-butadiene |
| 3108 | $\nu_{-CH_2}$ | 1,3-butadiene |
| 3100-3600 | $\nu_{O-H}$ | water |

[a]Denotes no band assignment.

In cases where catalyst composition significantly affected absorbance frequencies, a frequency range is indicated in parentheses. All species were observed independent of catalyst composition. Adsorbed butadiene species were assigned to a C=C stretching vibration typically centered at 1600 $cm^{-1}$, and weak olefinic C-H stretching vibrations at 3081 and 3108 $cm^{-1}$. Adsorbed maleic acid was assigned to a C=O stretching vibration at 1723 $cm^{-1}$; maleic anhydride was indicated by two carbonyl vibrations at 1773 and 1844 $cm^{-1}$. The vibrational-rotational bands of CO and $CO_2$ were observed at 2143 and 2350 $cm^{-1}$, respectively. A shoulder band at 1687 $cm^{-1}$ was not assigned, although infrared bands at this frequency are

characteristic of trans-2-olefin species, or possibly unsaturated

aldehyde species (18). Since butadiene was observed to form maleic acid,

maleic anhydride, CO, $CO_2$, and $H_2O$, the following selective oxidation

scheme is proposed.
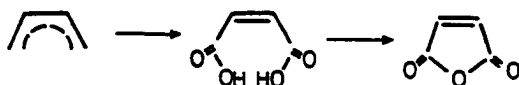


also $CO,CO_2,(H_2O)$

## 1-Butene Oxidation

Mechanisms for 1-butene selective oxidation to maleic anhydride

typically propose the reversible dehydrogenation of 1-butene to a methyl-

allyl species, which can be subsequently dehydrogenated to 1,3-butadiene,

or possibly hydrogenated to a 2-butene species. Once formed, butadiene

may be oxidized to crotonic acid or furan before maleic anhydride

formation (7, 11).

The _in situ_ infrared spectra collected during 1-butene selective

oxidation at 300-400°C revealed adsorbed 1-butene, a methyl-allyl species,

1,3-butadiene, maleic acid, maleic anhydride, CO, $CO_2$, and water on the

catalyst surface. Furan was not observed on either the P/V = 0.9, 1.0,

or 1.1 V-P-O catalysts. Adsorbed 1-butene was assigned to a shoulder

band $(\nu_{C=C})$ at 1645 cm$^{-1}$, and suggested by =CH and =CH$_2$ stretching

vibrations and 3010 and 3085 cm$^{-1}$. A firm assignment of the 3085 cm$^{-1}$

band to 1-butene is difficult since both 1-butene and 1,3-butadiene

display a distinct =CH$_2$ stretching vibration at 3085 cm$^{-1}$. Adsorbed

1,3-butadiene and additional reactive olefin species resembling a methyl

allyl species (19) or possibly cyclobutene (18) were indicated by C=C stretching vibrations in the region 1570-1615 $cm^{-1}$. An adsorbed maleic acid species was assigned to a C=O vibration at 1722-1727 $cm^{-1}$, maleic anhydride was assigned to C=O vibrations at 1777 and 1845 $cm^{-1}$. CO, $CO_2$, and water were indicated by infrared bands at 2143, 2350, and 3100-3600 $cm^{-1}$.

The effect of temperature on the relative intensity of infrared bands can reveal changes in reaction selectivity and offer additional evidence for reaction intermediates. At 400°C the intensity of infrared bands assigned to CO, $CO_2$, and water were observed to intensify more than did the carbonyl stretching vibrations of maleic anhydride. Consequently, catalyst selectivity was decreased by higher reaction temperatures. Furthermore, at 400°C the carbonyl stretching vibration of maleic acid (~1725 $cm^{-1}$) was observed to intensify more than was observed for the carbonyl stretching vibrations of maleic anhydride (1775 and 1845 $cm^{-1}$). For the basic series reaction of 1-butene $\xrightarrow{1}$ maleic acid $\xrightarrow{2}$ maleic anhydride, when $E_1 > E_2$ (very likely) a higher temperature should favor increased concentrations of maleic acid relative to maleic anhydride (20). Consequently, temperature effects support our hypothesis of reactive maleic acid intermediates during 1-butene selective oxidation.

Table 4 provides a summary of vibrational assignments for 1-butene selective oxidation on V-P-O catalysts at 400°C. Infrared band frequencies and assignments are presented for the P/V = 1.1 catalyst; in cases where catalyst composition affected the absorption frequency, a range is given in parenthesis. All species were observed on each V-P-O catalyst. Since 1-butene was readily dehydrogenated to a methyl-allyl

Table 4. Vibrational assignments for 1-butene oxidation at 400°C

| Frequency ($cm^{-1}$) | Assignment | Species |
|---|---|---|
| (1570–1580) | $\nu_{C=C}$ | methyl-allyl (cyclobutene) |
| (1605–1615) | $\nu_{C=C}$ | 1,3-butadiene |
| 1645 | $\nu_{C=C}$ | 1-butene |
| (1722–1727) | $\nu_{C=O}$ | maleic acid |
| 1777 | $\nu_{C=O}$ | maleic anhydride |
| 1845 | $\nu_{C=O}$ | maleic anhydride |
| 2143 | $\nu_{C\equiv O}$ | carbon monoxide |
| 2350 | $\nu_{O=C=O}$ | carbon dioxide |
| 3010 | $\nu_{=CH}$ | 1-butene |
| 3085 | $\nu_{=CH_2}$ | 1-butene (1,3-butadiene) |
| 3100–3600 | $\nu_{O-H}$ | water |

species and butadiene, and subsequently oxidized to maleic acid, maleic anhydride, carbon oxides, and water — a minor modification of the present reaction scheme is needed.



also $CO, CO_2, (H_2O)$

## n-Butane Oxidation

Escardino's et al. (2) reaction pathway for n-butane selective oxidation on V-P-O catalysts proposed the direct conversion of n-butane to maleic anhydride with the simultaneous combustion of n-butane and maleic anhydride to carbon oxides and water.

n-butane ⟶ maleic anhydride

$$CO_x, H_2O$$
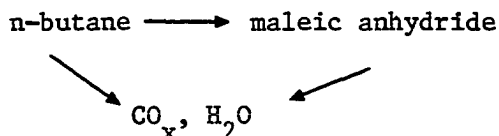
Both the _in situ_ infrared studies and the integral reactor studies for n-butane selective oxidation by V-P-O industrial catalysts, identified these four species on the catalyst surface (15) and in the reactor effluent (13). Furthermore, catalyst selectivity for maleic anhydride was found to be favored by lower reaction temperatures or higher catalyst phosphorus loadings, while specific rates of n-butane consumption were observed to increase with reaction temperature and to decrease with catalyst phosphorus content (13).

In addition to n-butane, maleic anhydride, CO, $CO_2$, and $H_2O$, three additional adsorbed species were observed during the _in situ_ n-butane oxidation studies. Adsorbed 1-butene and maleic acid were observed on the surface of the P/V = 0.9, 1.0, and 1.1 catalysts, while an additional conjugated or possibly strained olefin species was observed on the surface of the P/V = 1.0 and 1.1 catalysts.

Table 5 provides a summary of vibrational assignments for n-butane oxidation on the P/V = 0.9, 1.0, and 1.1 catalysts at 400°C. Infrared absorbance frequencies and band assignments are given for the P/V = 1.1

Table 5. Vibrational assignments for n-butane oxidation at 400°C

| Frequency ($cm^{-1}$) | Assignment | Species |
|---|---|---|
| 1461 | $\nu_{C-H}$ | n-butane |
| 1650 | $\nu_{C=C}$ | 1-butene |
| 1570[a] | $\nu_{C=C}$ | methyl allyl (cyclobutene) |
| (1705-1720) | $\nu_{C=O}$ | maleic acid |
| 1778 | $\nu_{C=O}$ | maleic anhydride |
| 1847 | $\nu_{C=O}$ | maleic anhydride |
| 2143 | $\nu_{\equiv O}$ | carbon monoxide |
| 2350 | $\nu_{O=C=O}$ | carbon dioxide |
| 2879 | $\nu_{-CH_2}$ | n-butane |
| 2933 | $\nu_{-CH_2}$ | n-butane |
| 2966 | $\nu_{-CH_3}$ | n-butane |
| 3010[b] | $\nu_{=CH}$ | --- |
| 3081 | $\nu_{-CH_2}$ | 1-butene |
| 3100-3600 | $\nu_{O-H}$ | water |

[a]Not observed for P/V = 0.9 catalyst.

[b]No band assignment.

catalyst; in cases where catalyst composition affected the vibrational frequency, the frequency range is placed in parenthesis. Adsorbed n-butane was assigned to C-H bending vibrations at 1461 $cm^{-1}$, and to C-H stretching vibrations at 2879, 2933, and 2966 $cm^{-1}$. Adsorbed 1-butene was assigned to C=C stretching vibrations at 1650 $cm^{-1}$. A distinct band

was observed for the P/V = 1.0 and 1.1 catalysts at 1570 cm$^{-1}$ and assigned

to the C=C stretching vibrations of an adsorbed methyl-allyl (19) or

cyclobutene (18) species. Maleic acid was assigned to a C=O stretching

vibration at 1705-1720 cm$^{-1}$, two C=O bands at 1778 and 1847 cm$^{-1}$ were

assigned to maleic anhydride. CO, $CO_2$, and water were assigned to

infrared bands at 2143, 2350, and a broad band from 3100-3600 cm$^{-1}$.

Since n-butane was observed to form 1-butene, a methyl-allyl or

pos.ibly a cyclobutene species, maleic acid, maleic anhydride, and carbon

oxides, the possibility of n-butane dehydrogenation to 1-butene followed

by the olefin selective oxidation scheme should be considered. This is

not unexpected since recent studies by Papera et al. (21) describe the

difficult activation of n-butane to form a $C_4H_9$· radical which is readily

dehydrogenated to a 1-butene species. The possibility of reactive olefin

and maleic acid intermediates in paraffin selective oxidation is also

indicated by a strengthening of the infrared bands of those adsorbed

species relative to maleic anhydride at higher reaction temperatures (20).

Since a strong 1570 cm$^{-1}$ C=C stretching vibration (18) was observed during

n-butane selective oxidation, a reactive cyclobutene species is now

included in the mechanism as a possible reaction intermediate.



also $CO, CO_2, (H_2O)$
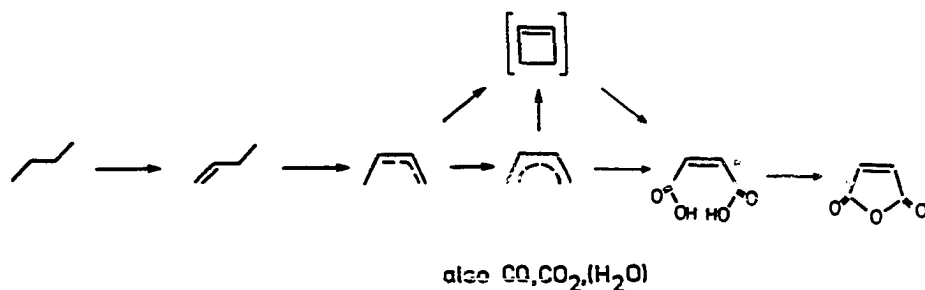
## 2-Buten-1-ol and 2-Butenoic Acid Oxidation

Since highly reactive olefin species and maleic acid were observed during the _in situ_ $C_4$ hydrocarbon oxidation studies (15, 16), crotyl alcohol (trans-2-buten-1-ol) and crotonic acid (trans-2-butenoic acid) oxidation studies were undertaken on the active and selective P/V = 1.1 V-P-O industrial catalyst (17). Crotyl alcohol was used as a mechanistic probe for allylic species on the catalyst surface, while crotonic acid was fed as a possible intermediate in butadiene selective oxidation to maleic anhydride.

Infrared spectra collected during crotyl alcohol oxidation (17) identified methyl-allyl species, butadiene, maleic acid, maleic anhydride, CO, $CO_2$, and water on the catalyst surface. A shoulder band at 1570 $cm^{-1}$ was assigned to the C=C stretch of methyl-allyl or possibly cyclo-butene species. Adsorbed butadiene was assigned to a C=C stretching vibration at 1605 $cm^{-1}$. Maleic acid was assigned to a C=O stretching vibration at 1720 $cm^{-1}$; two C-O vibrations at 1778 and 1847 $cm^{-1}$ were assigned to maleic acid. CO, $CO_2$, and $H_2O$ were assigned to infrared bands at 2143, 2350, and 3100-3600 $cm^{-1}$. Table 6 provides a summary of vibrational assignments for crotyl alcohol oxidation at 300°C.

Infrared spectra collected during crotonic acid oxidation (17) identified adsorbed crotonic acid, maleic acid, maleic anhydride, CO, $CO_2$, as well as "new" oxidation products not previously observed. Furthermore, adsorbed crotonic acid was distinguished by infrared bands not observed in any previous $C_4$ oxidation study (15, 16). Maleic acid and maleic anhydride were distinguished by carbonyl vibrations at 1720, 1780, and

Table 6. Vibrational assignments for crotyl alcohol oxidation at 300°C

| Frequency ($cm^{-1}$) | Assignment | Species |
|---|---|---|
| 1570 | $\nu_{C=C}$ | methyl-allyl (cyclobutene) |
| 1605 | $\nu_{C=C}$ | butadiene |
| 1720 | $\nu_{C=O}$ | maleic acid |
| 1778 | $\nu_{C=O}$ | maleic anhydride |
| 1847 | $\nu_{C=O}$ | maleic anhydride |
| 2143 | $\nu_{C\equiv O}$ | carbon monoxide |
| 2350 | $\nu_{O=C=O}$ | carbon dioxide |
| 3100-3600 | $\nu_{O-H}$ | water |

1845 $cm^{-1}$, while CO, $CO_2$, and water were assigned to infrared bands at 2143, 2350, and 3100-3600 $cm^{-1}$. Table 7 provides a summary of the vibrational assignments for crotonic acid oxidation at 300°C.

In these in situ oxidation studies (17), crotyl alcohol has been found to be an effective probe for reactive olefin species which participate in $C_4$ hydrocarbon oxidation. However, crotonic acid is not an intermediate in either n-butane or 1-butene oxidation, and probably forms maleic acid and maleic anhydride in a parallel reaction scheme. Consequently, butadiene appears to form maleic anhydride by the cyclic peroxide route proposed by Ostroushko et al. (11) and not by the oxidation of crotonic acid species. The proposed reaction scheme for $C_4$ hydrocarbon selective oxidation is presented in Figure 2.

Table 7. Vibrational assignments for crotonic acid oxidation at 300°C

| Frequency ($cm^{-1}$) | Assignment | Species |
|---|---|---|
| 1441 | $\nu_{O-H}$ | crotonic acid |
| 1625 | $\nu_{C=C}$ | crotonic acid |
| 1640 | $\nu_{C=C}$ | crotonic acid |
| 1681 | $\nu_{C=O}$ | crotonic acid |
| 1692 | $\nu_{C=O}$ | crotonic acid |
| 1720 | $\nu_{C=O}$ | maleic acid |
| 1760[a] | $\nu_{C=O}$ | -- |
| 1780 | $\nu_{C=O}$ | maleic anhydride |
| 1845 | $\nu_{C=O}$ | maleic anhydride |
| 2143 | $\nu_{C=O}$ | carbon monoxide |
| 2350 | $\nu_{O=C=O}$ | carbon dioxide |
| 3100-3600 | $\nu_{O=H}$ | water |

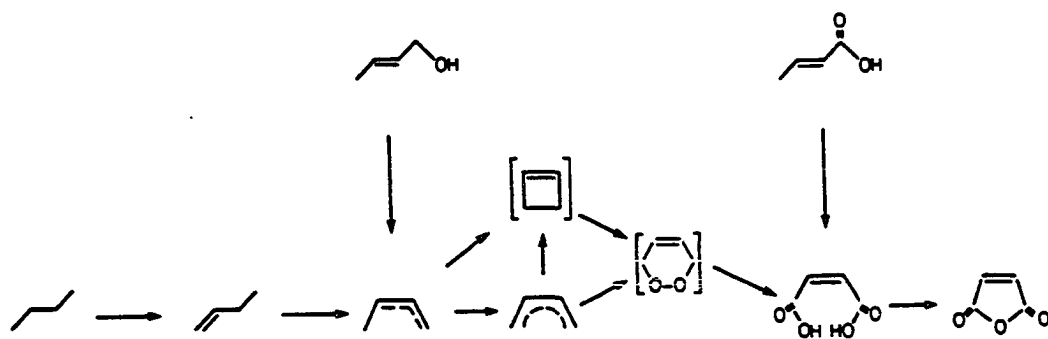[a]Denotes an unidentified oxidation product.

Figure 2. Reaction network for C$_4$ hydrocarbon selective oxidation

## CONCLUSIONS

A mechanism for the selective oxidation of $C_4$ hydrocarbons to maleic anhydride on V-P-O industrial catalysts has been developed. n-Butane is proposed to undergo a difficult dehydrogenation to 1-butene, followed by further dehydrogenation to 1,3-butadiene or cyclobutene species on the surface of catalysts having composition P/V = 1.0 and 1.1. The mechanism of n-butane dehydrogenation was not clear for the P/V = 0.9 catalyst—only 1-butene species were indicated. The oxidation of 1,3-butadiene or cyclobutene species does not seem to occur with crotonic acid or furan as reaction intermediates. Based on these studies, intramolecular peroxide formation across the butadiene double bond seems a likely route to the observed maleic acid intermediates in $C_4$ hydrocarbon selective oxidation to maleic anhydride.

## ACKNOWLEDGEMENT

REFERENCES

1. Burrington, J. D.; Kartisek, C. T.; Grasselli, R. K. Aspects of selective oxidation and ammoxidation mechanisms over bismuth molybdate catalysts - Allyl alcohol as a probe for the allylic intermediate. J. Catal. 63: 235-254; 1986.

2. Escardino, A.; Sola, C.; Ruiz, F. Oxidacion catalitica de butano a anhidrido maleico. Anales de Quimica 69: 385-396; 1973.

3. Wohlfahrt, K.; Hofmann, H. Kinetik der synthese von maleinsaure-anhdrid aus n-butan. Chem. Ing. Tech. 52(10): 811-814; 1980.

4. Wüstneck, N.; Wolf, H.; Seeboth, H. Role of vanadyl pyrophosphate in mild oxidation of hydrocarbons. React. Kinet. Catal. Lett. 21(4): 497-503; 1982.

5. Varma, R. L.; Saraf, D. N. Oxidation of butane to maleic anhydride. I. Kinetics and mechanism. Journal of Catalysis 55: 361-372; 1978.

6. Hodnett, B. K. Vanadium-phosphorus-oxide catalysts for the selective oxidation of $C_4$ hydrocarbons to maleic anhydride. Catal. Rev.-Sci. Eng. 27(3): 374-424; 1985.

7. Morselli, L.; Riva, A.; Trifiro, F.; Zucchi, M. Emig, G. The chemistry of V and P oxides based oxidation catalysts. I- Relationship between structure and activity for the oxidation of 1-butene to maleic anhydride. La Chimica E L'Industria 60(10): 791-797; 1978.

8. Ai, M.; Boutry, P.; Montarnal, R. Kinetics of the oxidation of butene to maleic anhydride on vanadium pentoxide-phosphorus pentoxide. I. Experimental kinetics. Bull. Soc. Chim. Fr. 8-9: 2775-2782; 1970.

9. Ai, M. A study of the partial catalytic oxidation of hydrocarbons. V. The effect of phosphorus addition to the vanadium catalyst on the oxidation of butene, butadiene, and furan. Bull. Chem. Soc. Jpn. 43(11): 3490-3495; 1970.

10. Van der Wieli, K.; Van den Berg, P. Heterogeneous oxidation processes. Comprehensive chemical kinetics. Vol. 20. 3rd ed. New York: Elsevier Scientific Publishing Company; 1978.

11. Ostroushko, V. I.; Kernos, Yu. D.; Ioffe, I. I. Oxidation of butenes with a vanadium-phosphorus catalyst. Neftekhimiya 12(3): 362-369; 1972.

12. Trimm, D. L. Design of industrial catalysts. New York: Elsevier Scientific Publishing Company; 1980.

13. Wenig, R. W.; Schrader, G. L. V-P-O industrial catalysts for n-butane oxidation: characterization and kinetic measurements. Ind. Eng. Chem. Fund.; accepted.

14. Moser, T. P.; Wenig, R. W.; Schrader, G. L. Maleic anhydride conversion by V-P-O catalysts. Appl. Catal.; submitted.

15. Wenig, R. W.; Schrader, G. L. In situ FTIR study of n-butane selective oxidation to maleic anhydride on V-P-O catalysts. J. Phys. Chem.; accepted.

16. Wenig, R. W.; Schrader, G. L. In situ FTIR study of 1-butene and 1,3-butadiene selective oxidation on V-P-O catalysts. J. Phys. Chem.; submitted.

17. Wenig, R. W.; Schrader, G. L. In situ FTIR study of crotyl alcohol, maleic acid, crotonic acid, and maleic anhydride oxidation on a V-P-O catalyst. J. Phys. Chem.; submitted.

18. Bellamy, L. J. The infrared spectra of complex molecules. New York: Chapman and Hall; 1980.

19. Dent, A. L.; Kokes, R. J. The nature of adsorbed propylene on zinc oxide: formation of $\pi$-allyl species. J. Amer. Chem. Soc. 92(23): 6709-6718; 1970.

20. Hill, C. G. An introduction to chemical engineering kinetics and reactor design. John Wiley and Sons, Inc.; 1977.

21. Papera, M.; Callahan, J.; Desmond, M.; Milberger, E.; Blum, P.; Bremer, N. Fundamental study of the oxidation of butane over vanadyl pyrophosphate. J. Am. Chem. Soc. 107: 4883-4892; 1985.

# SUMMARY AND RECOMMENDATIONS

## Summary

A fundamental understanding of the operation of vanadium-phosphorus-oxygen (V-P-O) catalysts in $C_4$ hydrocarbon oxidation to maleic anhydride has been gained. V-P-O industrial catalyst varying in P-to-V ratio have been synthesized, characterized, and the reactivity of these catalysts in n-butane selective oxidation has been studied in a fixed bed integral reactor system. Catalyst characterization studies were performed using X-ray diffraction, laser Raman spectroscopy, infrared spectroscopy, X-ray photoelectron spectroscopy, scanning electron microscopy, X-ray energy dispersive spectroscopy, and BET surface area measurements. A strong effect of P-to-V synthesis ratio on catalyst structure, catalyst morphology, vanadium oxidation state, and reactivity in n-butane selective oxidation to maleic anhydride was observed. A slight "excess" of catalyst phosphorus (P/V = 1.1 catalyst) was found to stabilize a $(VO)_2P_2O_7$ phase which was active and selective in n-butane oxidation. A larger "excess" of phosphorus was found to enhance selectivity of the $(VO)_2P_2O_7$ phase at the expense of catalyst activity. Used catalysts without "excess" phosphorus contained the active but nonselective $\alpha$-$VOPO_4$ phase. In addition, "excess" catalyst phosphorus was found to promote lower rates of maleic anhydride combustion on the V-P-O catalyst surface.

The reaction mechanism for n-butane selective oxidation to maleic anhydride has been studied by in situ Fourier-transform infrared spectroscopy. During n-butane selective oxidation highly reactive conjugated or possibly strained olefin species and maleic acid were observed on the

catalyst surface. The _in situ_ 1-butene and 1,3-butadiene studies also revealed reactive olefin and acid species on the catalyst surface. These studies taken together indicate that olefins and maleic acid could be reaction intermediates in paraffin, as well as olefin selective oxidation.

In situ infrared adsorption studies were also undertaken using crotyl alcohol, maleic acid, crotonic acid, and maleic anhydride feeds. Crotyl alcohol was used as a mechanistic probe for the formation of allylic species on the catalyst surface. Following crotyl alcohol introduction, methyl-allyl species and butadiene were observed. Maleic acid and crotonic acid were used as probes for the adsorbed acid species which were observed during the previous _in situ_ n-butane, 1-butene, and 1,3-butadiene studies. Adsorbed maleic acid was identified by the same infrared vibrations observed earlier, while adsorbed crotonic acid was distinguished by "new" infrared bands. Since both acid species formed maleic anhydride, it appears maleic acid is an intermediate in paraffin and olefin selective oxidation, while crotonic acid is a participant in a parallel reaction scheme. Adsorbed maleic anhydride was characterized by the same carbonyl vibrations which were observed during the previous _in situ_ studies, and was found to be readily oxidized on the catalyst surface to carbon oxides and water.

## Recommendations

V-P-O industrial catalysts with different P-to-V ratios have proven to be complex, often multi-phase systems with distinct structure, morphology, and reactivity. Some specific suggestions for further

investigations involving $C_4$ hydrocarbon selective oxidation to maleic anhydride follow:

1. Long-term kinetic measurements should be coupled with X-ray fluorescence studies and solid state $^{31}P$ and $^{51}V$ magnetic resonance studies, to investigate the effects of catalyst phosphorus loss on structure and reactivity.

2. The in situ incorporation of oxygen-18 into maleic acid, maleic anhydride, and carbon oxides can be studied by infrared spectroscopy using a V-P-$^{16}O$ catalyst, $^{18}O_2$, and n-butane.

3. The mechanism of n-butane activation can be revealed by the infrared identification of surface fragments which result from the adsorption of specifically deuterated n-butane.

4. An identification of the strength and population of catalyst acid sites can be made by infrared adsorption studies using basic "probe" molecules like ammonia or pyridine.

5. Commercial V-P-O catalysts are typically supported on silica or alumina. A determination of support effects on catalyst structure, vanadium oxidation state, and reactivity can be made.

6. Commercial V-P-O catalysts often contain Zn, Co, Mo, Ti, or Cr promoters. An understanding of promotional effects on catalyst structure, vanadium oxidation state, and reactivity is needed.

ADDITIONAL LITERATURE CITED

1. Gates, G. C.; Katzer, J. R.; Schuit, G. C. Chemistry of catalytic processes. New York: McGraw-Hill, Inc.; 1979.

2. Malow, M. Benzene on butane for MAN. Hydrocarbon Processing. November 1980: 149-153.

3. Hodnett, B. K. Vanadium-phosphorus oxide catalysts for the selective oxidation of $C_4$ hydrocarbons to maleic anhydride. Catal. Rev.-Sci. Eng. 27(3): 373-424; 1985.

4. Varma, R. L.; Saraf, D. M. Selective oxidation of $C_4$ hydrocarbons to maleic anhydride. Ind. Eng. Chem. Prod. Res. Dev. 18(1): 7-13; 1979.

5. Garbassi, F.; Bart, J.; Montino, F.; Petrini, G. Preparation and characterization of vanadius-phosphorus oxidation catalysts. Appl. Catal. 16: 271-287; 1985.

6. Bordes, E.; Courtine, P. Some selectivity criteria in mild oxidation catalysis - V-P-O phases in butene oxidation to maleic anhydride. J. Catal. 57: 236-252; 1979.

7. Hodnett, B. K.; Permanne, Ph.; Delmon, B. Influence of P/V ratio on the phase composition and catalytic activity of vanadium phosphate based catalysts. Appl. Catal. 6: 231-244; 1983.

8. Hodnett, B. K.; Demon, B. Influence of calcination conditions on the phase composition of vanadium-phosphorus oxide catalysts. Appl. Catal. 9: 203-211; 1984.

9. Escardino, A.; Solá, C.; Ruiz, F. Oxidacion catalitica de butano a anhidrido maleico. Anales de Quimica 69: 385-396; 1973.

10. Wohlfahrt, K.; Hofmann, H. Kinetic der Synthese von Maleinsäure-anhydrid aus n-Butan. Chem. Ing. Tech. 52(10): 811-814; 1980.

11. Wüstneck, N.; Wolf, H.; Seeboth, H. Role of vanadyl pyrophosphate in mild oxidation of hydrocarbons. React. Kinet. Catal. Lett. 21(4): 497-503; 1982.

12. Papera, M.; Callahan, J.; Desmond, M.; Milberger, E.; Blum, P.; Bremer, N. Fundamental study of the oxidation of butane over vanadyl pyrophosphate. J. Am. Chem. Soc. 107: 4883-4892; 1985.

13. Morselli, L.; Riva, A.; Trifirò, F.; Zucchi, M.; Emig, G. The chemistry of V and P oxides based oxidation catalysts. I - relationship between structure and activity for the oxidation of 1-butene to maleic anhydride. La Chimica E L'Industria 60(10): 791-797; 1978.

14. Ai, M. A study of the partial catalytic oxidation of hydrocarbons. V. The effect of phosphorus addition to the vanadium catalyst on the oxidation of butene, butadiene, and furan. Bull. Chem. Soc. Jpn. 43(11): 3490-3495; 1970.

15. Varma, R. L.; Saraf, D. N. Oxidation of butene to maleic anhydride. I. Kinetics and mechanism. J. of Catal. 55: 361-372; 1978.

16. Trimm, D. L. Design of industrial catalysts. New York: Elsevier Scientific Publishing Co.; 1980.

17. Mars, P.; van Krevelen, D. W. Oxidation carried out by means of vanadium-oxide catalysts. Chem. Eng. Sci. 3: Spec. Suppl.; 41-59; 1954.

18. Batist, Ph. A.; Kapteijns, C. J.; Lippens, B. C.; Schuit, G. C. A. The catalytic oxidation of 1-butene over bismuth molybdate catalysts. J. Catal. 7: 33-49; 1967.

## ACKNOWLEDGEMENTS

APPENDIX

Gas Chromatograph Analytical System

A five column gas chromatograph analytical system having two flame ionization detectors, one thermal conductivity detector, and three heated gas sampling values was used for analyzing the feed and product streams. A description of the chromatographic columns and possible separations follows:

A1) A Porapak Q column capable of separating hydrocarbons, $CO_2$, water, and air (A $N_2$, $O_2$, CO peak was unresolved) was used with the thermal conductivity detector.

A2) A 5 $\overset{o}{A}$ molecular sieve column able to separate $O_2$, $N_2$, and CO was connected in series to the Porapak Q column.

B) The reference column for the thermal conductivity detector packed with Chromosorb PAW SE 30.

C) A Carbopack B/5% carbowax column which provided a separation of furan, crotonaldehyde, and maleic anhydride from $C_4$ olefins. This column fed a flame ionization detector.

D) A Carbopack C/19% picric acid column which was capable of separating butane, 1-butene, cis-2-butene, trans-2-butene, 1,3-butadiene, and furan. This column fed the second flame ionization detector.

Columns A1, A2, B, and C were placed within the temperature programmed oven; column D was placed external to the gas chromatograph and maintained at 60°C. Helium was used as the carrier gas to each column.

The sampling procedures for analysis of product or feed gases follows:

t < 0              Cool oven to 30°C.

t = 0              Introduce sample to column A1 and start the first
                   integrator.

t = 1 min          Introduce the sample to column C and start the second
                   integrator.

t = 2 min          Introduce the sample to column D and start the third
                   integrator.

t = 2 min 45 sec   Switch the isolation valve so that $N_2$, $O_2$, and CO are
                   isolated to the molecular sieve column.

t = 4 min 50 sec   Begin heating the g.c. oven to 180°C at a rate of
                   15°C per minute.

t = 17 min         Begin cooling the g.c. oven to 40°C.

t = 28 min         Switch the isolation valve so that $N_2$, $O_2$, and CO are
                   eluted.

The concentrations of species were calculated from the integrated
peak areas using relative response factors which were obtained from
mixtures of known composition. For example, the amount (concentration) of
species b in a mixture was calculated by the relationship

$$N_b = \frac{N_a}{A_a} \times \frac{A_b}{f_b} \times f_a$$

where $N_b$ = moles of species b

$N_a$ = moles of standard a

$A_b$ = raw peak area of species b

$A_a$ = raw peak area of standard a

$f_b$ = molar response factor of species b relative to a

$f_a$ = molar response factor of standard a which is unity by
        definition.

Table 1 lists response factors relative to n-butane which were used in these studies.

Table 1. Response factors relative to n-butane

| Species | Response factor |
|---------|-----------------|
| cis-2-butene | 0.991 |
| trans-2-butene | 0.991 |
| 1,3-butadiene | 0.980 |
| maleic anhydride | 0.352 |
| carbon dioxide | 0.589 |
| furan | 0.887 |